High Axial Ratio Nanostructures

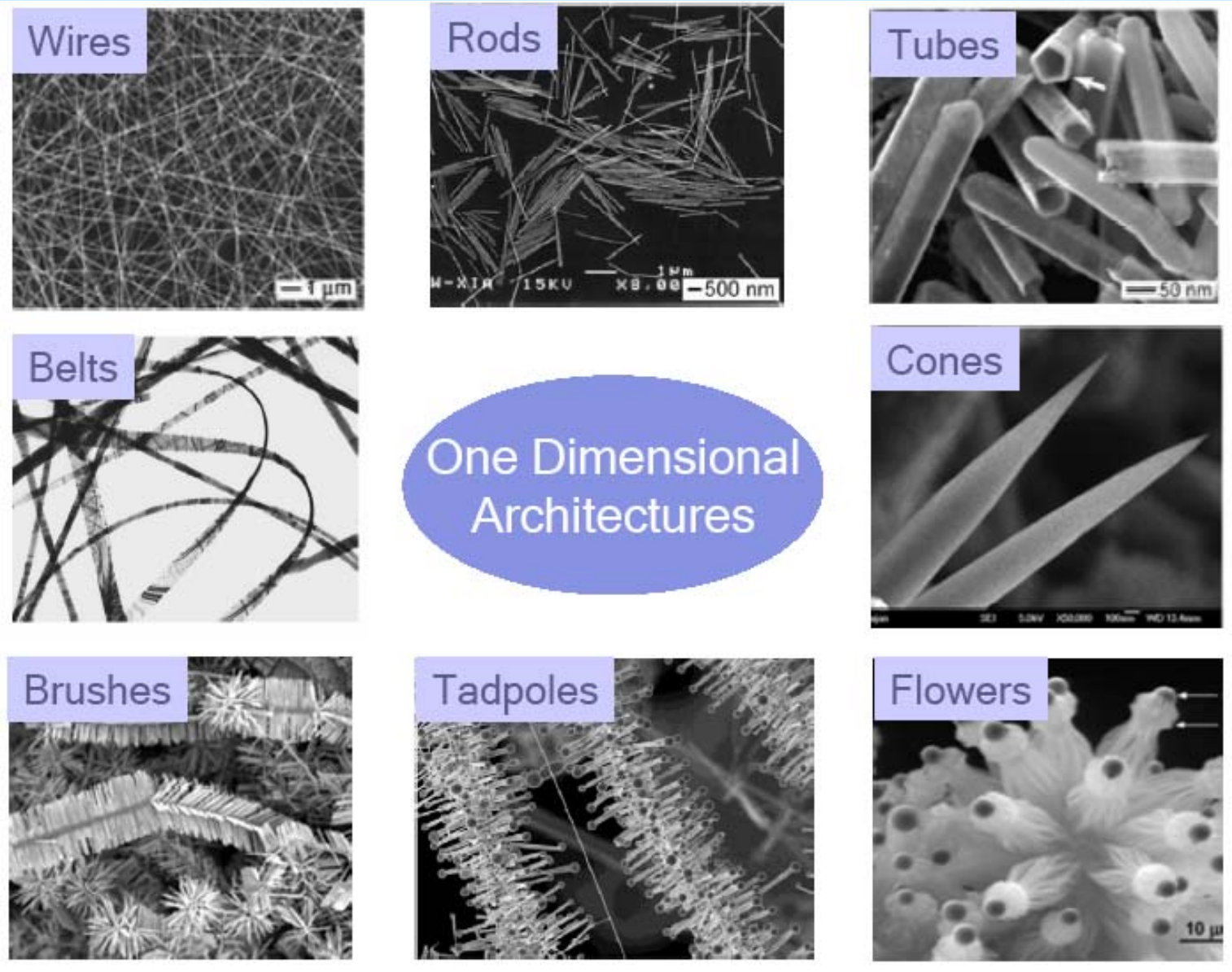

Dimension-Properties Interplay

Carbon allotropes

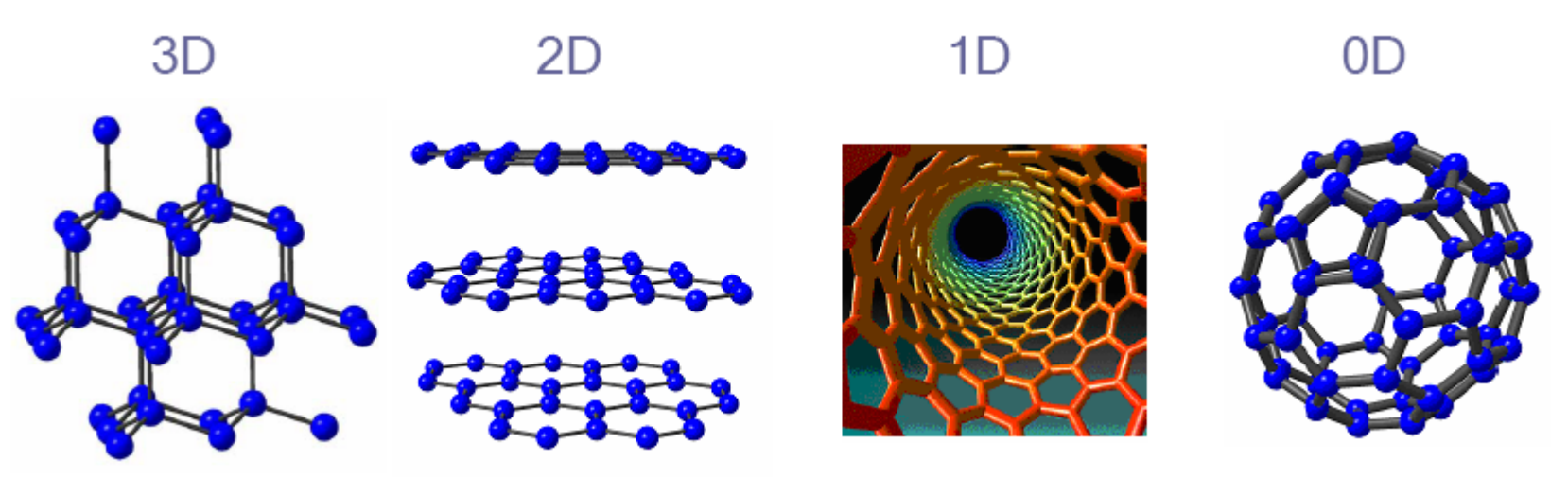

Brilliant, Transparent	**Metallic lusture Opaque**	**Black, Fibrous**	**Black Shiny Crystals**
Mohs Hardness 10	**1-2**	**1-1.2**	**-**
20 W/cmK	**25**	**6000**	**-**
High Melting point	**Lubricant**	**Unusual Electrical Behaviour**	**Superconductor (10-40 K)**

Role of Dimensionality

From continuous bands to discrete energy levels

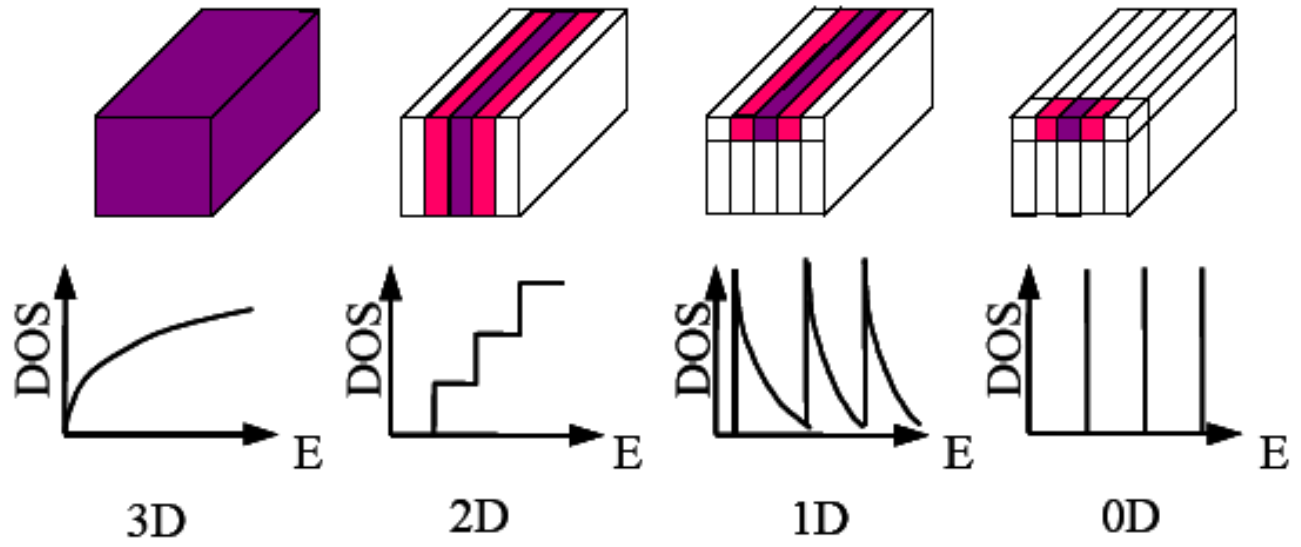

3 D: $E = \frac{\hbar^2}{2m}\left[k_x^{\,2} + k_y^{\,2} + k_z^{\,2}\right]$

2 D: $E = \frac{\hbar^2}{2m}\left[k_x^{\,2} + k_y^{\,2} + \left(n_z \frac{\pi}{L}\right)^2\right]$ $\quad n_z = 1,2,3\ldots$

1 D: $E = \frac{\hbar^2}{2m}\left[k_x^{\,2} + \left(n_y \frac{\pi}{L}\right)^2 + \left(n_z \frac{\pi}{L}\right)^2\right]$ $\quad n_y, n_z = 1,2,3\ldots$

0 D: $E = \frac{\hbar^2}{2m}\left[\left(n_x \frac{\pi}{L}\right)^2 + \left(n_y \frac{\pi}{L}\right)^2 + \left(n_z \frac{\pi}{L}\right)^2\right]$ $\quad n_x, n_y, n_z = 1,2,3\ldots$

1D Nanostructures

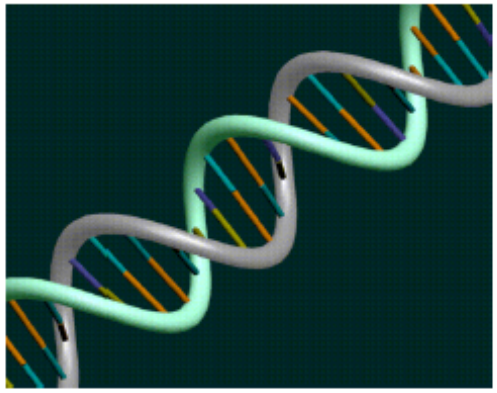

DNA

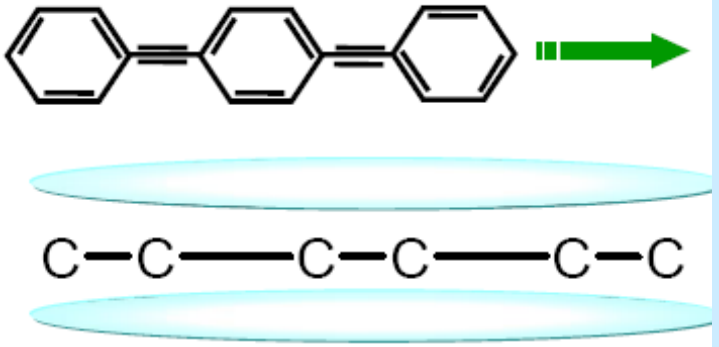

Molecular Wire

The Nano World

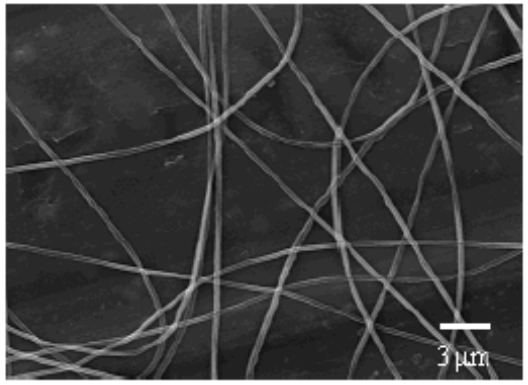

Poly (ethylene oxide)

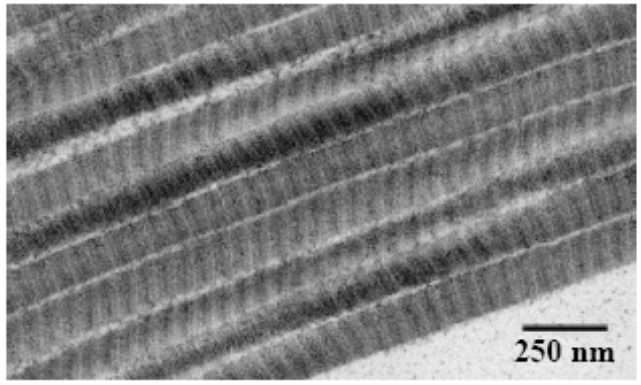

Collagen Fibrils

Potential of Nanowires

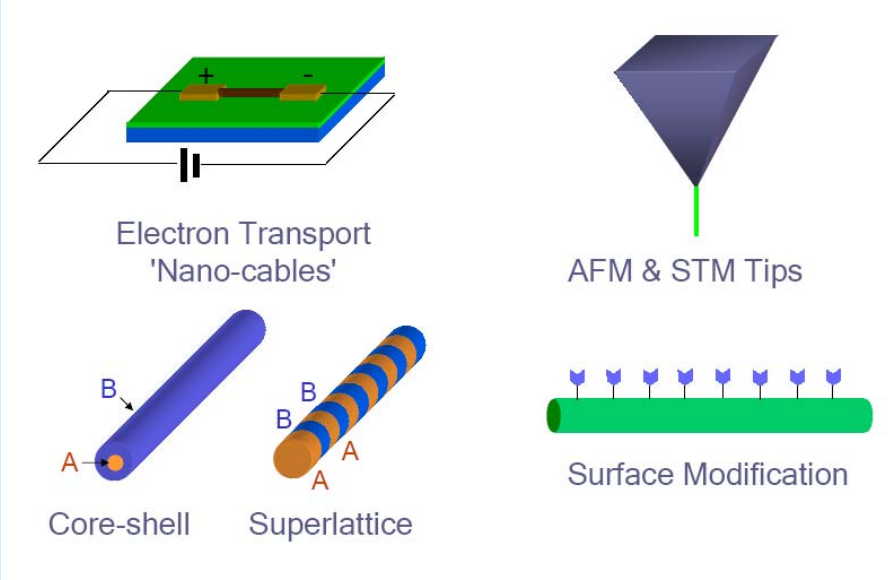

Potential applications

Interconnects
Novel Probes
Multifunctional
Hierarchical alignment
Building blocks for devices

Effect of Confinement

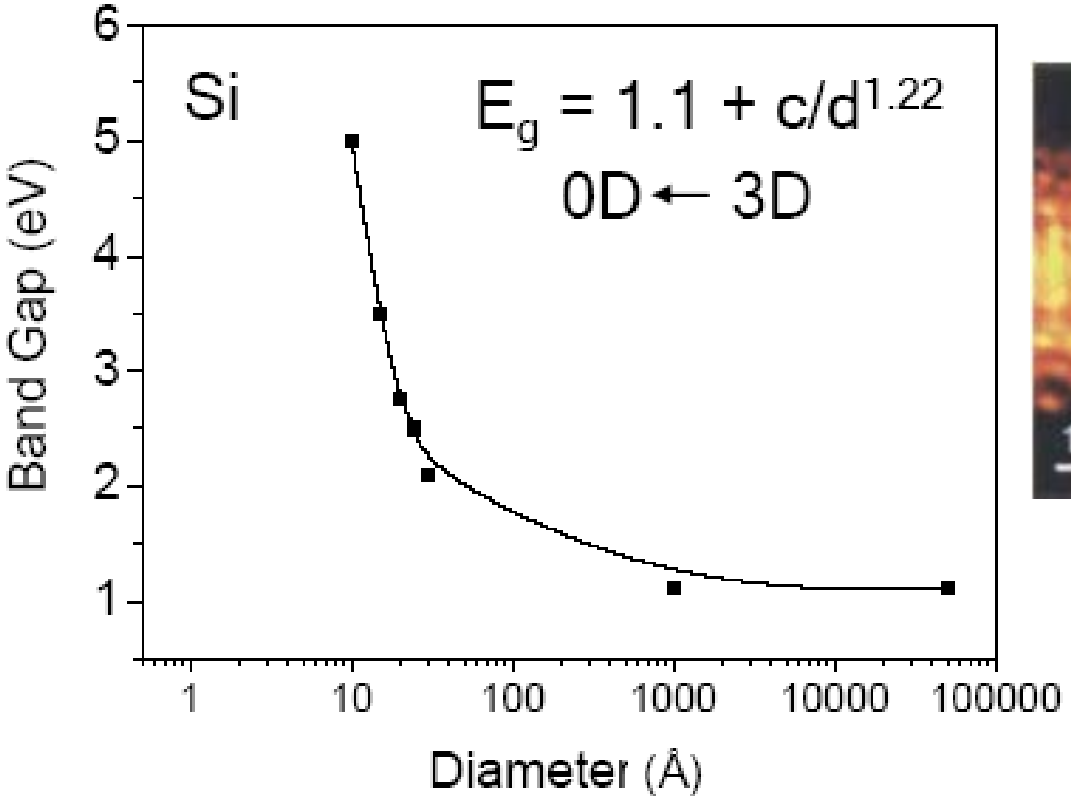

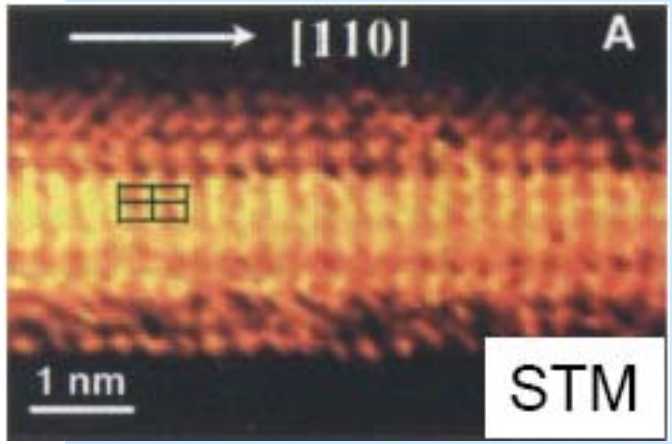

The band gap increases with decreasing diameter (quantum confinement)

Mechanical properties

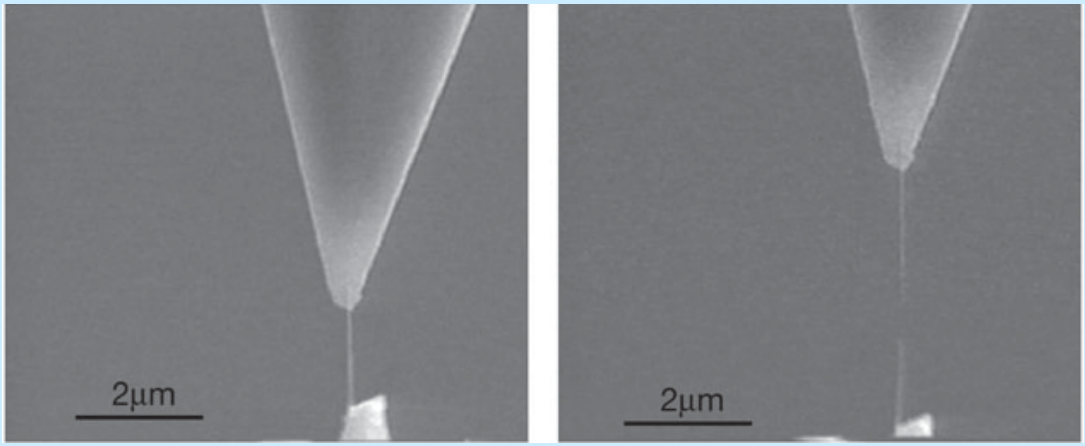

WS_2 nanotube during a tensile test before (left) and after (right) failure

WS_2 nanotube

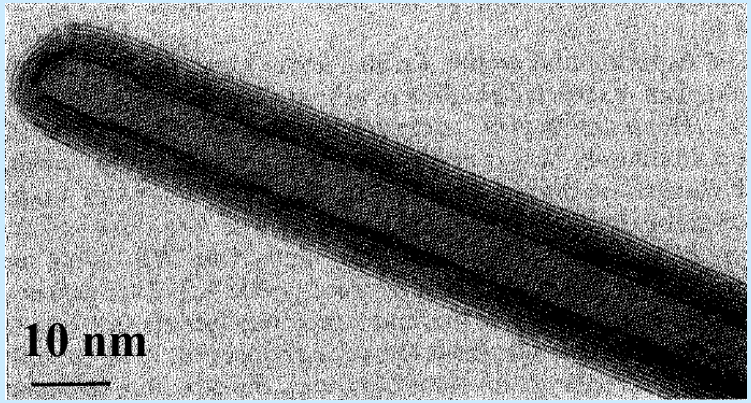

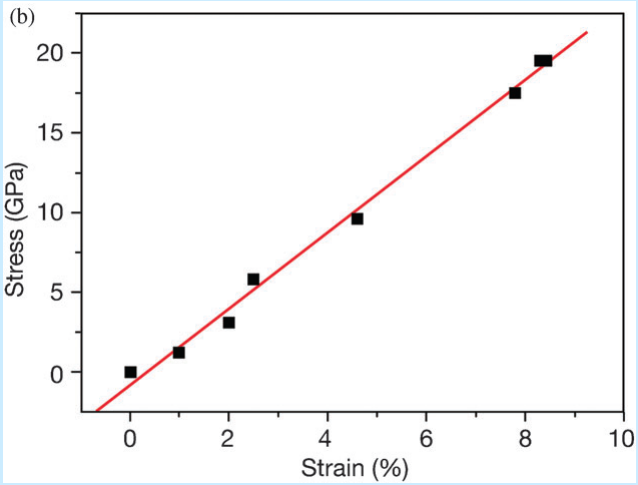

Strain–stress curve of a nanotube

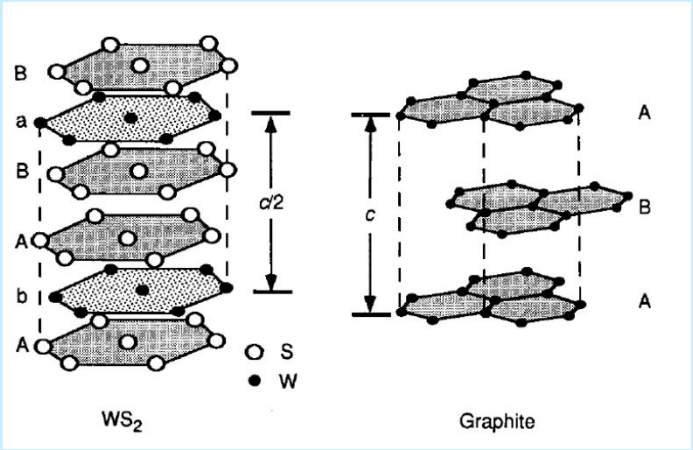

Carbon Nanotubes

- (Re)discovered by Iijima (1991, NEC)
- 1952 Russians (CO + Fe hot, SEM)
- Rolled up sheet of graphene
- Capped at the ends with half a fullerene

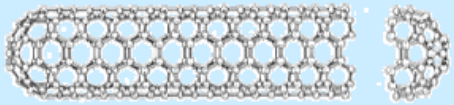

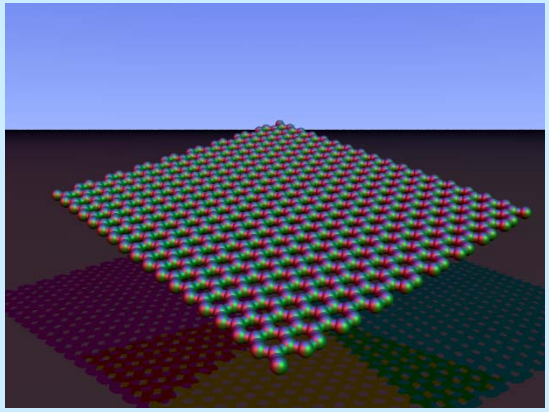

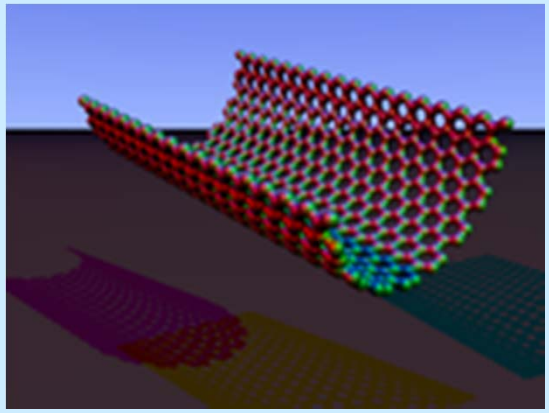

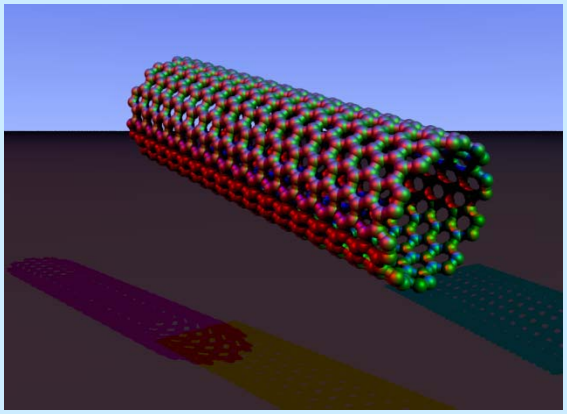

Carbon Nanotubes

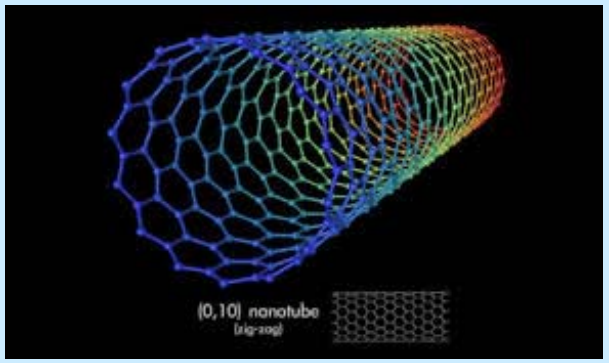

Single Walled Nanotube (SWNT)

- Single atomic layer wall
- Diameter of 0.7 – 5 nm
- Length several microns to centimeters

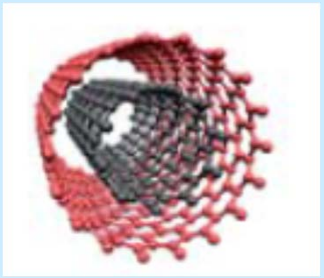

Double Walled Nanotube (SWNT)

- exactly two concentric CNT
- the outer wall selectively functionalized while maintaining an intact inner-tube

Multi Walled Nanotube (MWNT)

- Concentric tubes ca. 50 in number, separation 0.34 nm
- Inner diameters : 1.5 – 15 nm
- Outer diameters : 2.5 – 150 nm

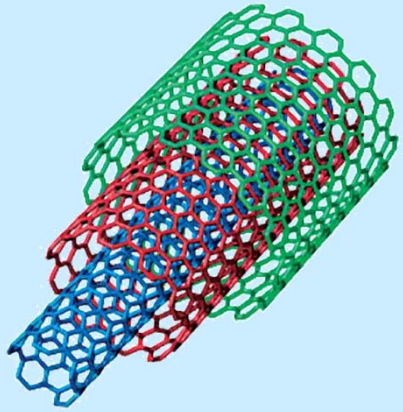

Lengths: micrometers to centimeters
Aspect Ratio: up to 10^7

SWCNT diameter from Raman spectroscopy

- RBM (Radial Breathing Mode): 100 to 300 cm^{-1}, vibration at which the nanotube diameter contracts and expands
- D-band: vicinity of 1350 cm^{-1}, defect-derived peak
- G-band: vicinity of 1550 -1605 cm^{-1}, in-plane vibration of graphite
- G'-band: 2700 cm^{-1}, overtone of D-band

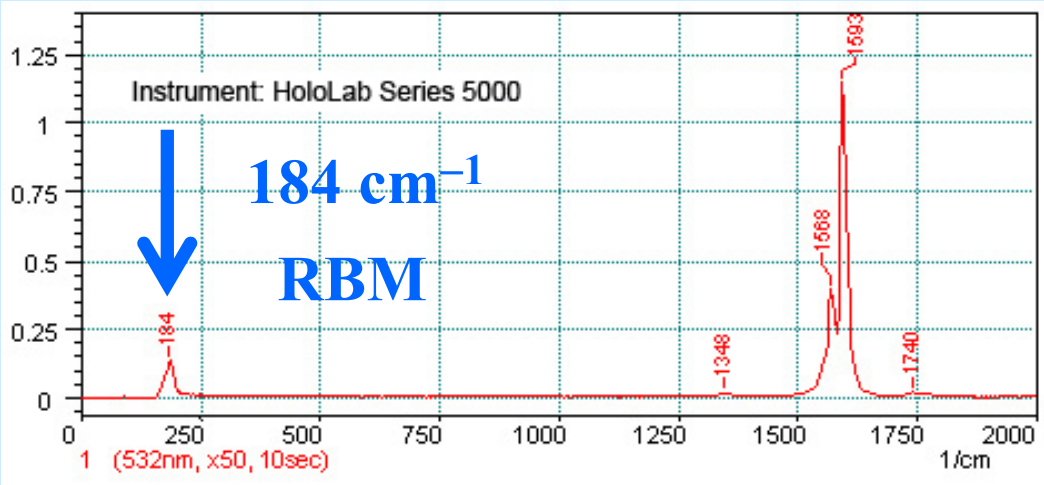

The wavenumber of RBM is inversely proportional to the tube diameter D

$$\mathbf{D\ (nm) = 248/\omega} = 248/184 = 1.3\ (nm)$$

Raman spectroscopy

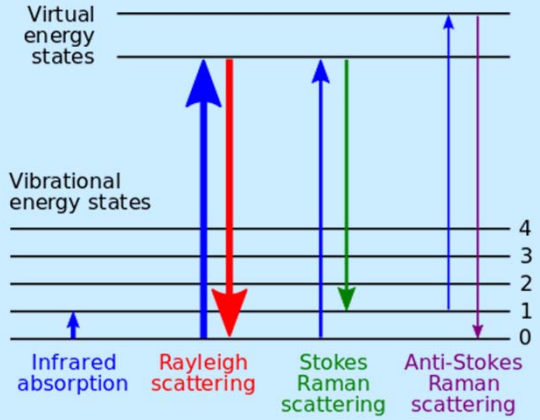

Raman scattering is an extremely weak process - only one in every 10^6 - 10^8 photons scatters

Raman effect

- interaction between the electron cloud of a molecule and the external electrical field of the monochromatic light
- a change in polarizability with respect to the vibrational coordinate

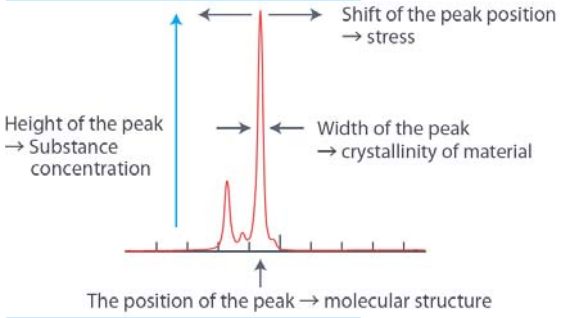

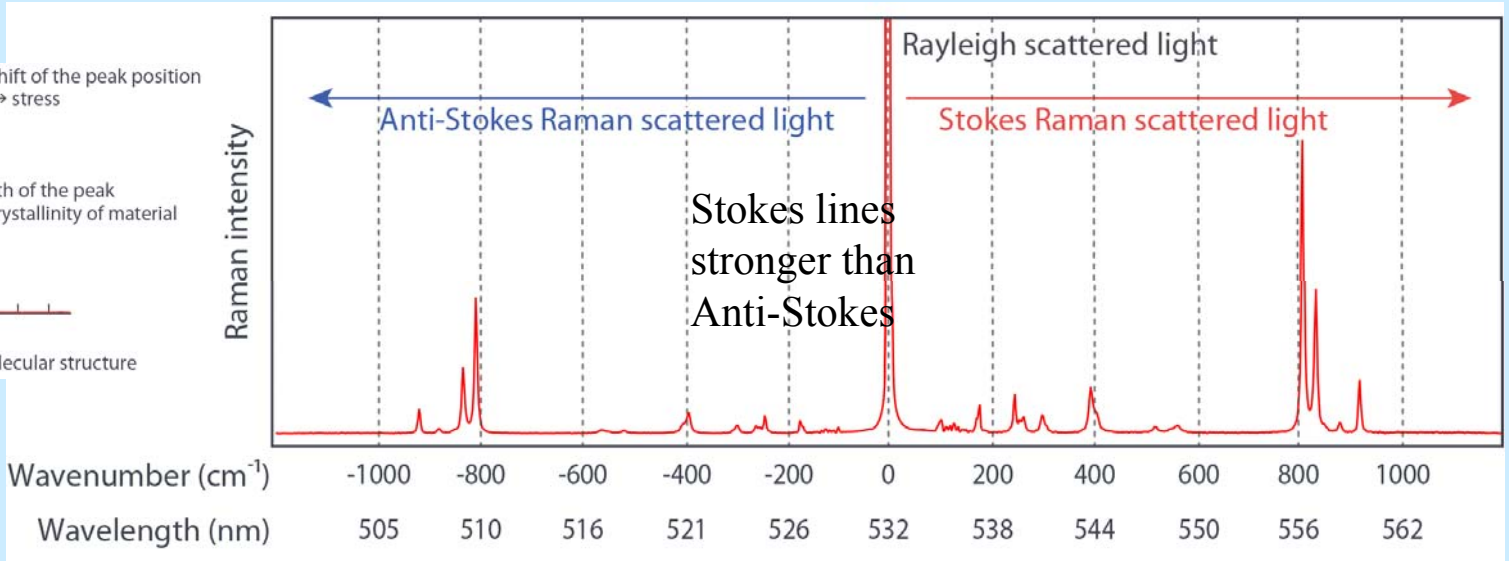

CNTs: Properties and Potential

Electronic: Bandgap $E_g \sim 1/d$
Ballistic conductivity in metallic CNTs,
the highest current density 10^9 A/cm^2 (Cu only 10^6 A/cm^2)
SWNT – metallic or semiconducting, MWCNT - metallic

Magnetic: Anisotropic magn. susceptibility $\chi_\perp >> \chi_\parallel$

Mechanical: Young's Modulus
1.8 TPa (SWNT, axial), 0.95 TPa (MWNT) (Steel: 230 GPa)
tensile strength above 100 GPa (steel: 1–2 GPa) the highest known

Thermal: Conductivity theor. 6600 W/m K axial, 1.5 perpendicular , 3500 experim. (Diamond 3000, Cu 400 W/m K) 300 W/m K bulk SWCNTs, 3000 W/m K individual MWCNTs

Thermal stability 650 °C (SW)–800 °C (MW) in air, 2800 °C in Ar (anealing to graphitize defects), 320 °C with metal oxides on the surface – O vacancies, Mars-van Krevelen catatlytic mechanism

Synthetic routes to CNT

- **DC arc discharge**: growth on a cathode C electrode at 3000 °C, MWCNTs and SWCNTs (with catalyst), easy design, few structural defects, short tubes, low yield, low purity, random diameters

- **Laser ablation**: primarily SWCNTs, few defects, good control over diameter, most costly method, poor scalability, requires Class 4 lasers, Co and Ni catalyst

- **Molten salt**: primarily MWCNTs, simple process, used for filling CNTs, low yield and crystallinity, poor controllability

- **Chemical vapor deposition**: both types, high yields, easy scalability, long tubes, alignment and pattern growth, some defects, medium purity

Synthetic routes to CNT

DC Arc discharge

NTs observed in carbon soot of graphite electrodes during arc discharge (during production of fullerenes)
The most used method of synthesis in early 1990´s

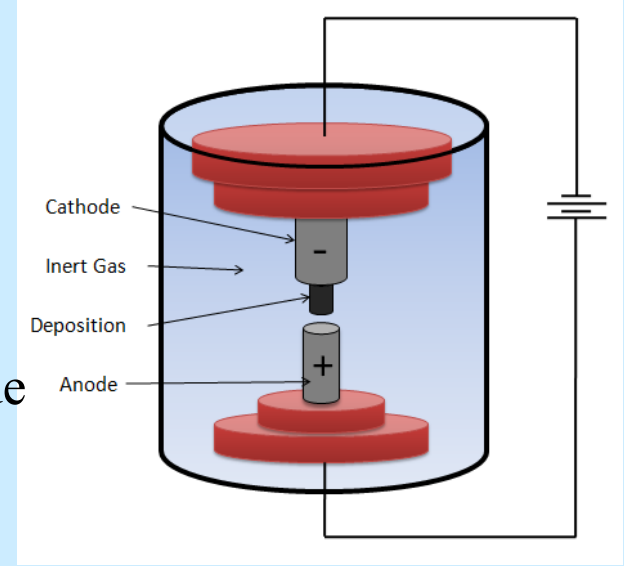

2 carbon electrodes touch, T rises, gap,
electric arch, fast e^- from cathode ionize He gas
He^+ attracted to cathode (–)
Carbon (with catalyst) contained in negative electrode sublimes thanks to high temperatures of the electric discharge (3000 °C)

Yield up to 30 %wt, produces both SWNTs, MWNTs
Length up to 50 μm, few structural defects

Synthetic routes to CNT

Laser ablation

Pulsed laser vaporizes graphite target in a high-temperature reactor filled with inert gas (650 mbar, Ar, N_2)

CNTs develop on the cooler surfaces of reactor as the carbon condenses

Pure graphite – MWNTs

Graphite + metal catalyst particles (Co + Ni) – SWNTs

Yield up to 70%wt, few defects

Controllable diameter of SWNTs by changing p, T

More expensive than arc discharge, CVD

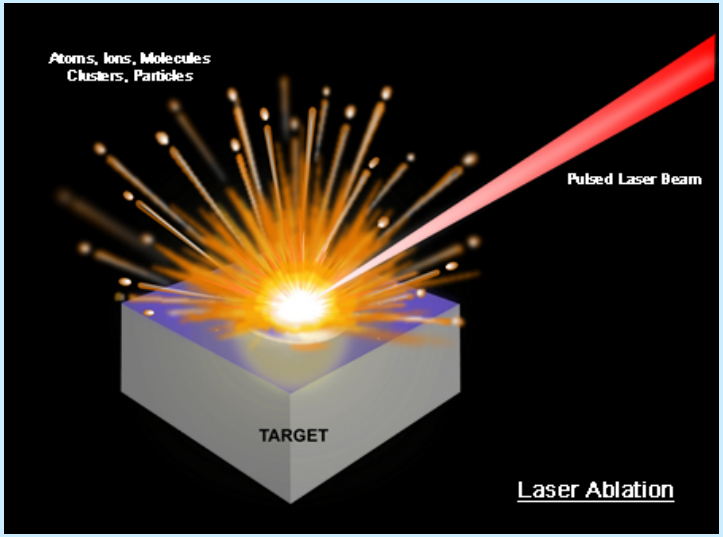

Synthetic routes to CNT

Molten salt

LiCl, LiBr, 600 °C, graphite electrodes
Cathode exfoliates and graphite sheet wraps
MWCNTs
Yield up to 30%wt, low purity
Large number of defects, amorphous carbon impurity, salt encapsulating

Synthetic routes to CNT

CVD (Chemical Vapor Deposition)

Substrate + metal catalyst particles (cobalt, nickel, iron)
Distribution of metal catalyst and the size of the particles influence the diameter of NTs
Patterned (or masked) deposition of metal, annealing, plasma etching
Substrate is heated
Two gasses are bled into the reactor – process gas (ammonia, nitrogen, hydrogen) and carbon-containing gas (acetylene, methane, ethylene)
Carbon-containing gas is broken apart at the surface of the metal catalyst particle, carbon is transported to the edges of the particle, where it forms the NT
Catalyst is removed by acid treatment
Resulting NTs are randomly oriented

Synthetic routes to CNT

CVD (Chemical Vapor Deposition)

CH_4 + metal catalyst particles (cobalt, nickel, iron) → $Fe_3C/C + H_2$

Tip growth
Base growth

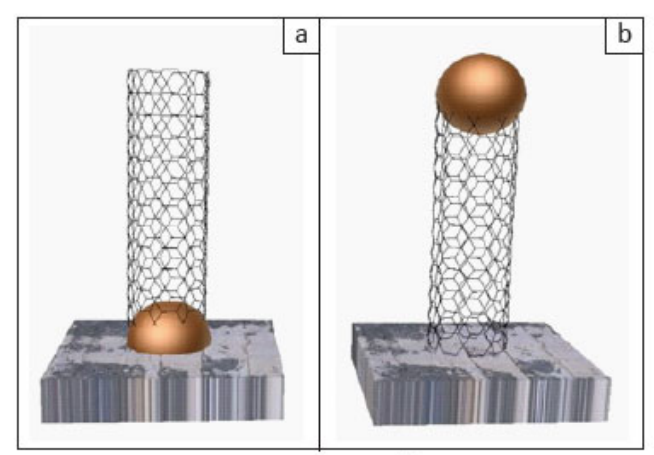

FIGURE 9: Carbon nanotube mechanistic models: (a) root-growth mechanism and (b) tip-growth mechanism.

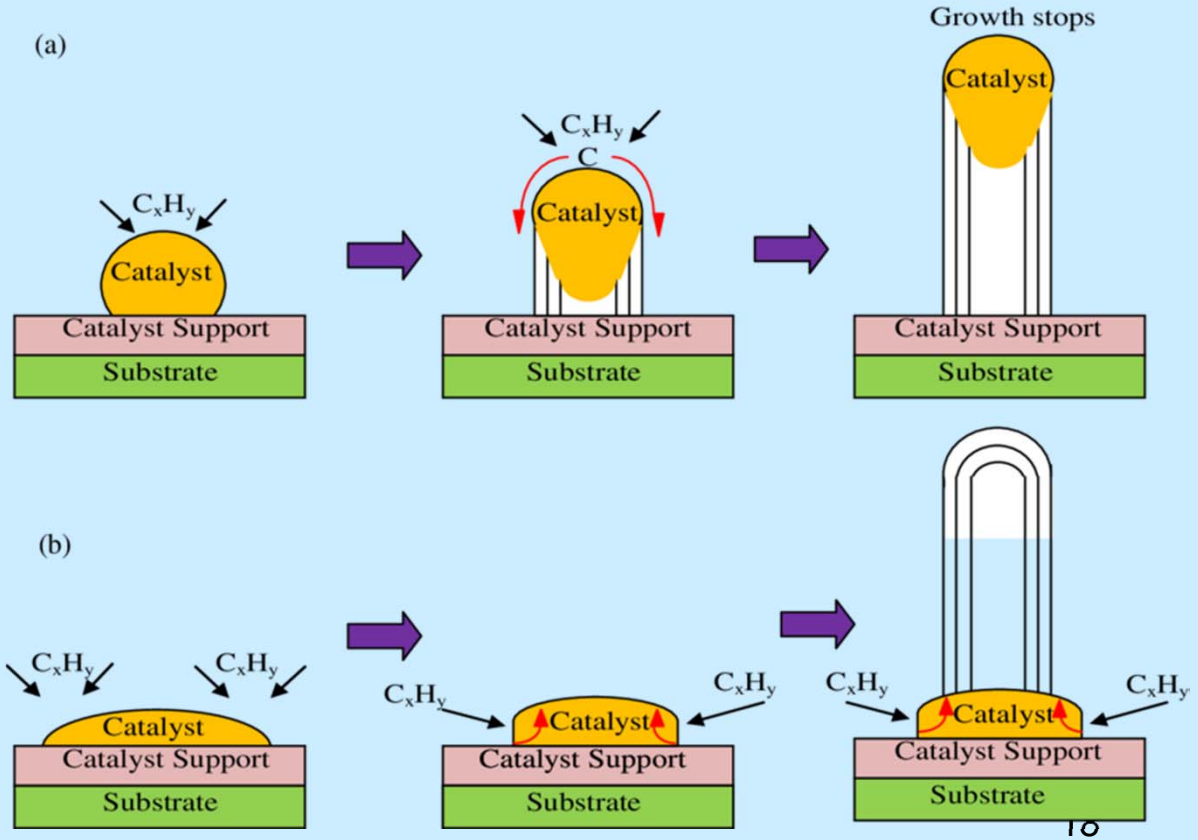

Synthetic routes to CNT

CVD (Chemical Vapor Deposition)

Plasma Enhanced CVD
Plasma is generated by the application of strong electric field during growth
Growing NTs follow the direction of the electric field
With the correct use of reactor geometry, vertically aligned (perpendicular to substrate) NTs can be grown

Substrate patterned (lithography) with Fe NPs

CDV shows the best promise for industrial manufacturing of CNTs
Better price/unit ratio
NTs grown on desired substrates

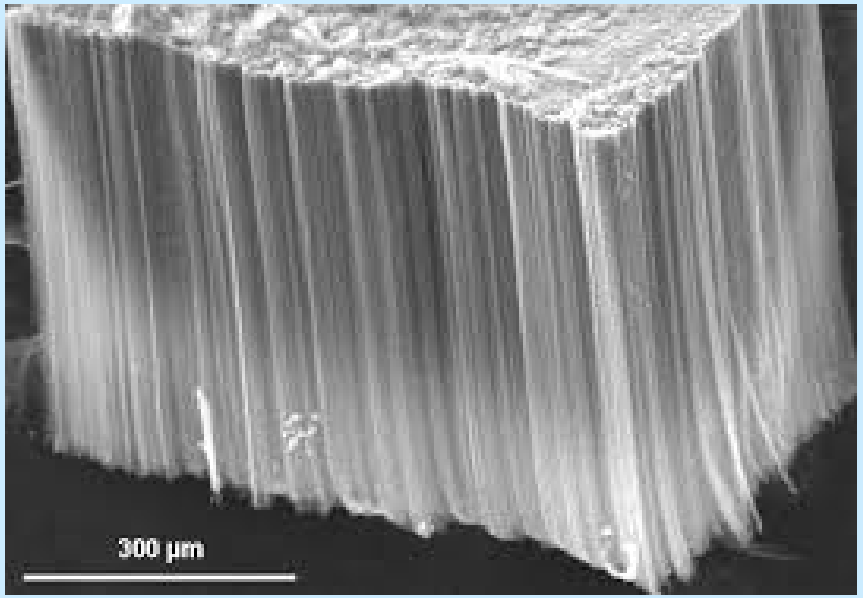

Synthetic routes to CNT

Super-growth CVD

New methods of CVD using different substrates, catalysts
Activity and lifetime of catalyst can be enhanced by adding water into the reactor
Growing CNTs then form „forests“ up to several mm high, aligned normaly
Improved efficiency, reaction time and purity of CNTs (more than 99,9%)

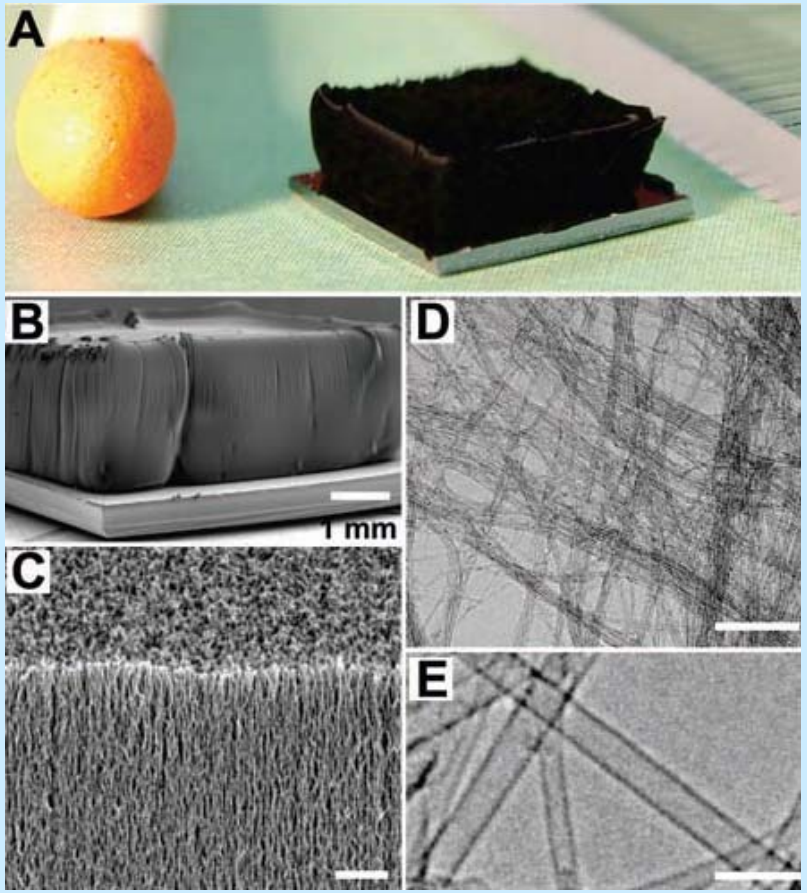

Hata, K.; Futaba, DN; Mizuno, K; Namai, T; Yumura, M; Iijima, S (2004). "Water-Assisted Highly Efficient Synthesis of Impurity-Free Single-Walled Carbon Nanotubes". *Science* **306** (5700): 1362–1365. doi:10.1126/science.1104962. PMID 15550668

Synthetic routes to CNT

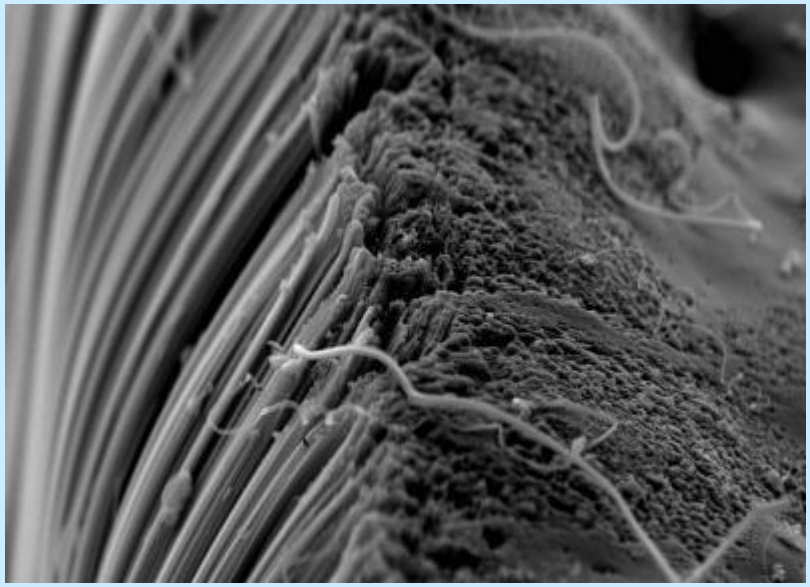

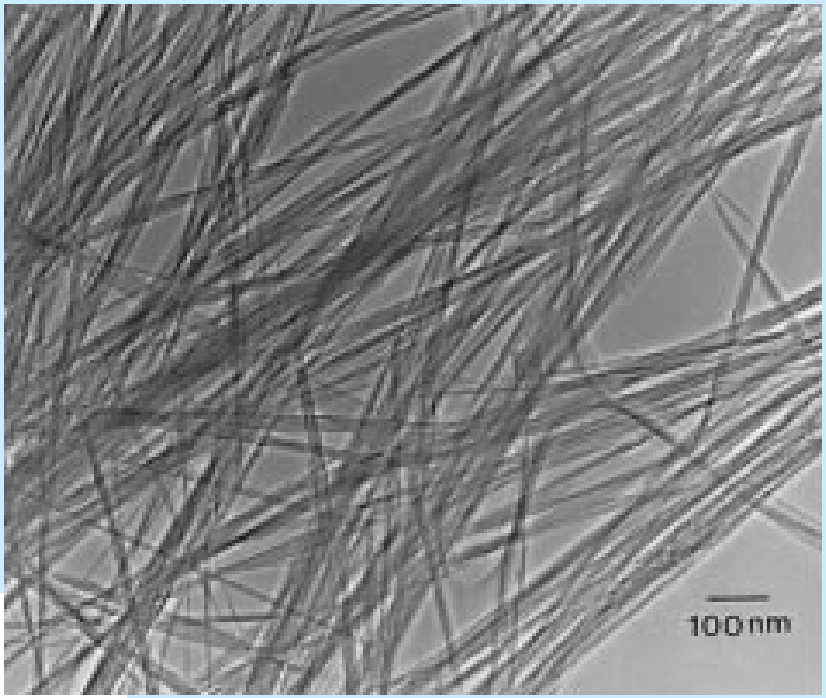

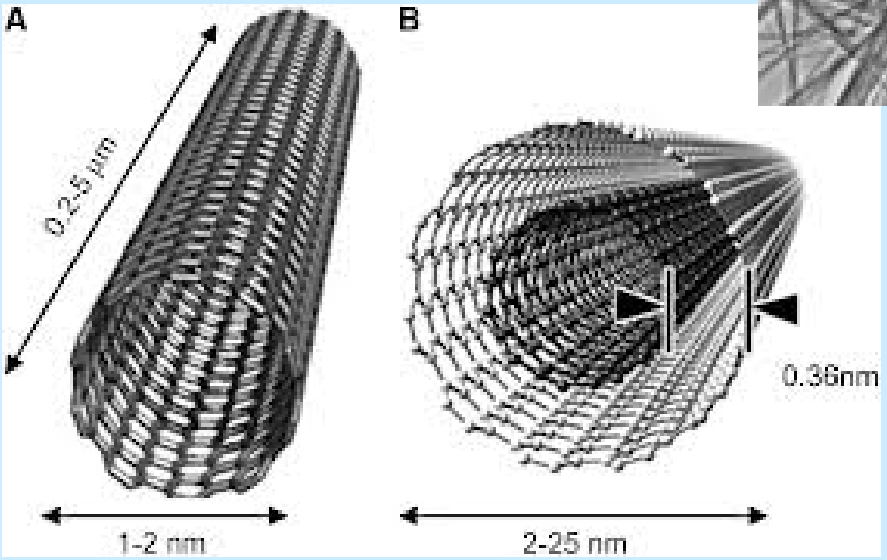

Defect-free (n,m) SWNTs with open ends

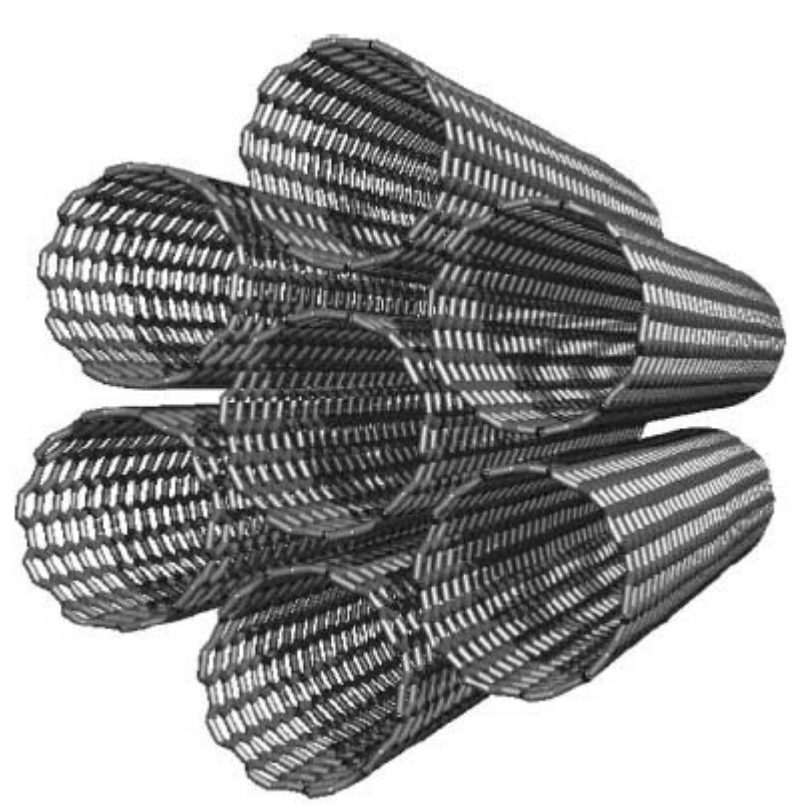

A bundle of (10,10) nanotubes held together with strong π-π-stacking interactions

Roll-up of (n,m) SWNTs

Chiral vector (n,m)

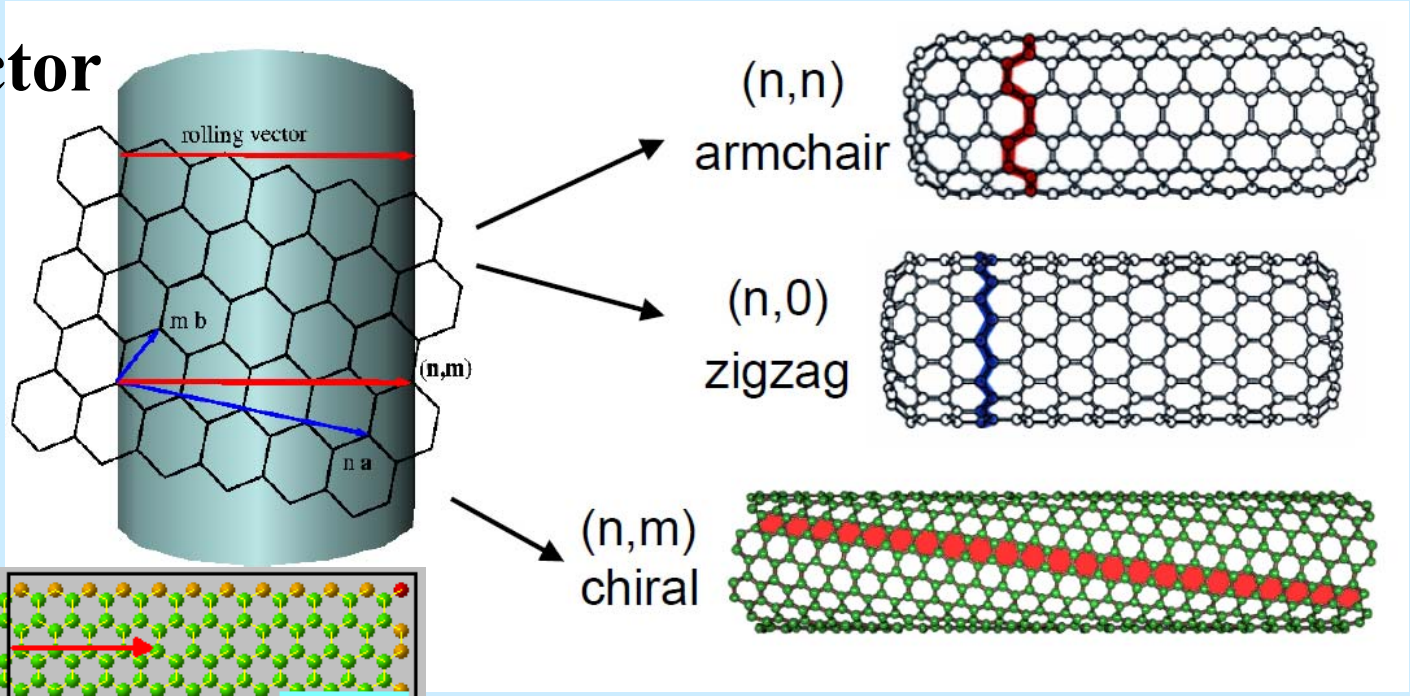

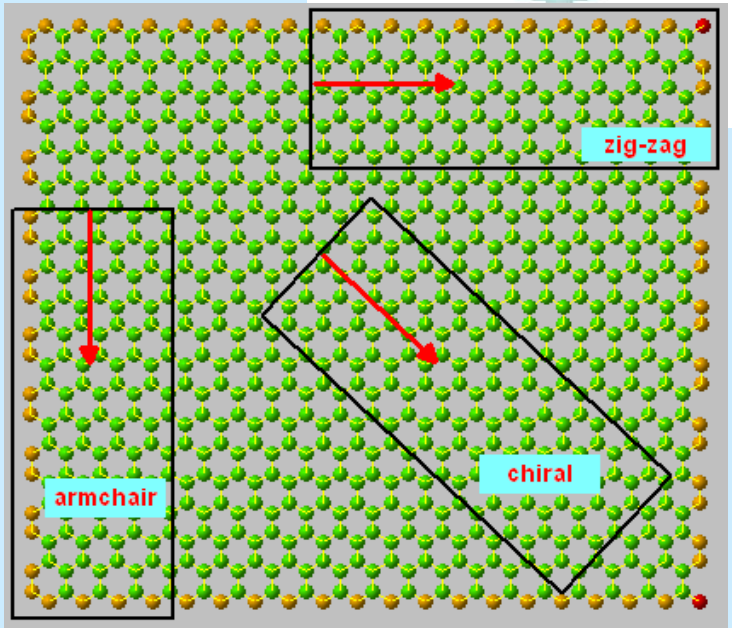

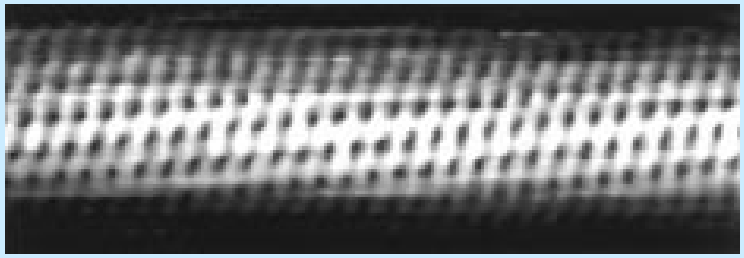

TEM of a chiral CNT

Roll-up of (n,m) SWNTs

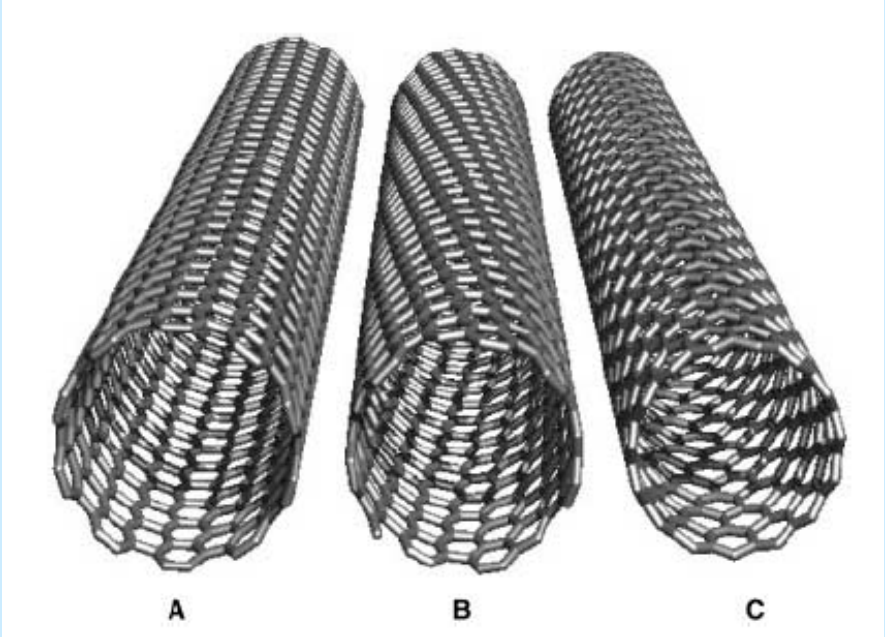

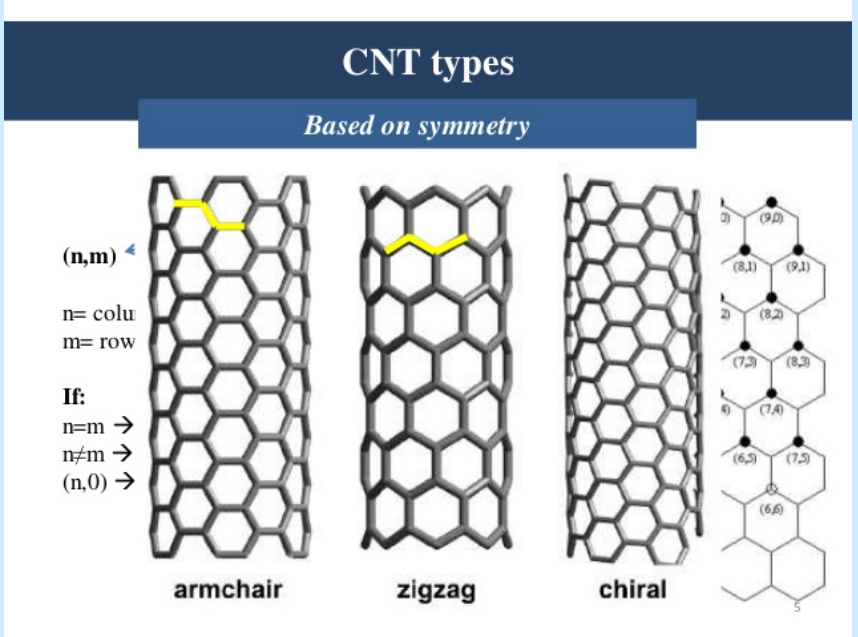

A) Armchair - an achiral metallic conducting (10,10) tube
B) Chiral - semiconducting (12,7) tube
C) Zigzag - an achiral conducting (15,0) tube

All the (n,n) armchair tubes are metallic
Chiral or zigzag tubes are metallic only if (n-m)/3 is a whole number, otherwise, they are semiconductors

Roll-up of (n,m) SWNTs

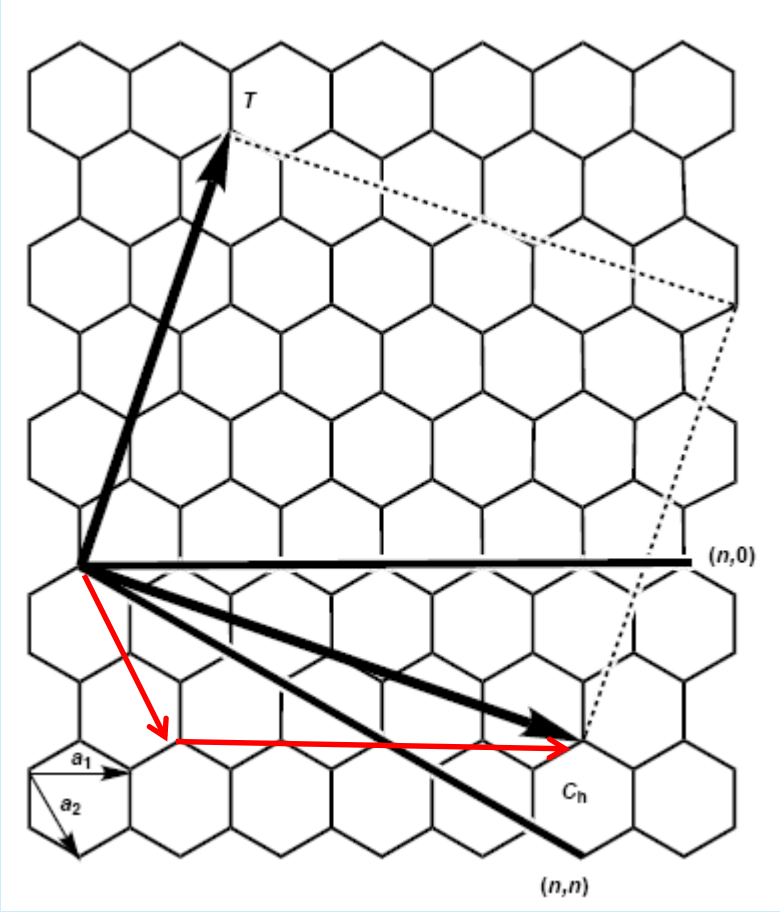

A 2D graphite layer
the lattice vectors a_1 and a_2

The roll-up vector $C_h = na_1 + ma_2$
Achiral tubes exhibit roll-up vectors derived from (n,0) (zigzag) or (n,n) (armchair).

The translation vector T is parallel to the tube axis and defines the 1D unit cell.

The rectangle represents an unrolled unit cell, defined by T and C_h

(n,m) = (4,2)

Roll-up of (n,m) SWNTs

Chiral vector:

$$C_h = na_1 + ma_2$$

(n,m) = (3,3)

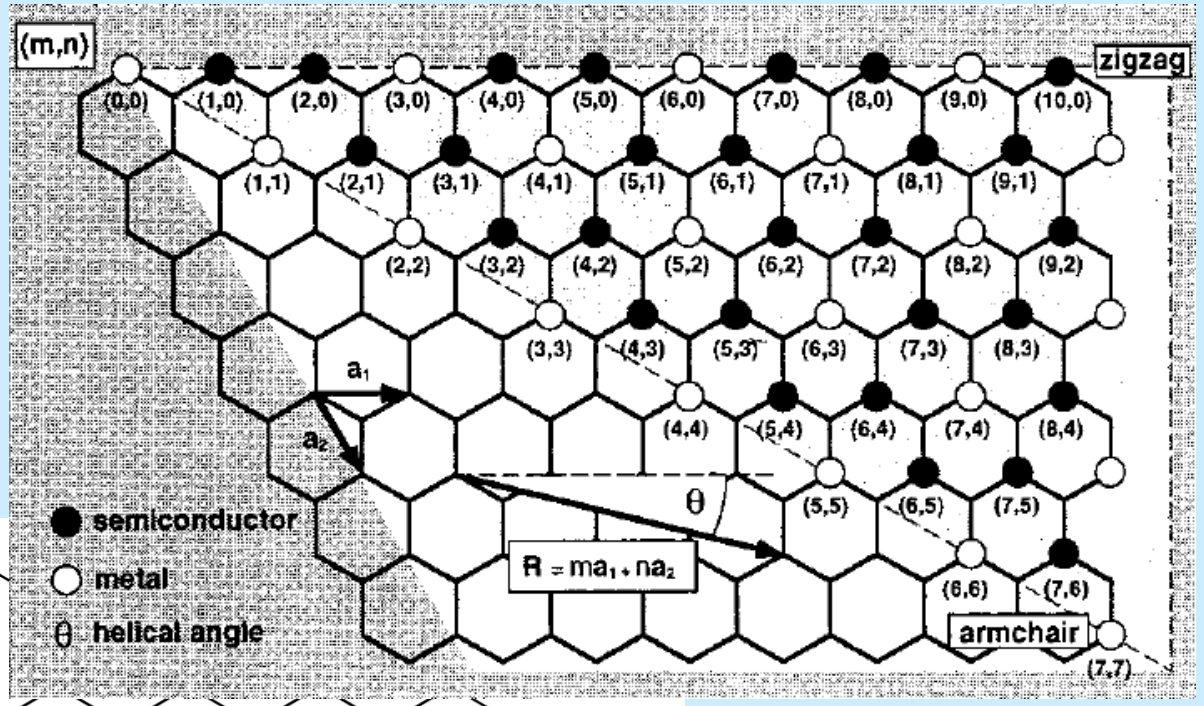

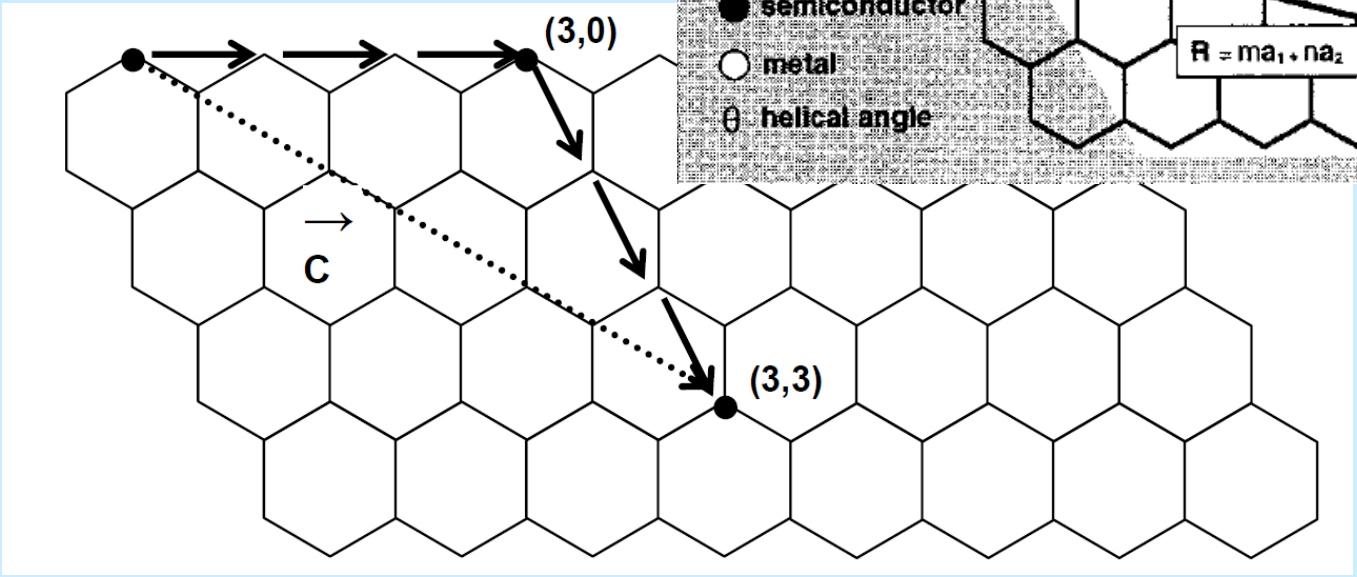

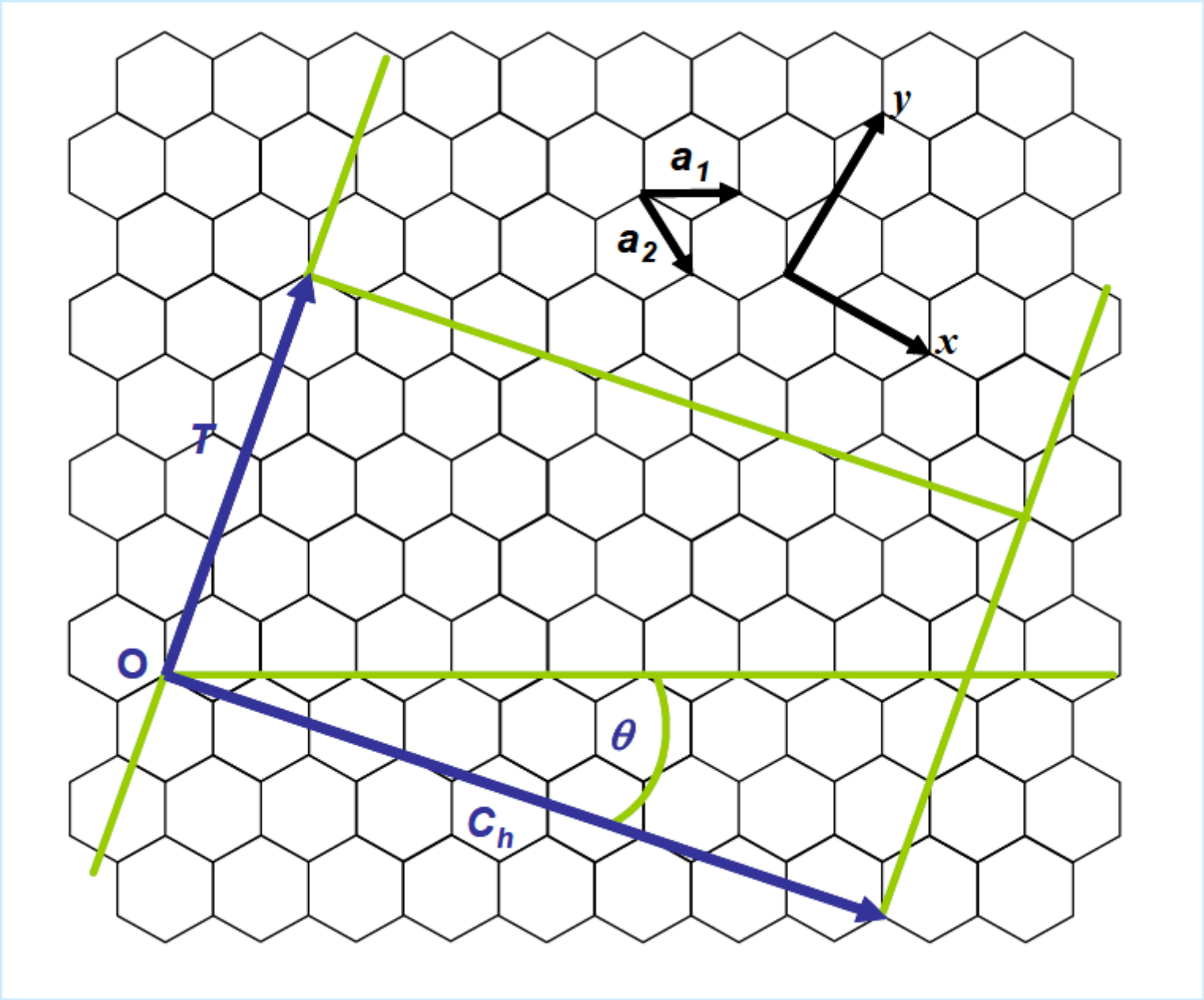
y
a_1
a_2
x
T
O
θ
C_h

Roll-up of (n,m) SWNTs

$$\vec{C_h} = n\vec{a_1} + m\vec{a_2} \equiv (n,m) \qquad (\text{ and } \; 0 \le |m| \le n \;)$$

Tube diameter

$$d_t = \frac{|C_h|}{\pi} = \frac{a_0\sqrt{\left(n^2 + nm + m^2\right)}}{\pi}$$

$$|a_1| = |a_2| = a_0 = 0.249 \text{ nm}$$

$$\theta = \tan^{-1}\left[\sqrt{3}m/\left(m + 2n\right)\right]$$

$\theta = 0 - 30°$

$a = 1.42\ \sqrt{3} = 2.49$ Å

$d(Csp^2\text{-}Csp^2) = 1.42$ Å

Defects in SWNTs

Atomic vacancies – reduction of tensile strength, electrical and thermal conductivity

Topological (Stone Wales) defect – rearrangement of bonds into pentagonic and heptagonic pair (connected, no other types of rings known)

Defects lead to phonon scattering – increased phonon relaxation rate – reduction of mean free path (reduction of ballistic conductivity) leads to reduced thermal conductivity

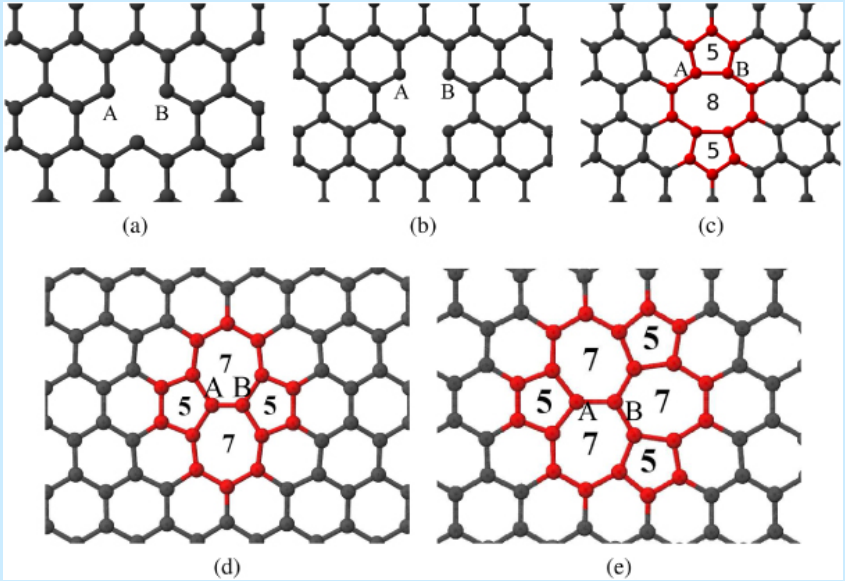

Defects in SWNTs

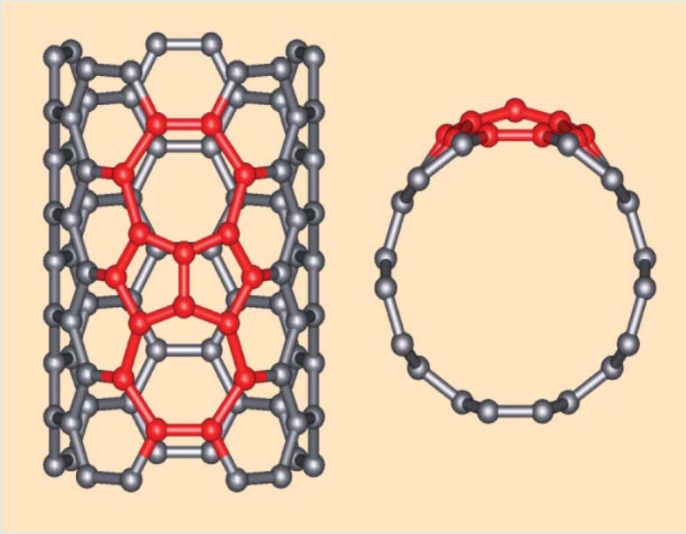

Stone-Wales defect (7-5-5-7 defect) ⇒ Larger curvature, esp. where the 5-membered rings are condensed ⇒ addition reactions at this C=C favored

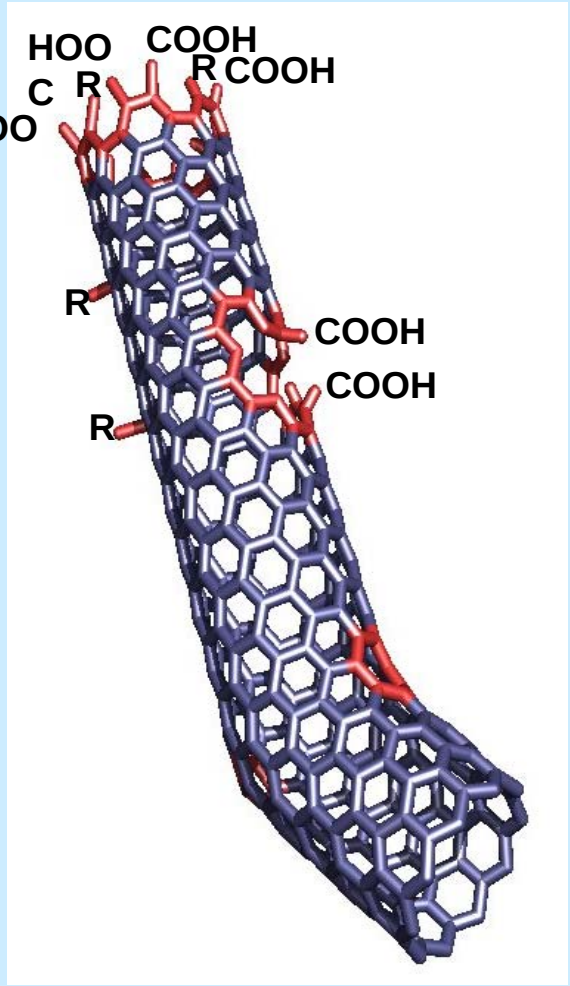

Separation of CNTs

Semiconducting CNTs
- Separation by surfactants, (octadecylamine), a strong affinity

Metallic CNTs
- Separation by diazonium reagents, biomolecules, DNA
- AC dielectrophoresis – 10 MHz, induced dipole, causes the two types of CNTs to migrate along the electric field gradient in opposite directions

Doping of CNTs

Intercalation CNTs
- Between walls of MWCNT – during synthesis or posttreatment

On-wall substitution CNTs
- N or B substitute for C
- In-situ – element-containing precursor
- Ex-situ – removal of C atom – graphite (n) or pyridine (n or p) type of group

Functionalization possibilities for SWNTs

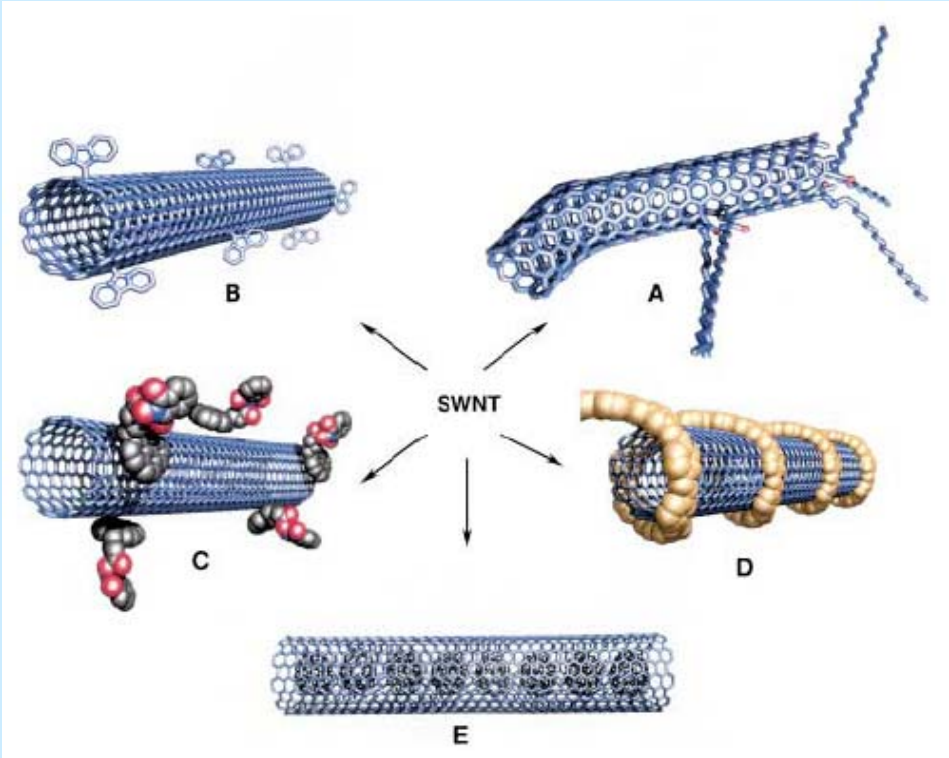

A) defect-group functionalization

B) covalent sidewall functionalization

C) noncovalent exohedral functionalization with surfactants – wrapping

D) noncovalent exohedral functionalization with polymers

E) Endohedral functionalization with C_{60} (C_{60}@CNT, "peapods)

Functionalization possibilities for SWNTs

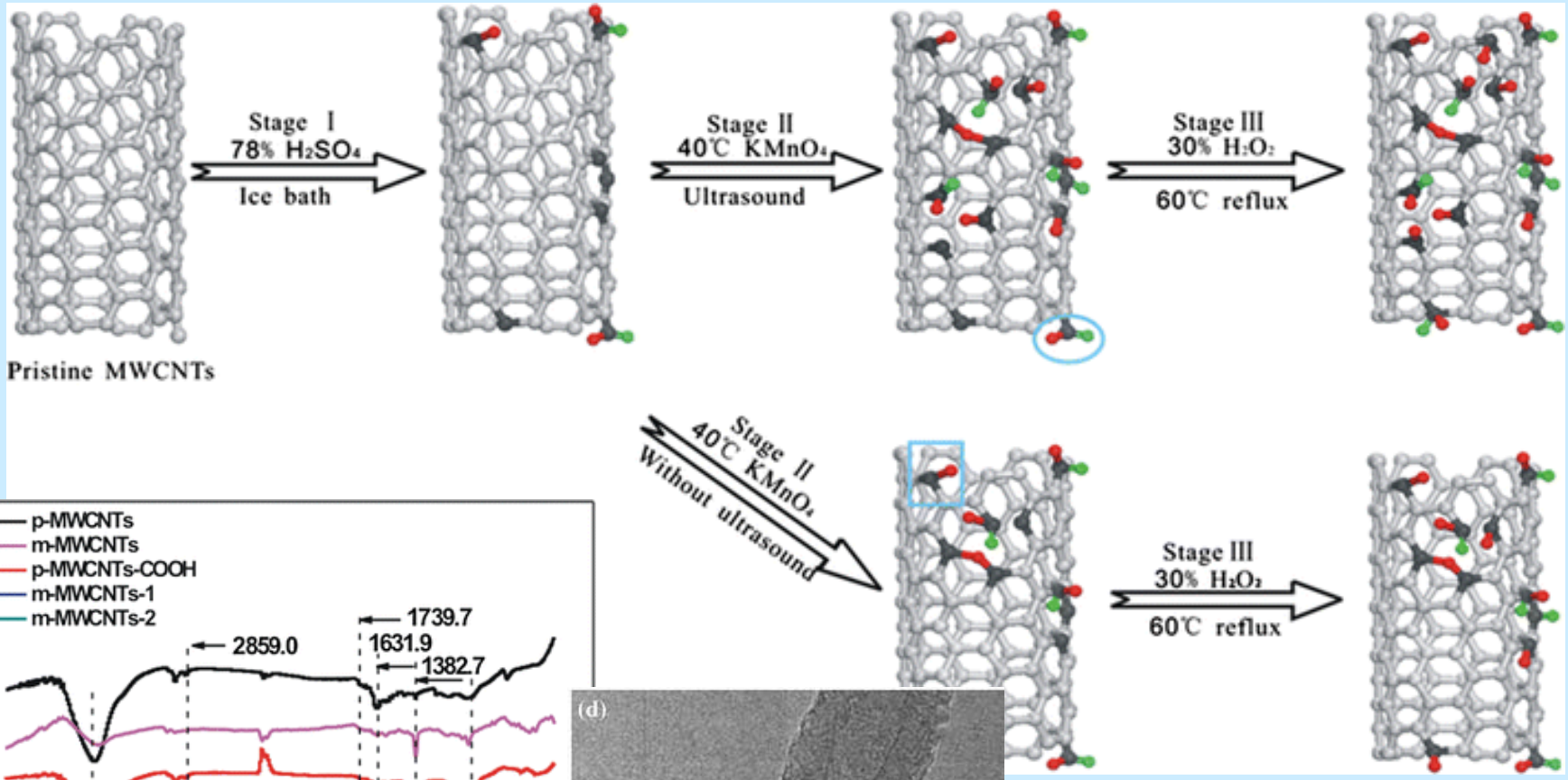

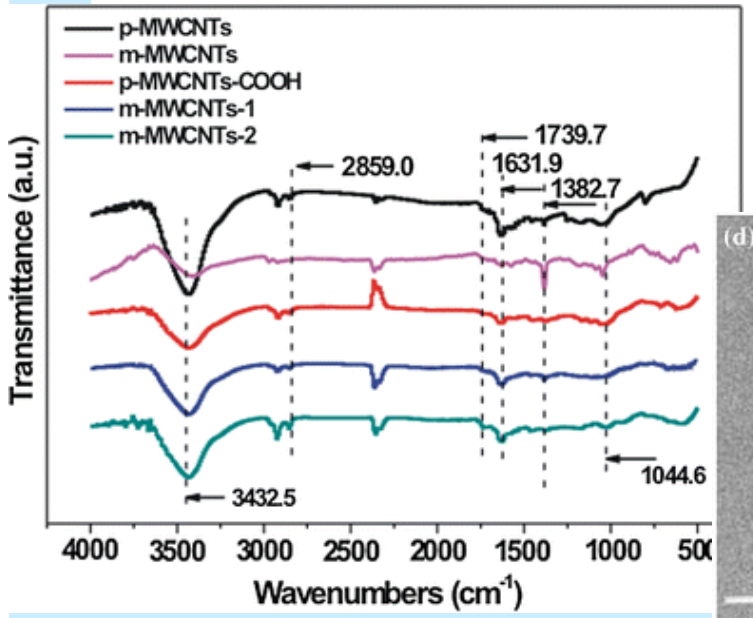

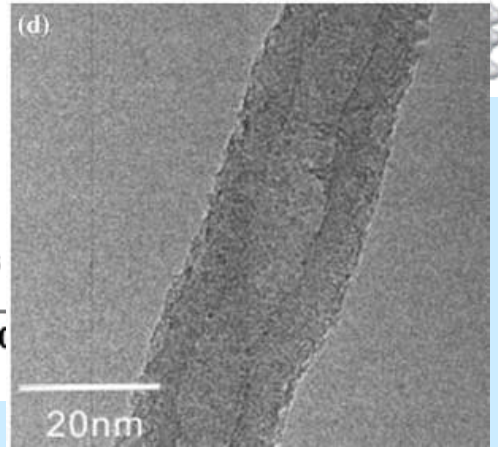

Functionalization possibilities for CNTs

reactions will occur first at the end caps, then on the surface, at structural defects

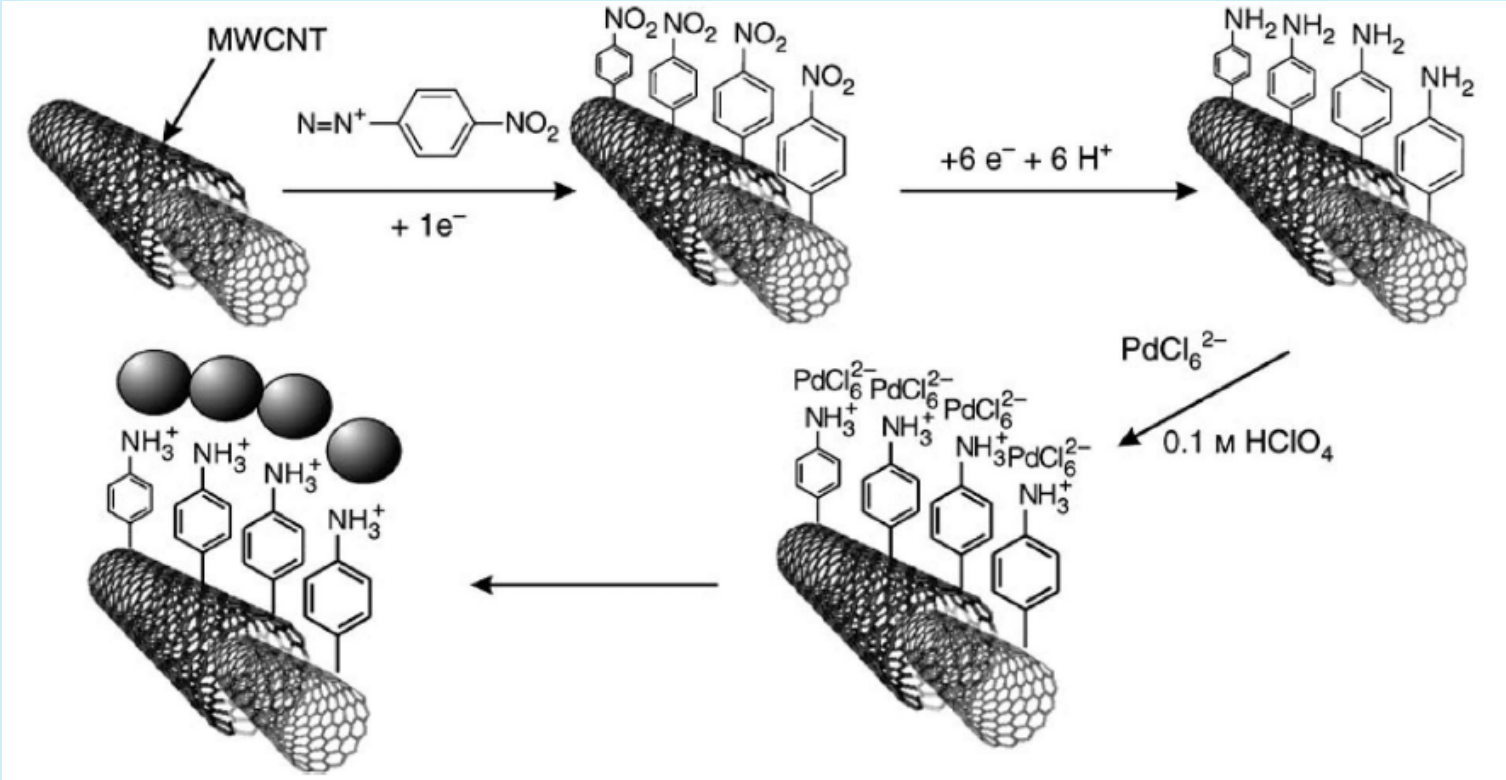

Functionalization possibilities for CNTs

TiO_2 and SiO_2 on acid-treated CNTs via ALD
SEM image for the case of SiO_2
TEM image of vertically grown CNT coated with RuO_2 both outside and inside.

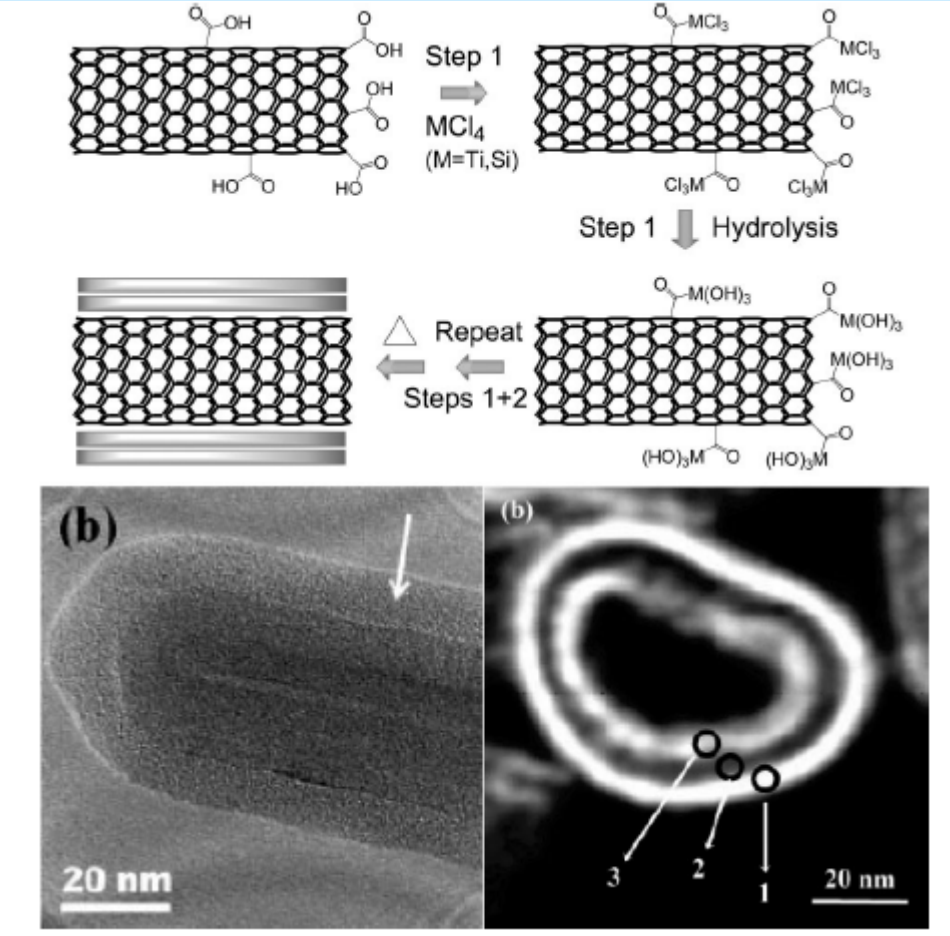

Interconnect

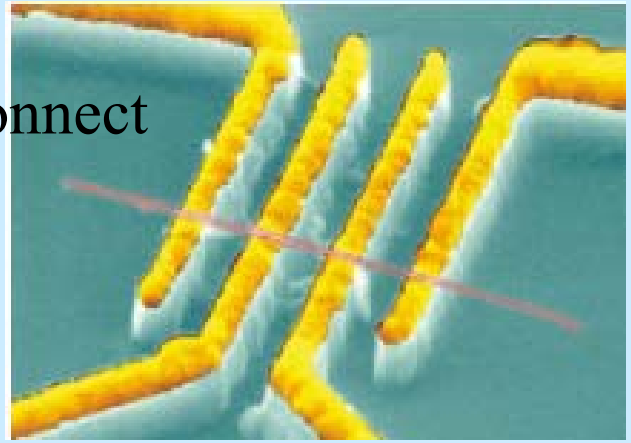

Nanomanipulator

Transistor

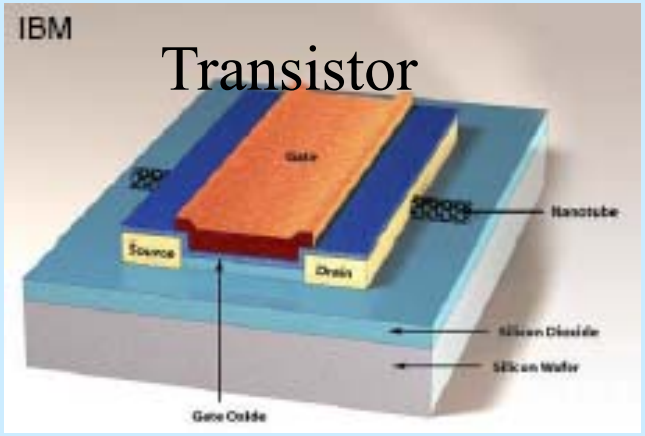

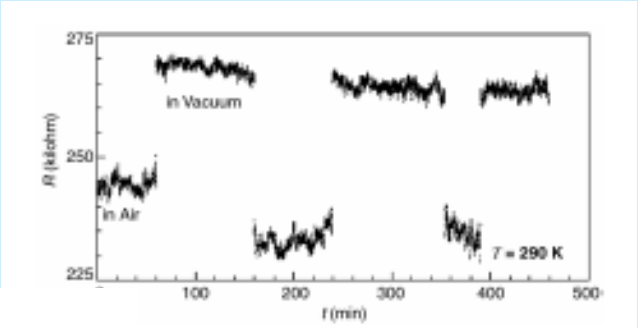

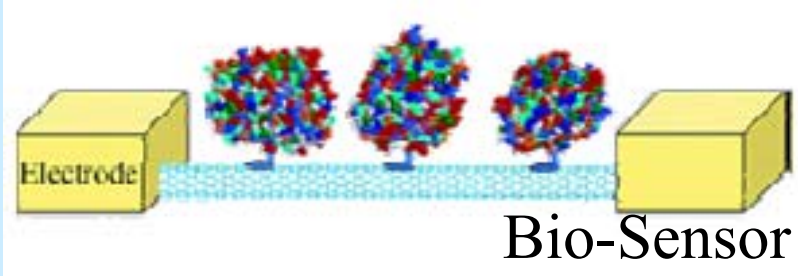

Bio-Sensor

Chemical Sensor

Assembly of CNTs

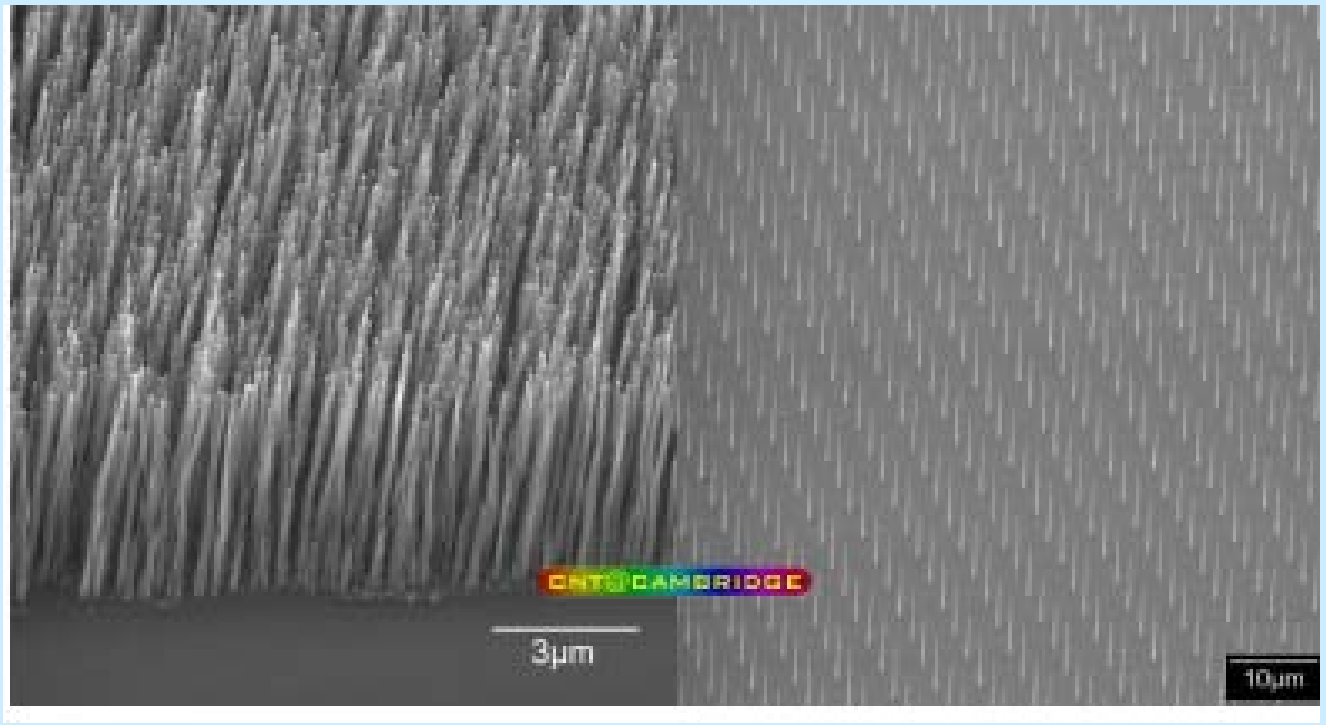

CNT applications:
Ultra-hard Composites
Nanopipettes
Field Emission Transistor
Nanomanipulator

CNT applications

CNTs as photosensitizers:

(a) electron injection into the conduction band of TiO_2

(b) electron back-transfer to CNTs with the formation of a hole in the valence band of TiO_2 and reduction of the hole by oxidation of adsorbed OH^- species

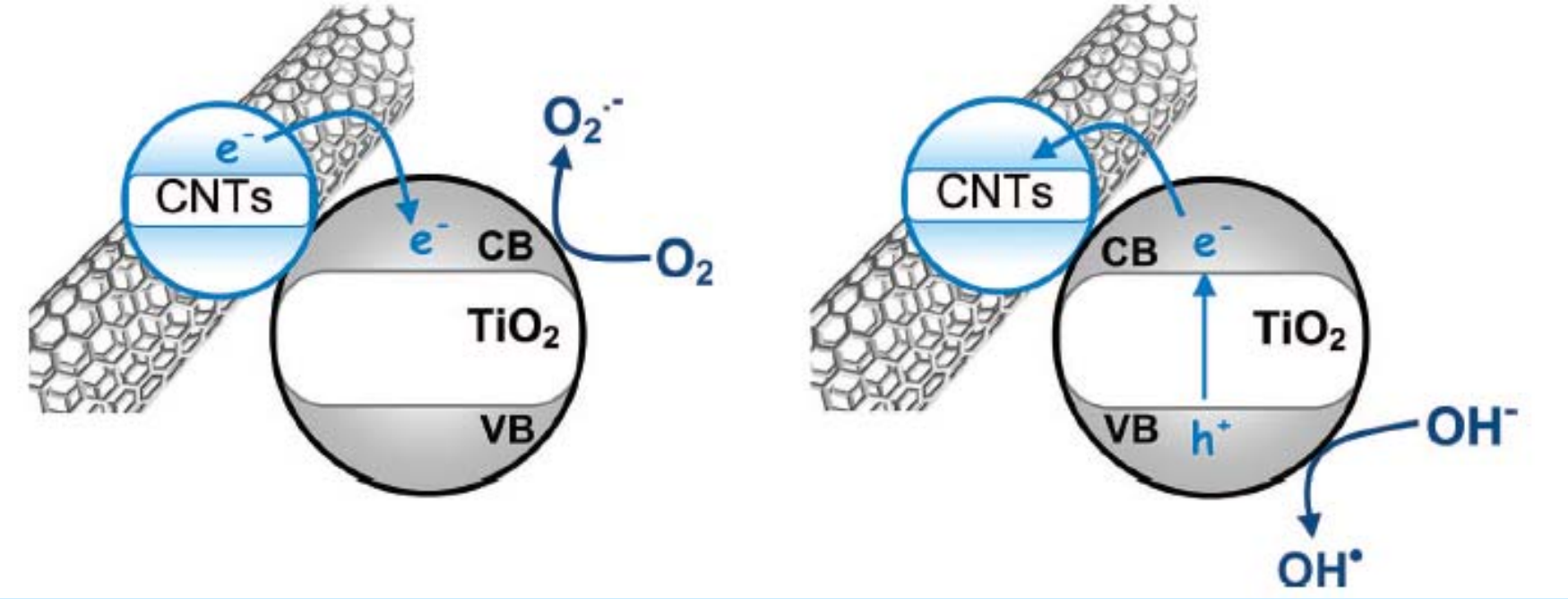

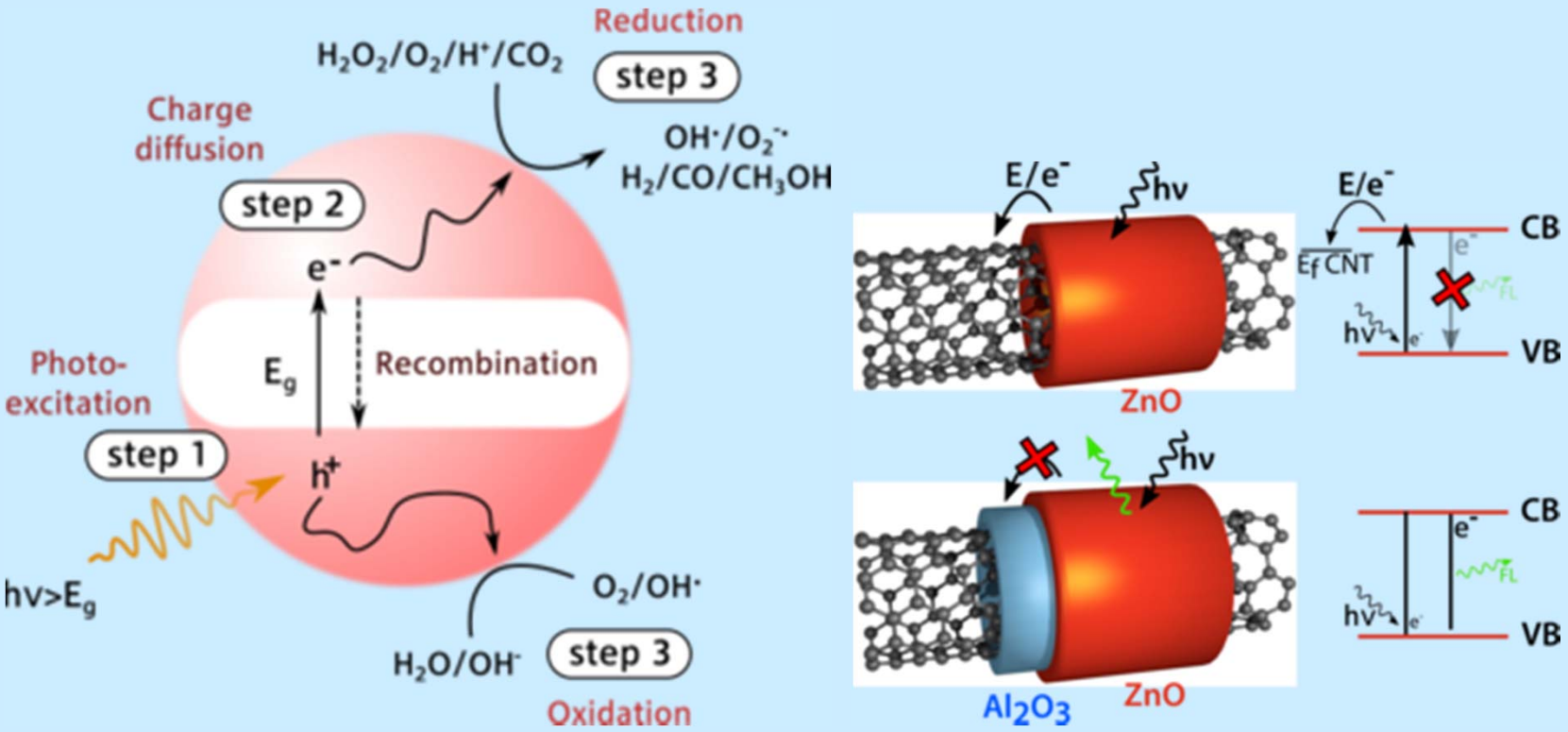
Reduction
$H_2O_2/O_2/H^+/CO_2$
step 3
$OH^·/O_2^{-·}$
$H_2/CO/CH_3OH$
Charge diffusion
step 2
e^-
E_g
Recombination
Photo-excitation
step 1
h^+
$hv>E_g$
$O_2/OH^·$
H_2O/OH^-
step 3
Oxidation
E/e⁻
hv
ZnO
E/e⁻
Ef CNT
CB
VB
hv
e⁻
FL
Al_2O_3
ZnO
hv
CB
VB
hv
e⁻
FL

Metallic CNTs

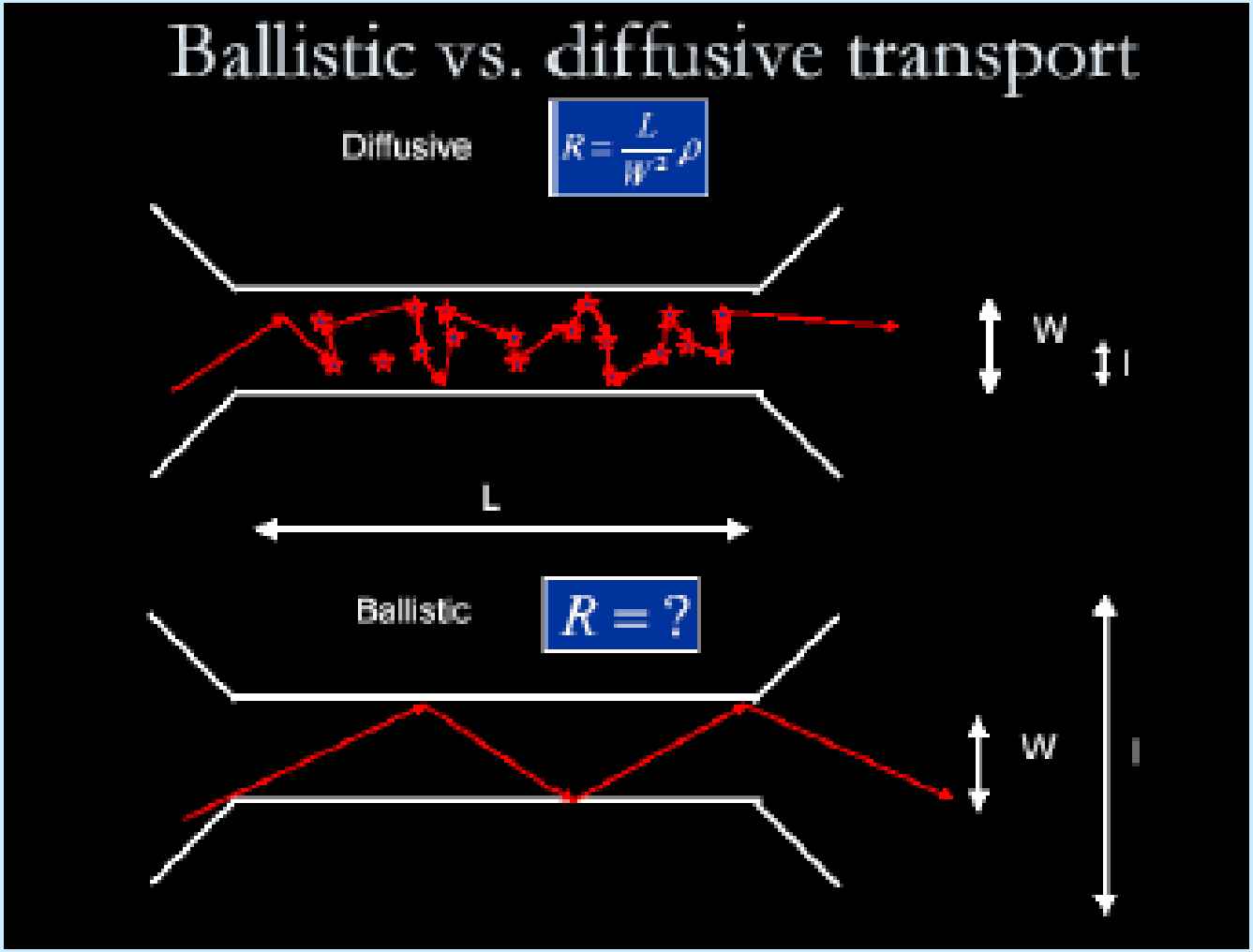

Carbon Nanotubes

Difficult to obtain in pure form (SWNT, MWNT, C_x, soot etc.)

As-synthesized CNTs are a mixture of conducting, semiconducting and insulating ones

Not stable under oxidizing conditions

Little manufacturing control over tube diameter

Nanowires

Good transport properties – Single crystalline nature

Mechanically robust – Defect free

Flexibility in composition

Doping possible to create p- and n-type nanowires

Nanowires-based FETs and basic logic circuits demonstrated in the laboratory

Techniques for mass manufacture

Transport in Nanowires

Conductance Quantization:

The Landauer equation

$G = (2e^2/h)N$, N = no. of conduction channels

When NW diameter is smaller than the Fermi wavelength, conductance changes in steps of $2e^2/h$

Synthetic Routes to Nanowires

Epitaxial growth

Catalytic VLS growth

Catalytic base growth

Defect nucleation

Templated growth

Arrested growth

Assembly of nanoparticles

Epitaxial growth

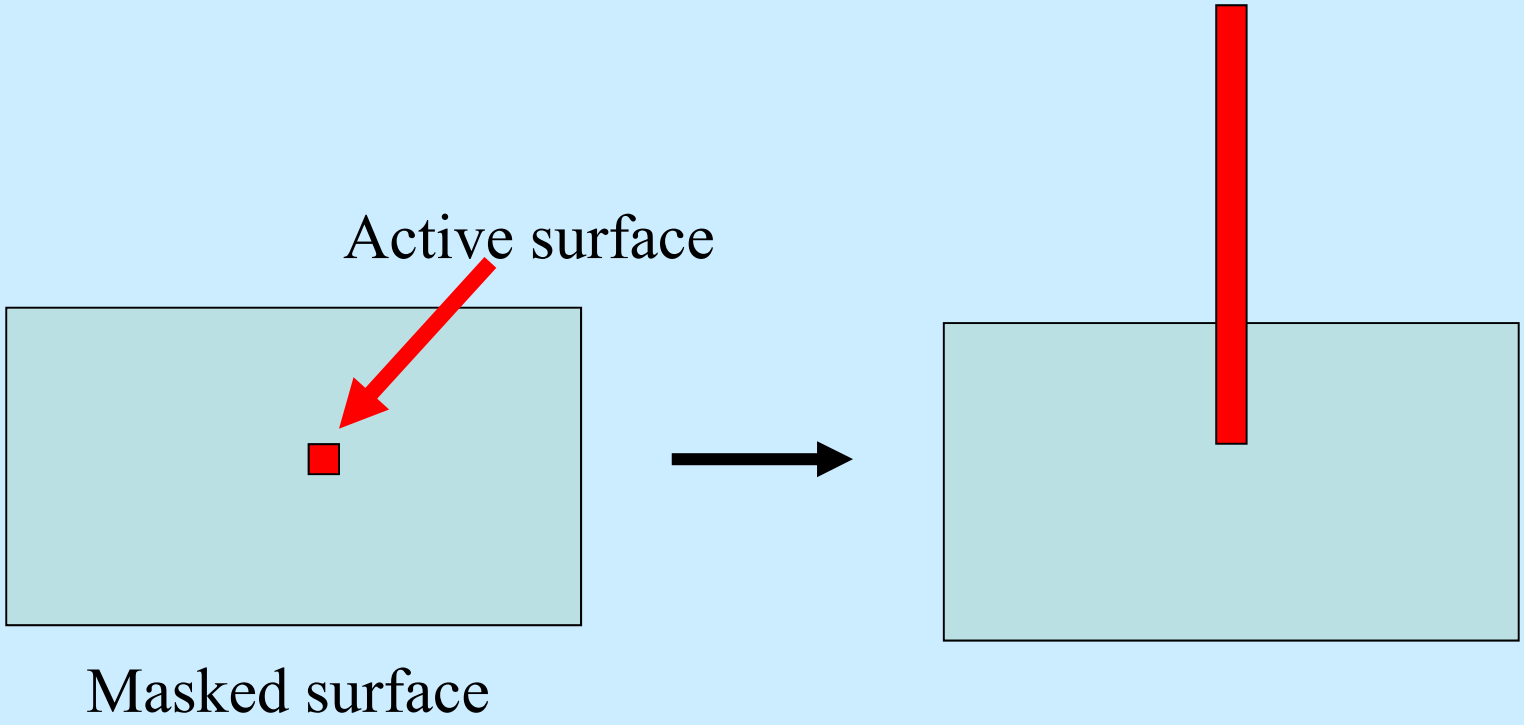

Vapor-Liquid-Solid (VLS) Growth

(1) Metal catalyst nanoparticles - Au(s)

Feed another element (Ge vapor, GeH_4 or SiH_4) at an elevated temperature (440-800 °C/ultra-high-vacuum)

Gaseous precursor feedstock is absorbed/dissolved in Au(s) till the solid solubility limit is reached (2)

A liquid phase appears, melts to a droplet (3)
The droplet becomes supersaturated with Ge

When the solubility limit is reached (4), an excess material is precipitated out to form solid NWs beneath the droplet

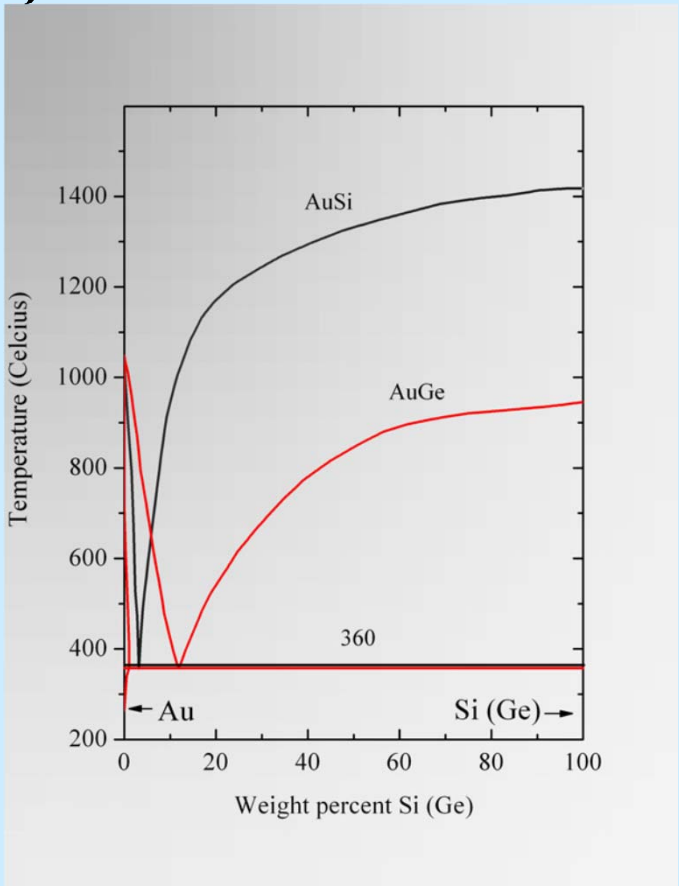

Eutectic 360 °C
Au (mp 1064 °C)
Si (mp 1410 °C)
Ge (mp 938 °C)

Vapor-Liquid-Solid (VLS) Growth

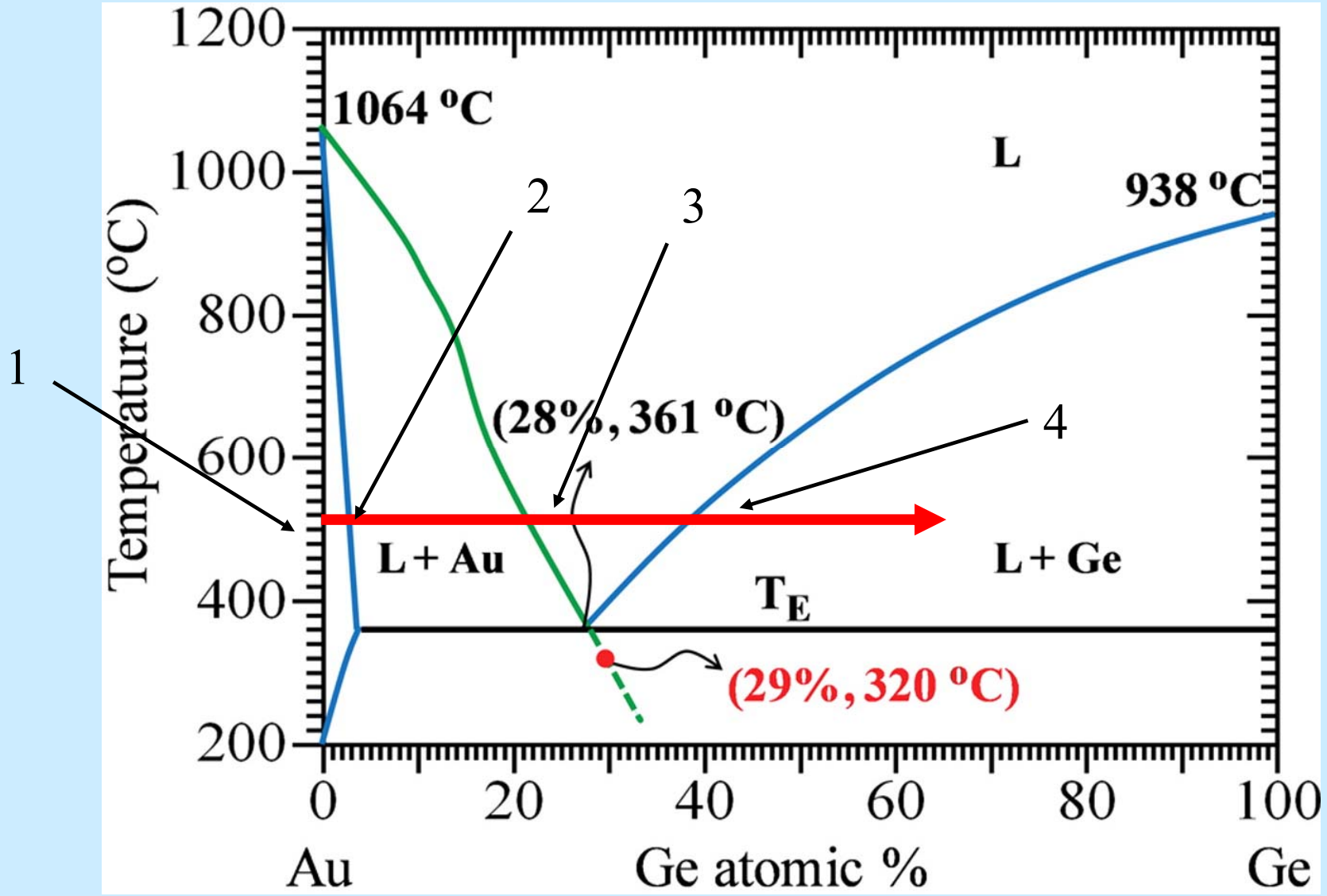

Vapor-Liquid-Solid (VLS) Growth

Au/Ge Eutectic Liquid Alloy

Au Particles

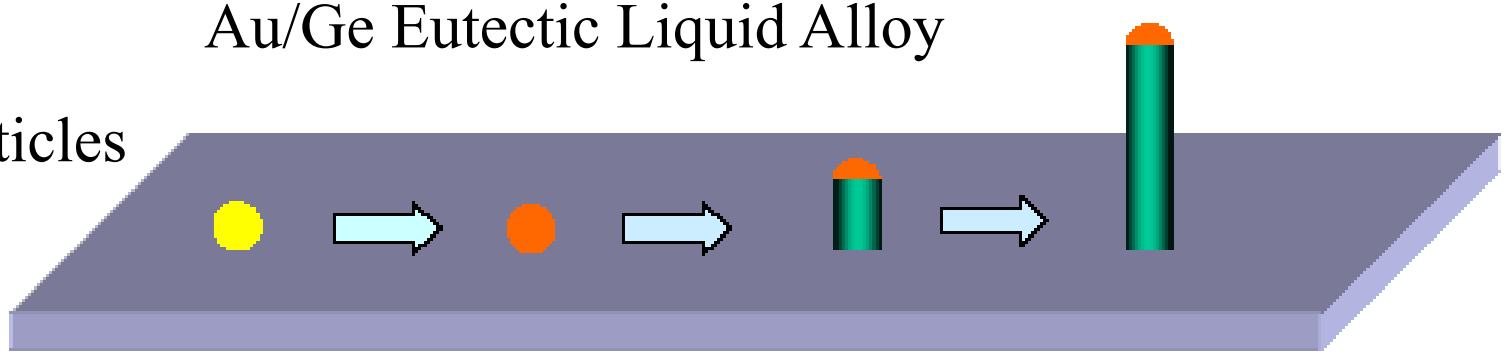

Nucleation of NWs

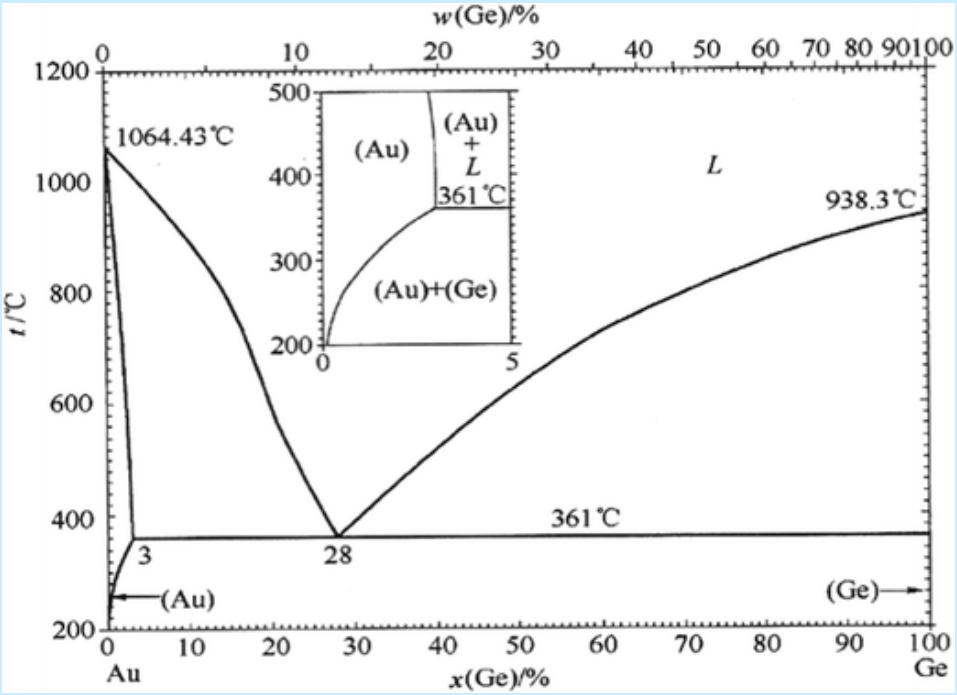

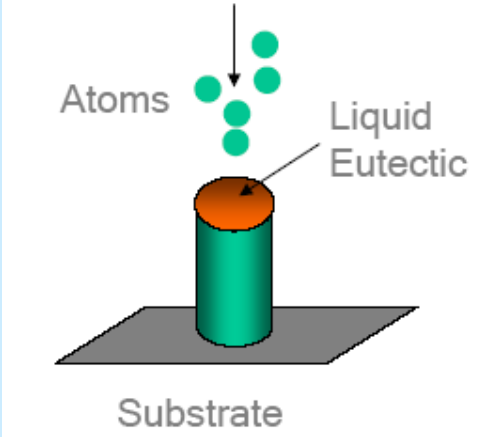

NW Growth

In-situ TEM images of the VLS process

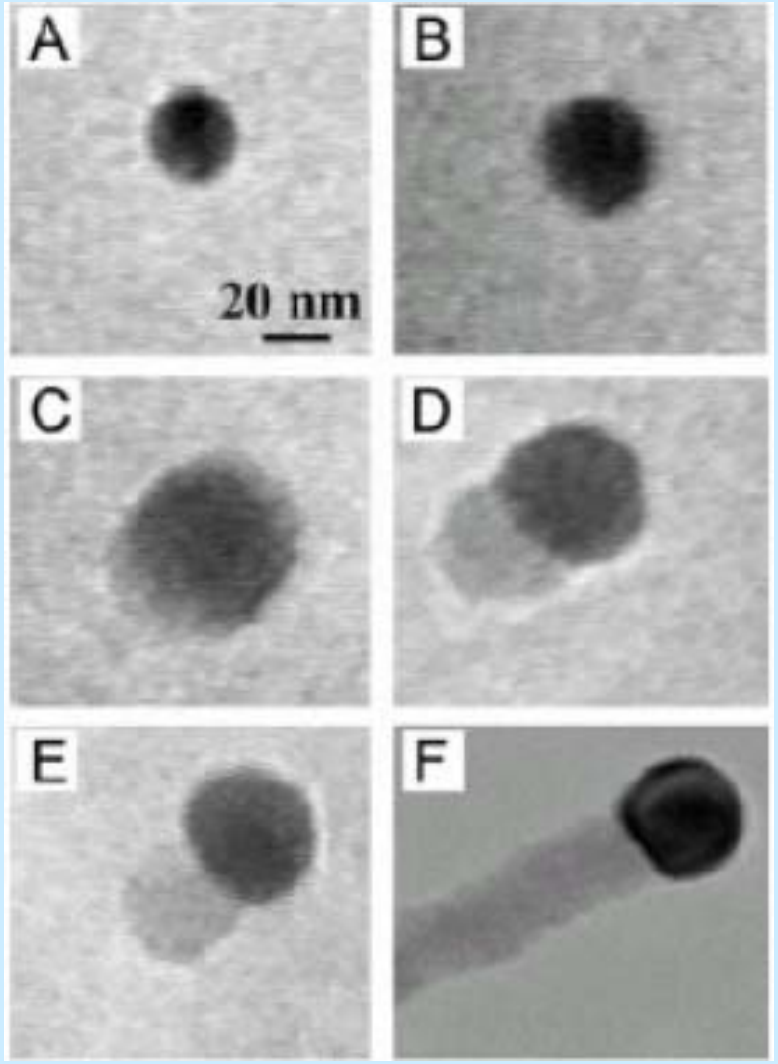

In-situ TEM images recorded during the process of nanowire growth:
(a) Au nanoclusters in solid state at 500 °C
(b) alloying initiated at 800 °C, at this stage Au exists mostly in solid state
(c) liquid Au/Ge alloy
(d) the nucleation of Ge nanocrystal on the alloy surface
(e) Ge nanocrystal elongates with further Ge condensation
(f) Ge forms a wire

Ge NWs on the bare Ge(110) substrate

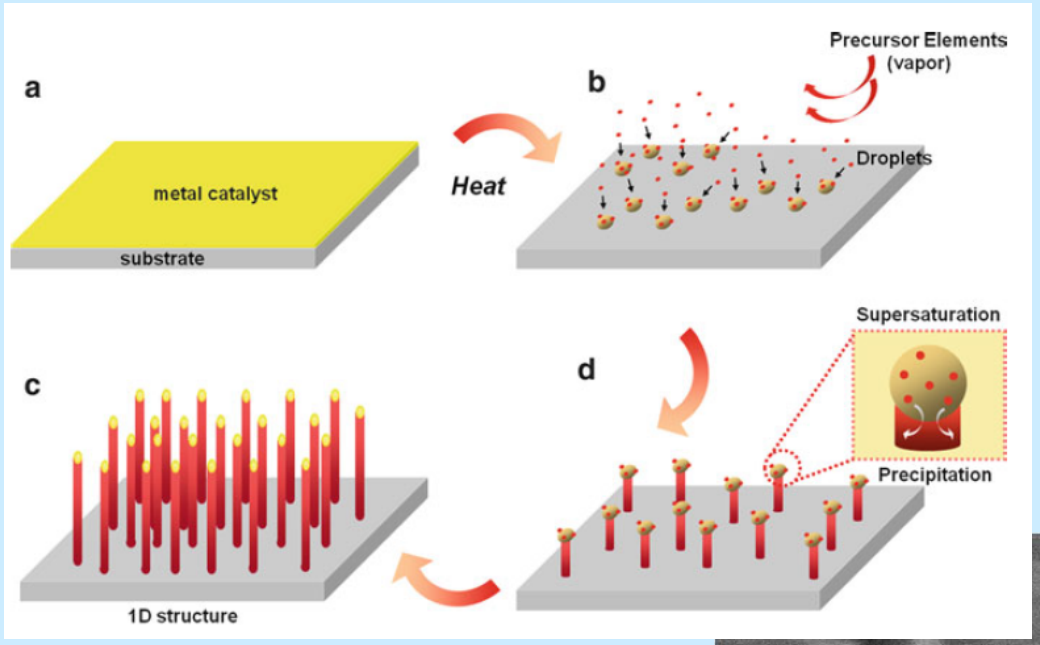

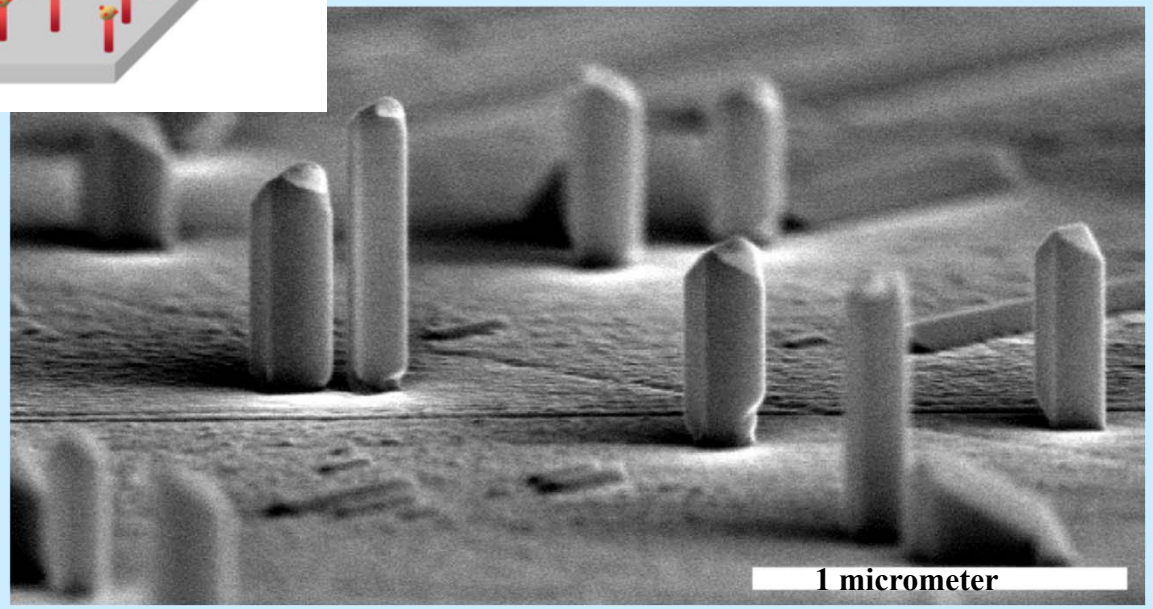

Si Nanowire Growth

$$SiH_4 \rightarrow Si + 2H_2$$

Mass transport in the gas phase

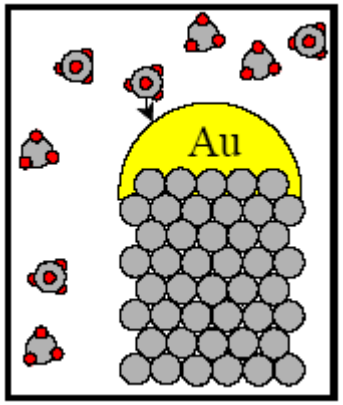

Diffusion in molten catalyst

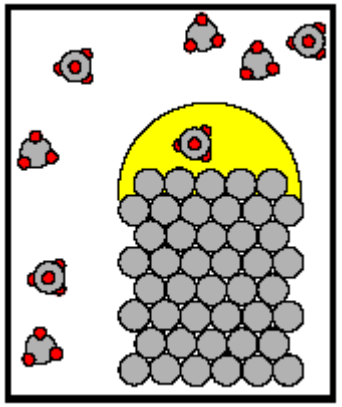

Chemical reaction at the V-L interface

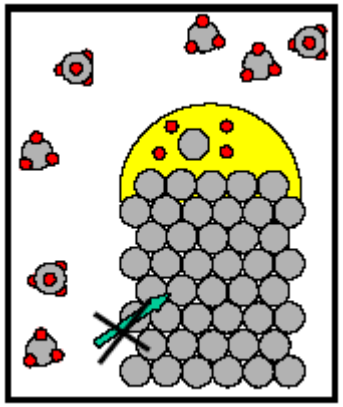

Incorporation of material in the crystal lattice

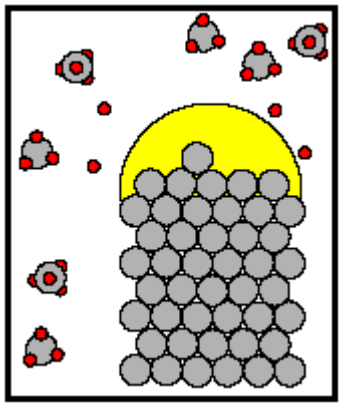

Si Nanowires

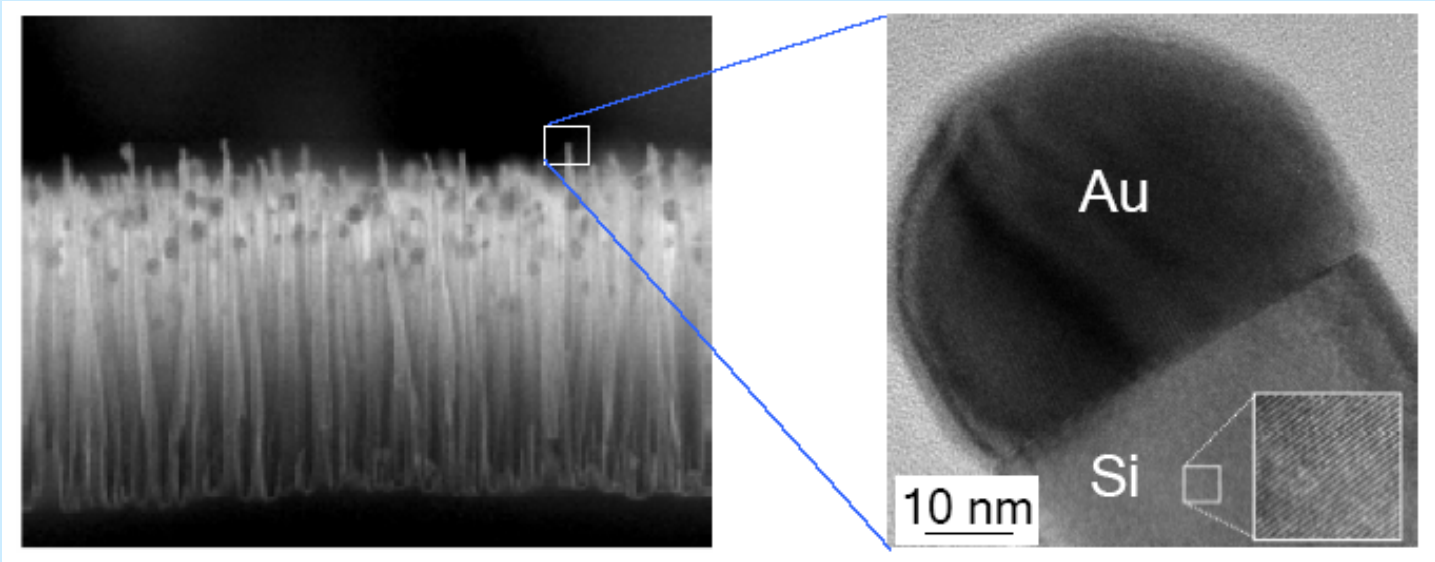

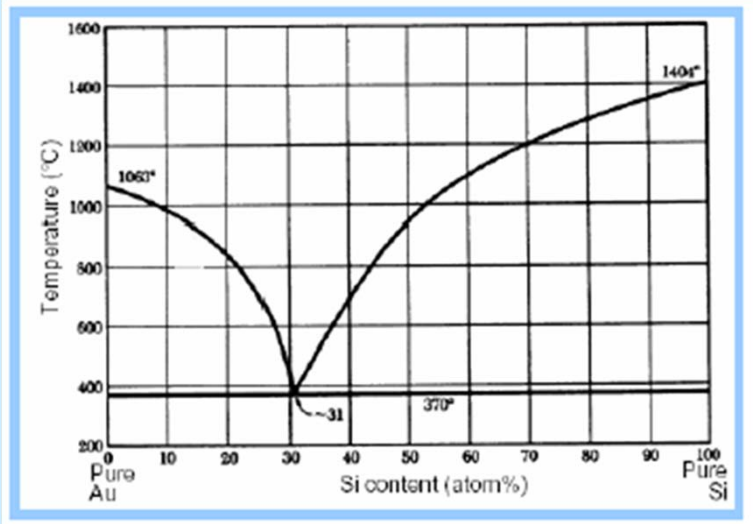

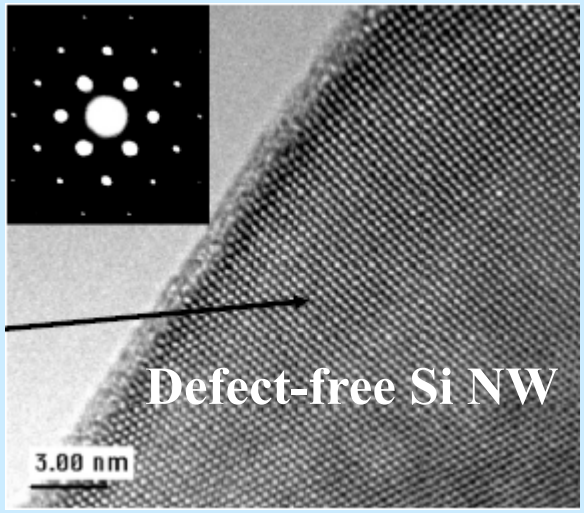

Size Control

Metal particle acts as a soft template to control the diameter of the nanowire

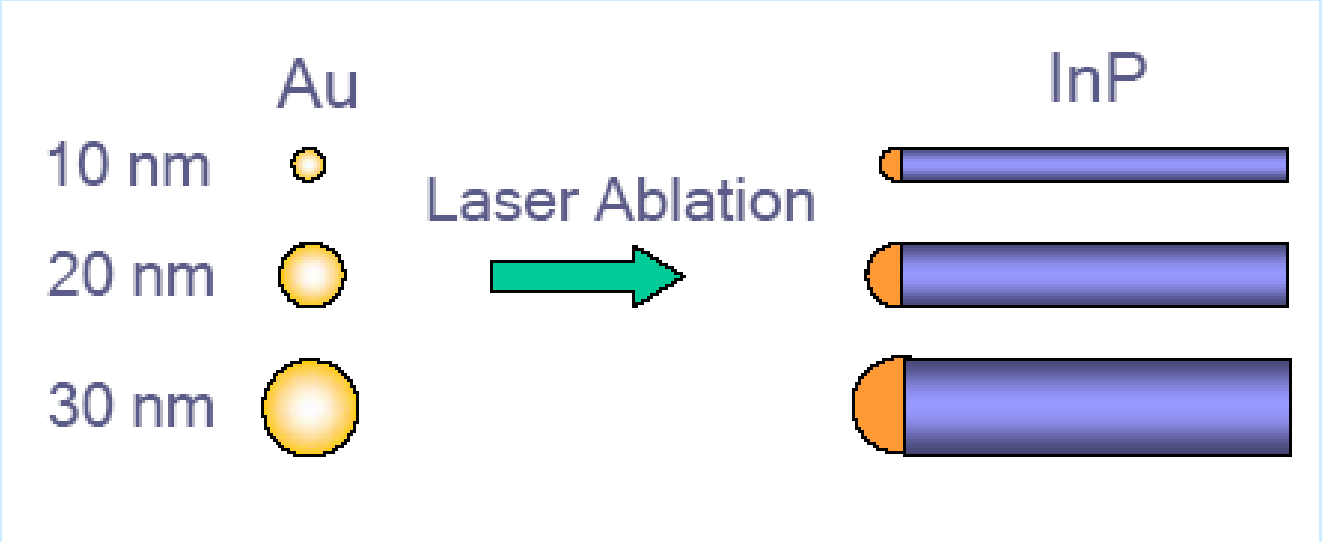

Catalytic base growth

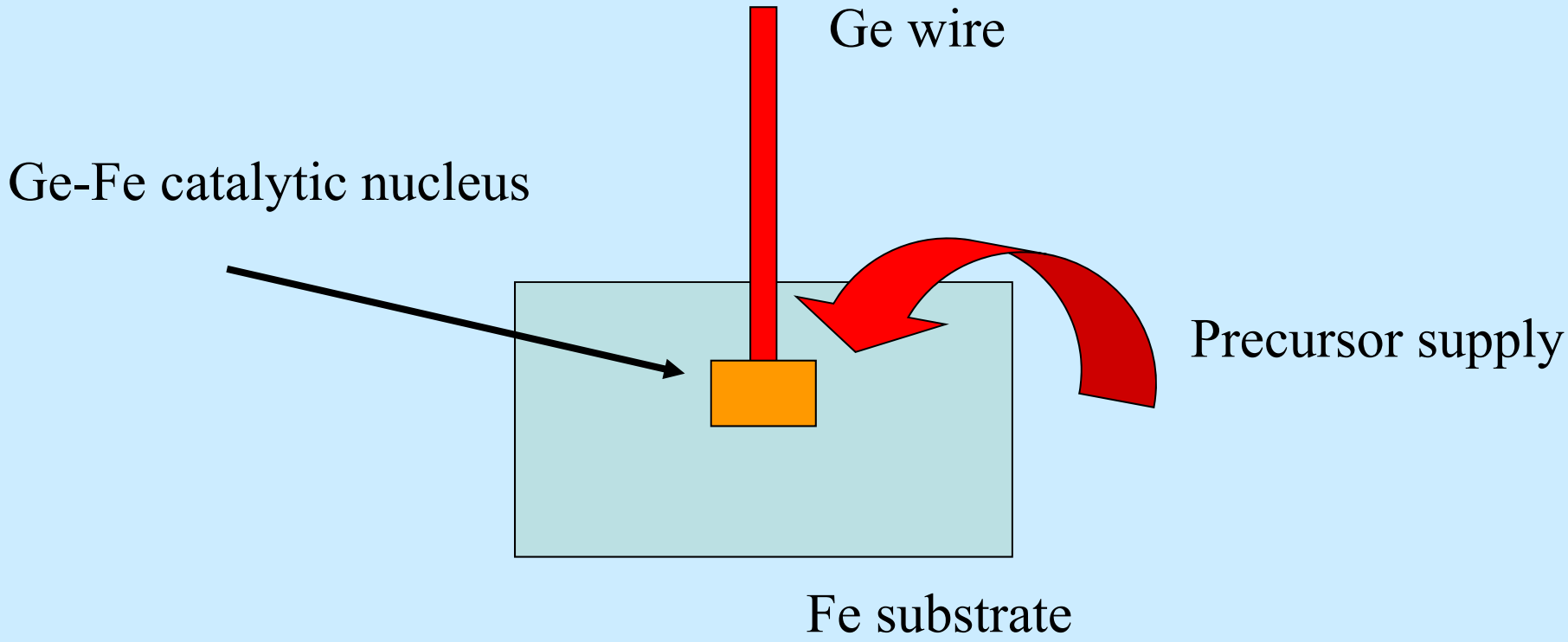

Templated growth

1. Pores filled with material by CVD

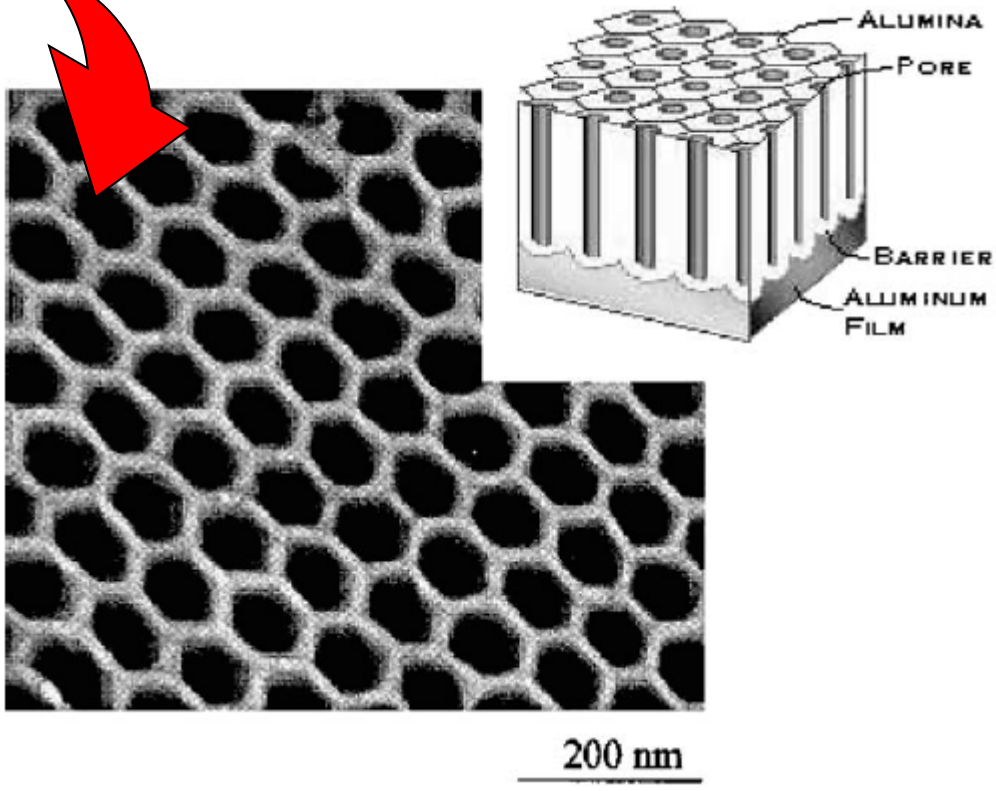

2. Alumina matrix dissolved
3. Wires separated

Arrested growth

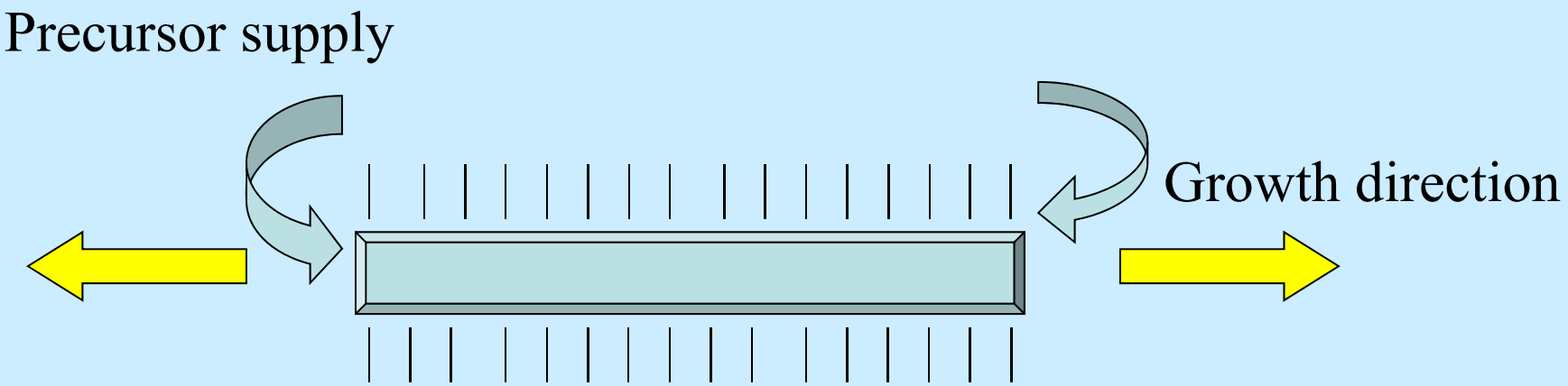

Selective binding of a compound to certain crystal faces

CdTe, TOPO blocks (111)

Alivistos

SLS-growth mechanism

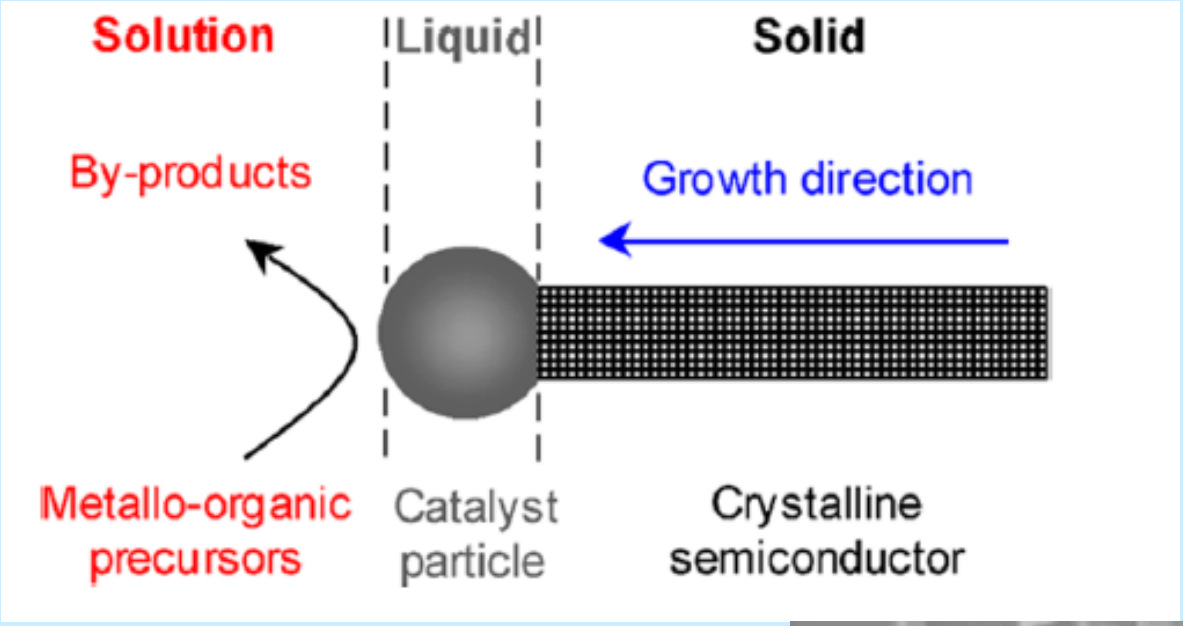

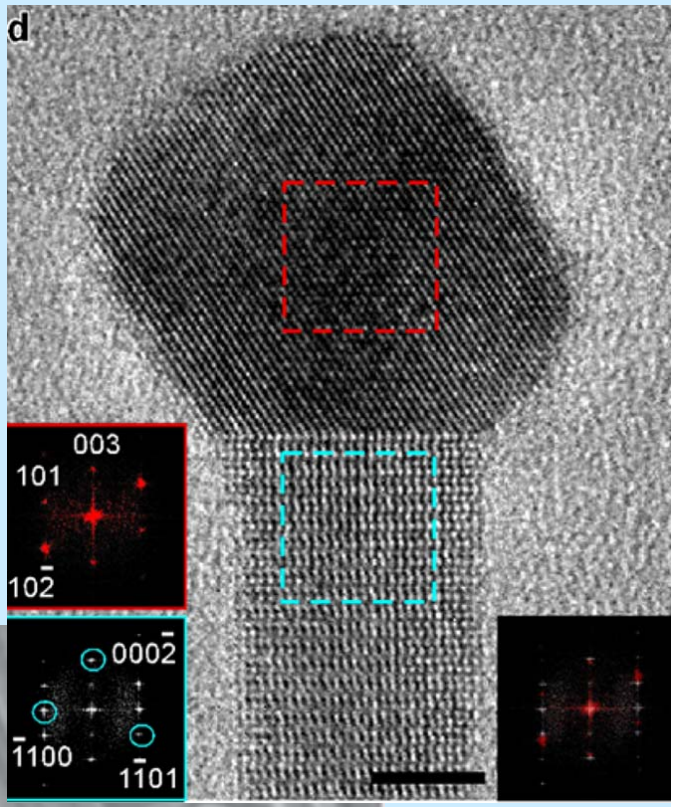

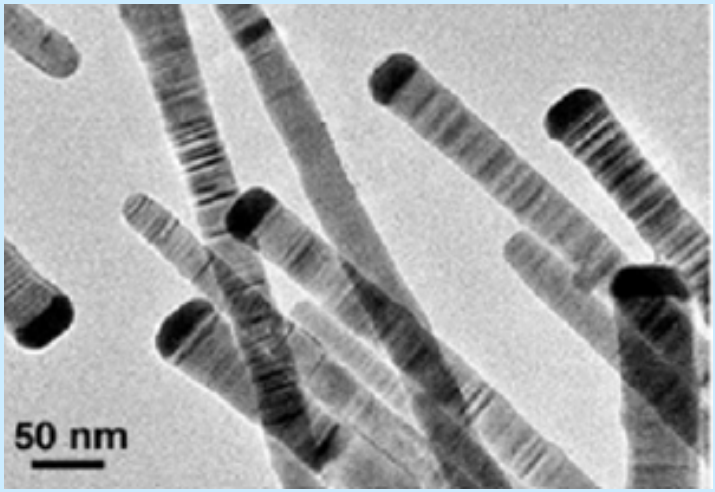

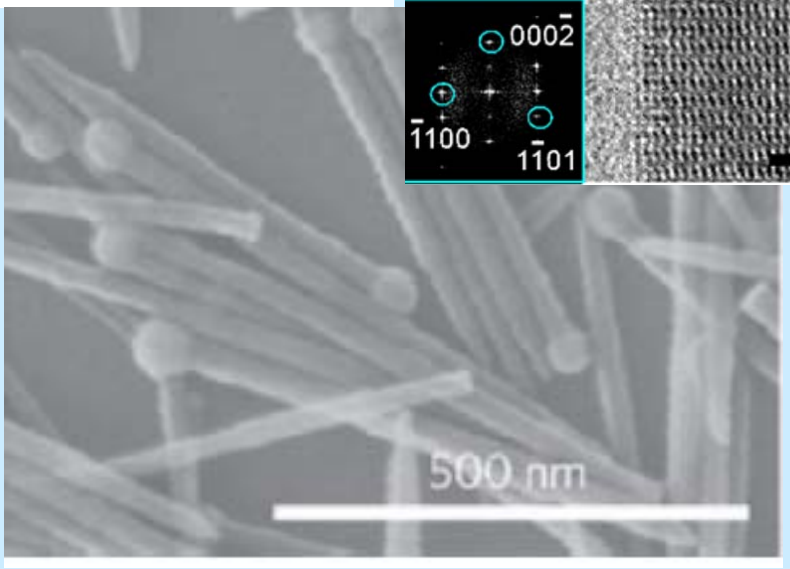

Inorganic NanoTubes INT - MoS_2, WS_2

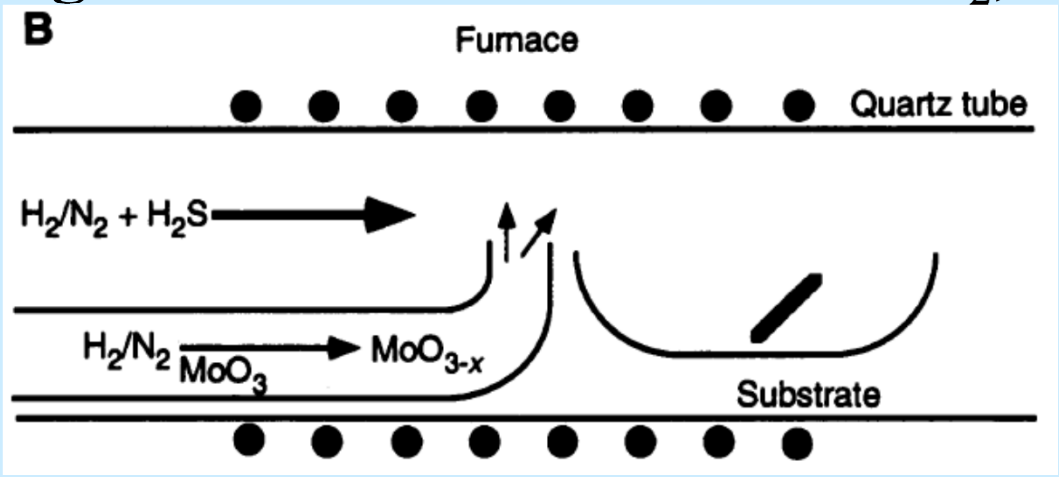

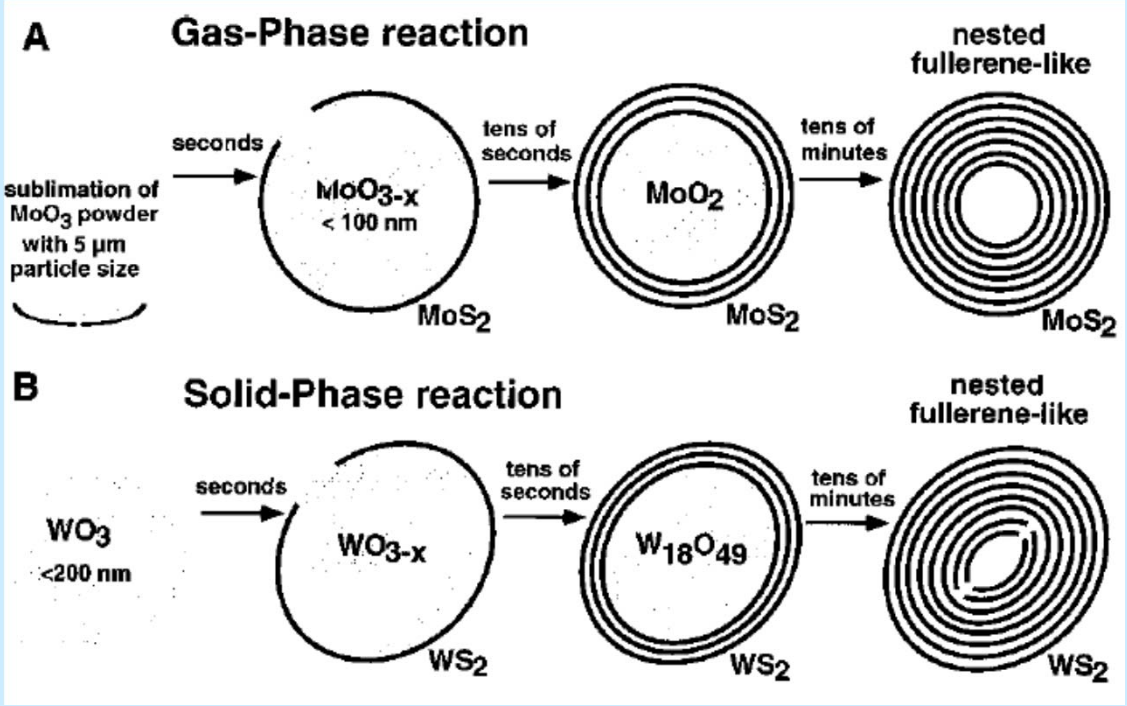

Inorganic NanoTubes INT

$$WO_3 + 2\,H_2S + H_2 \rightarrow 3\,H_2O + WS_2$$

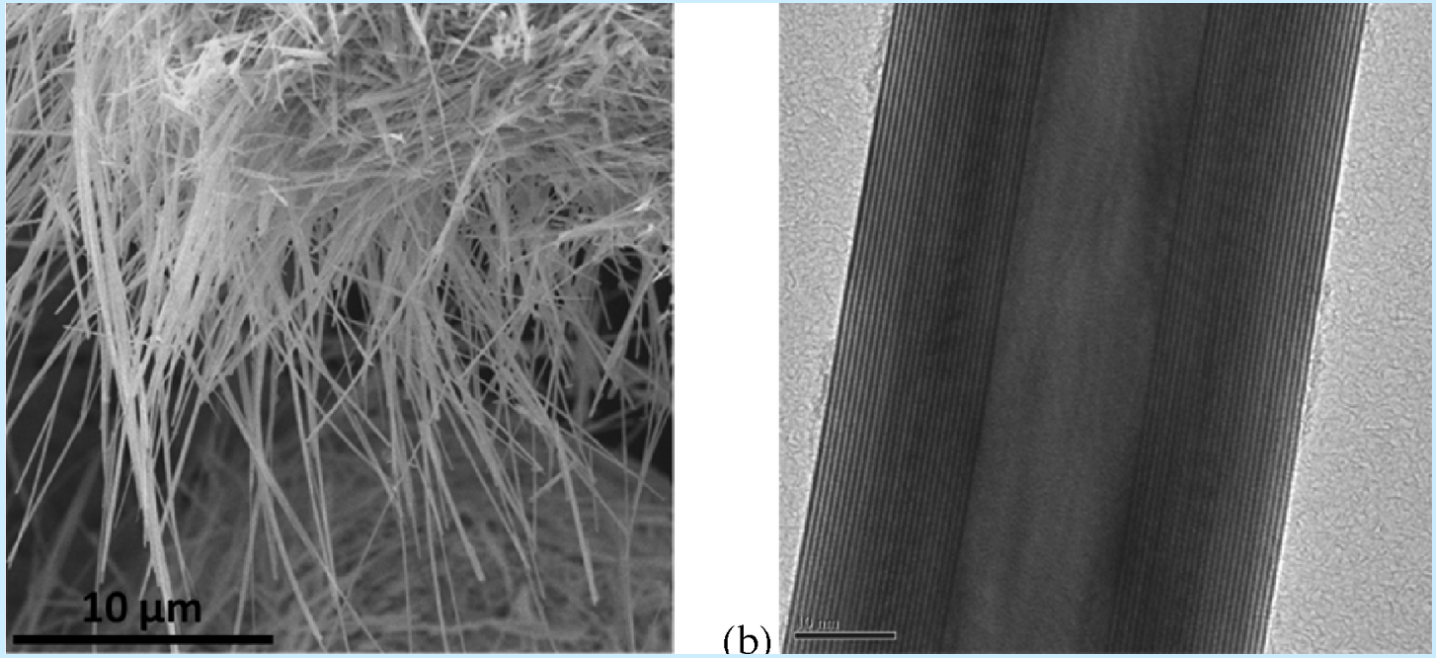

Defect free INT-WS_2; (a) SEM image. (b) TEM image (scale bar 10 nm).

Molecular rods

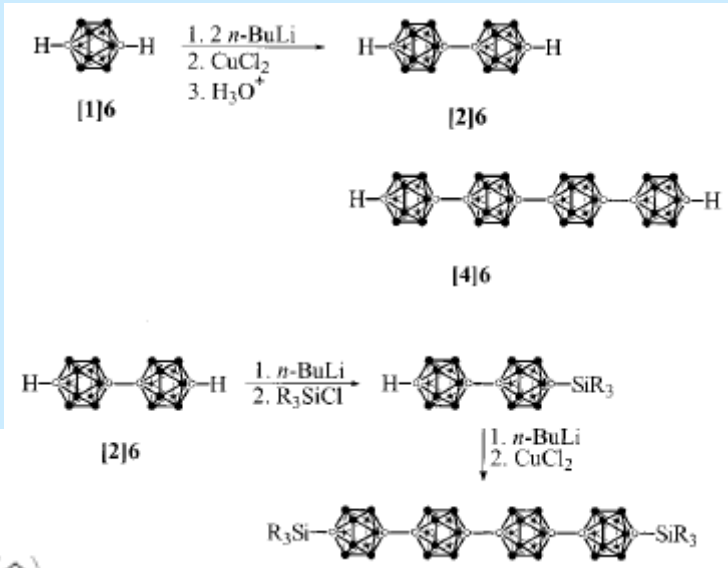

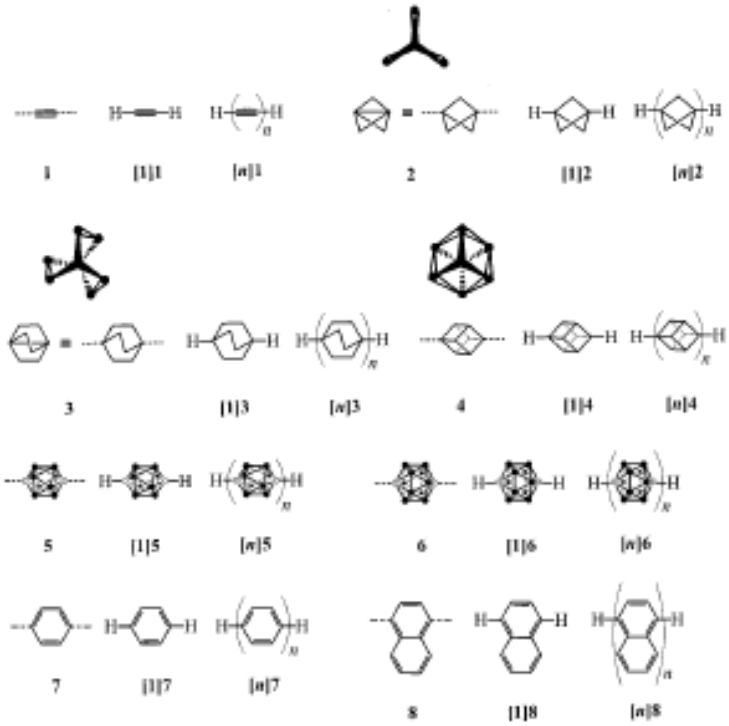

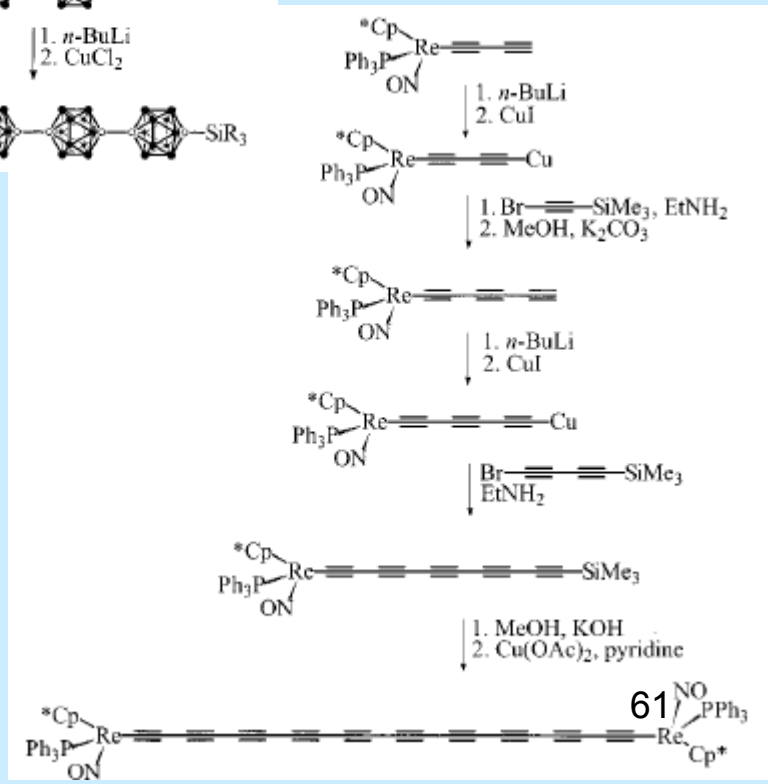

Fibers

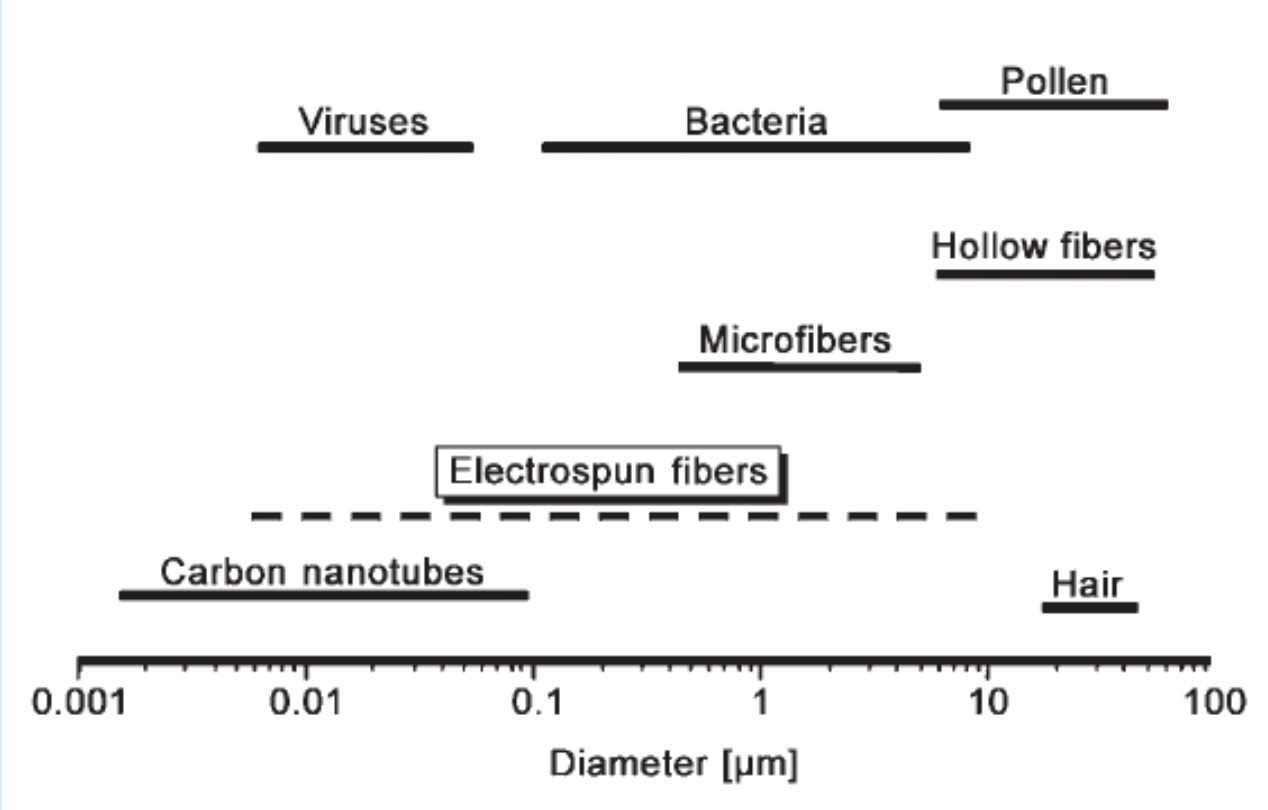
Pollen
Viruses
Bacteria
Hollow fibers
Microfibers
Electrospun fibers
Carbon nanotubes
Hair
0.001
0.01
0.1
1
10
100
Diameter [μm]

Electrospinning

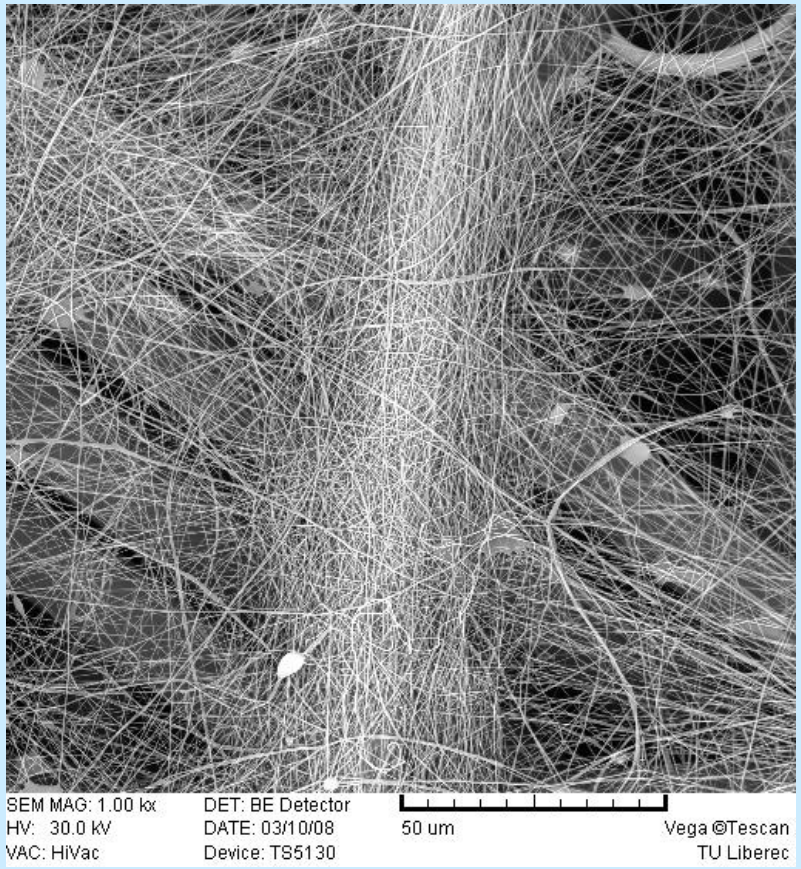

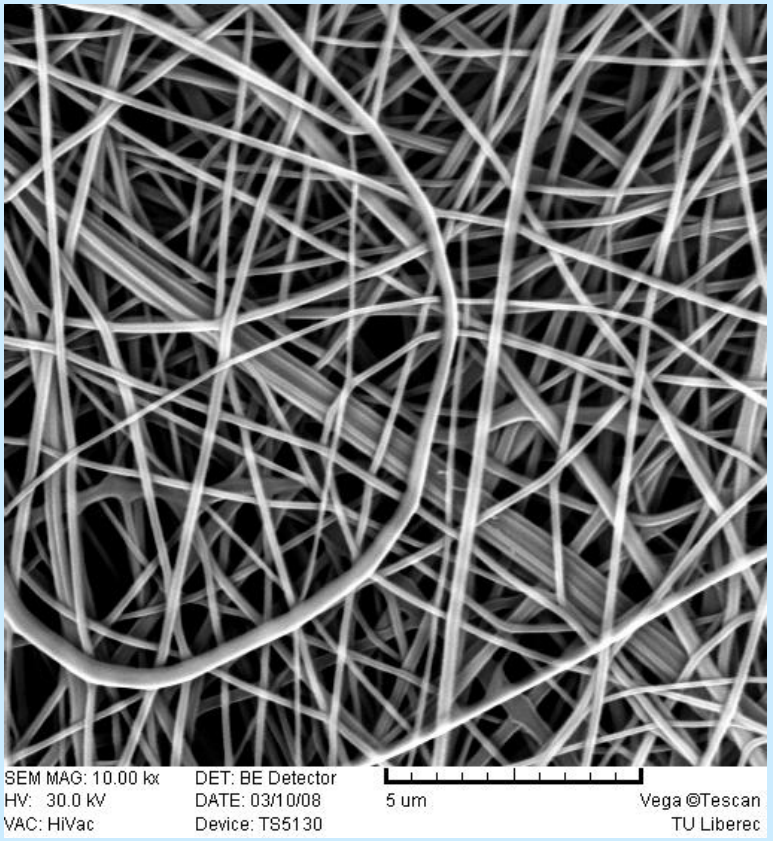

Electrospinning

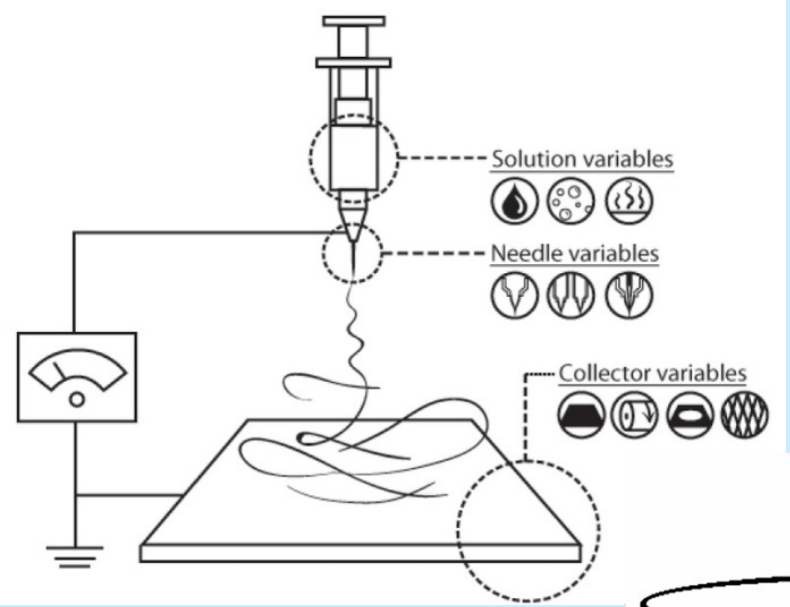

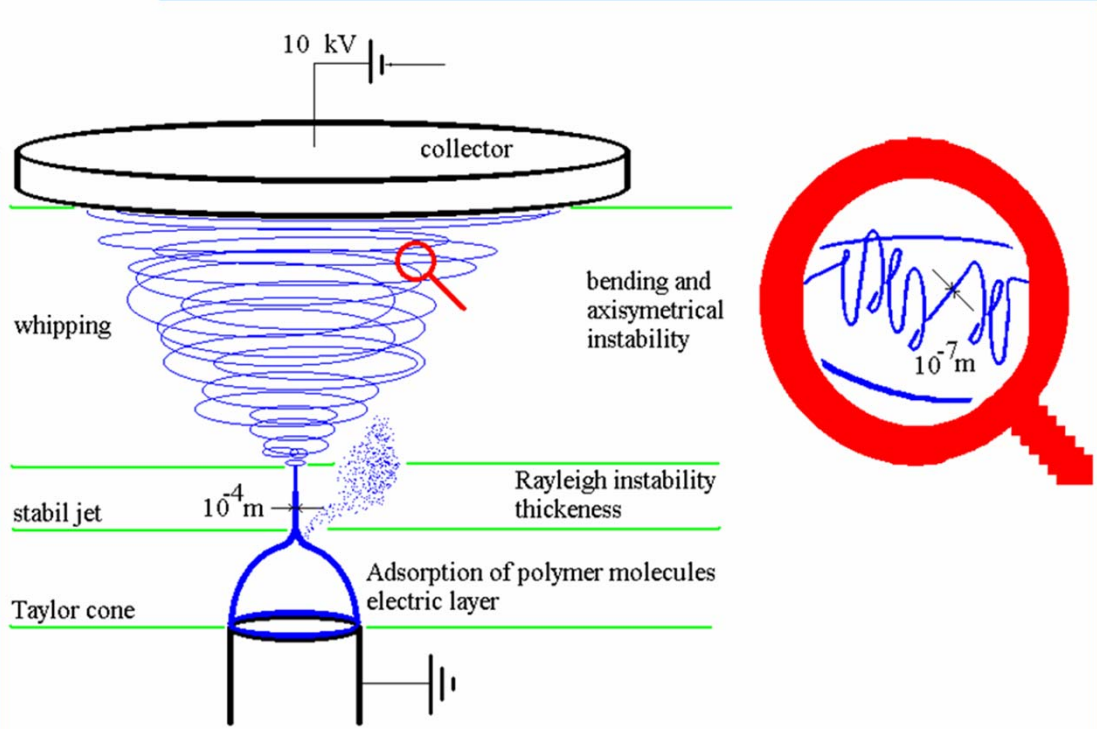

Electrospinning

electrospraying

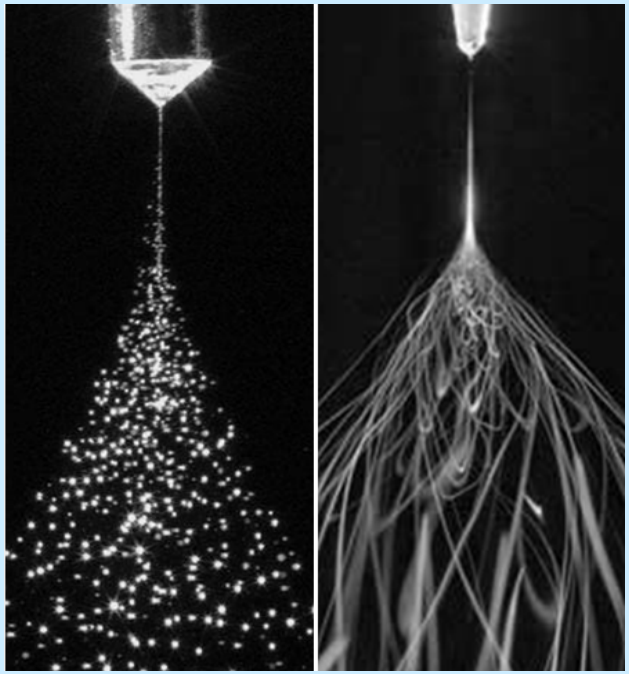

electrospinning

Parameters:

- Solution (viscosity, conductivity, surface tension)
- Instruments (voltage, distance b/w electrodes, collector shape)
- Ambient (temperature, humidity, atmosphere)

Electrospinning

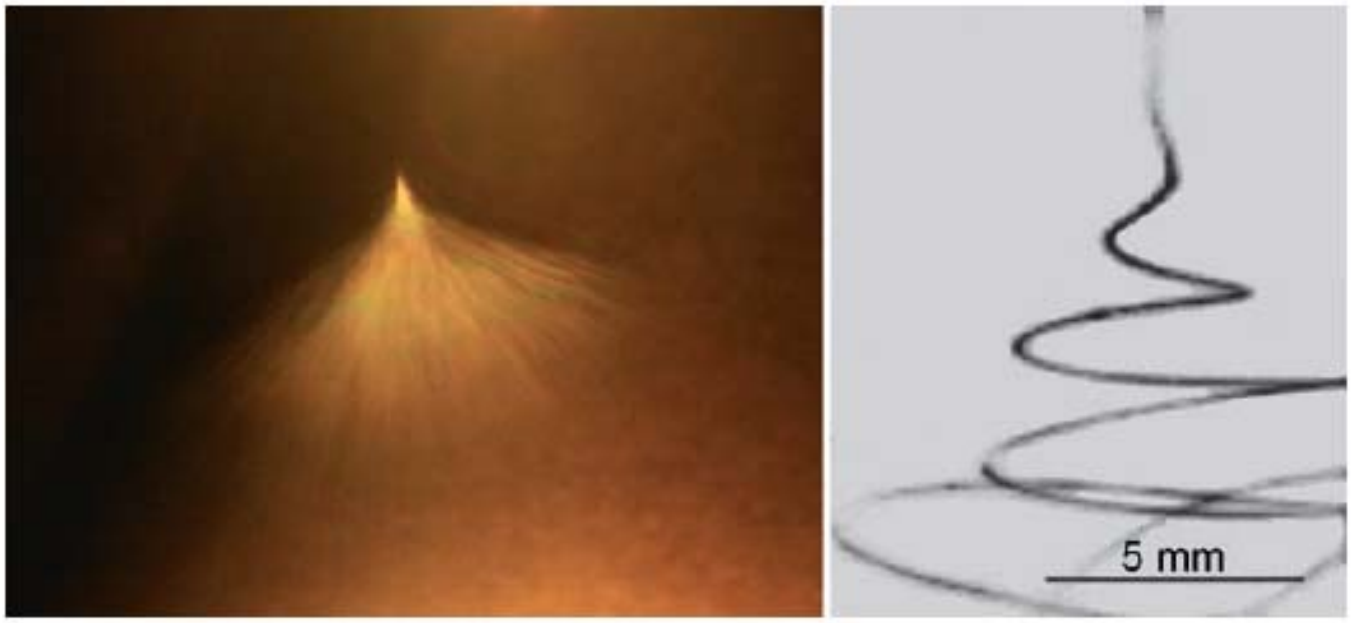

Left: Photograph of a jet of PEO solution during electrospinning.
Right: High-speed photograph of jet instabilities.

Taylor cone

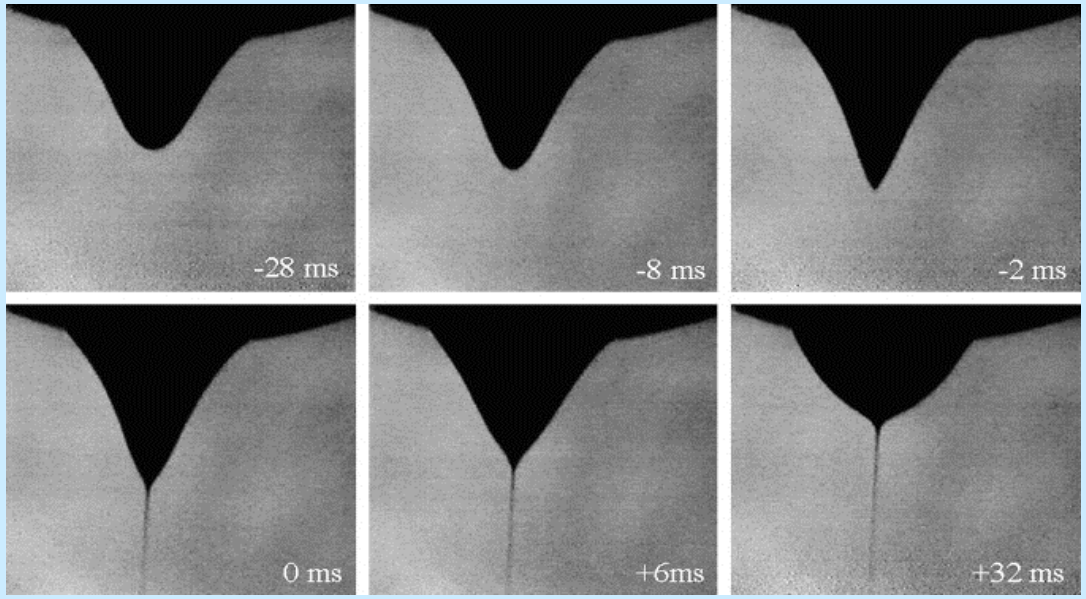

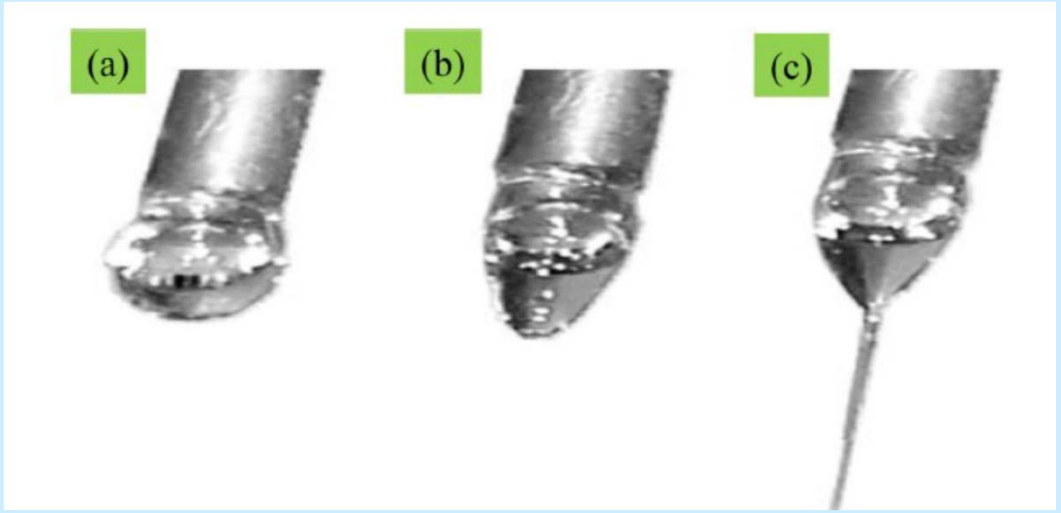






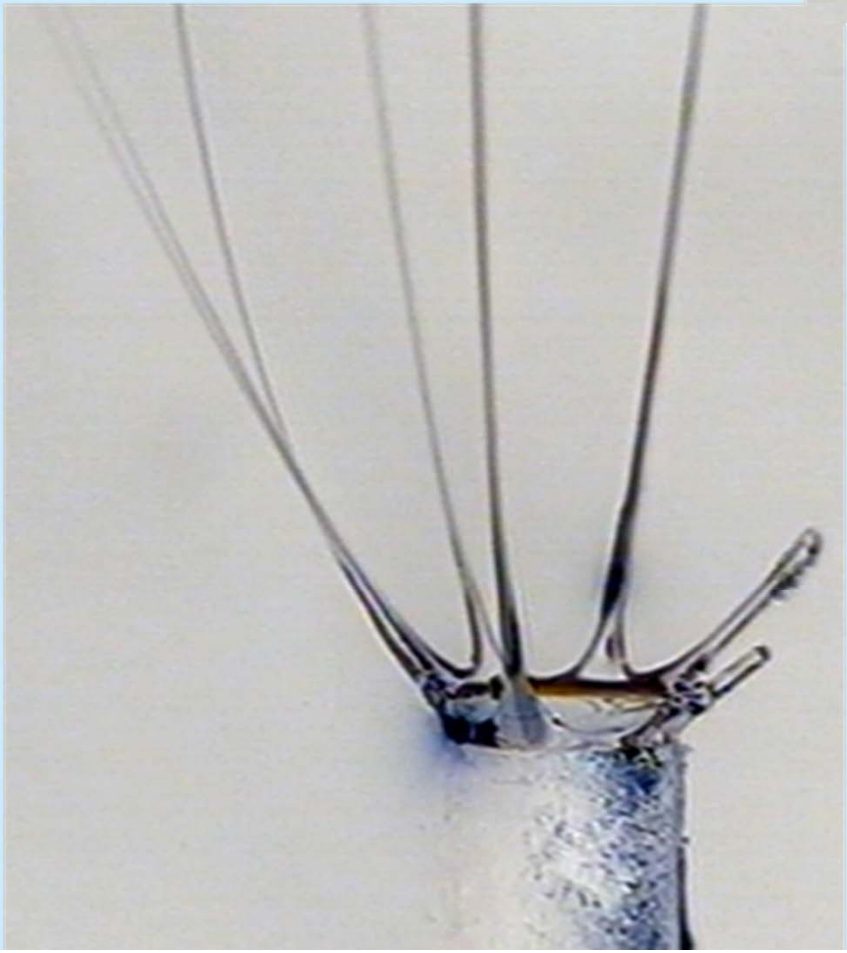

Viscosity

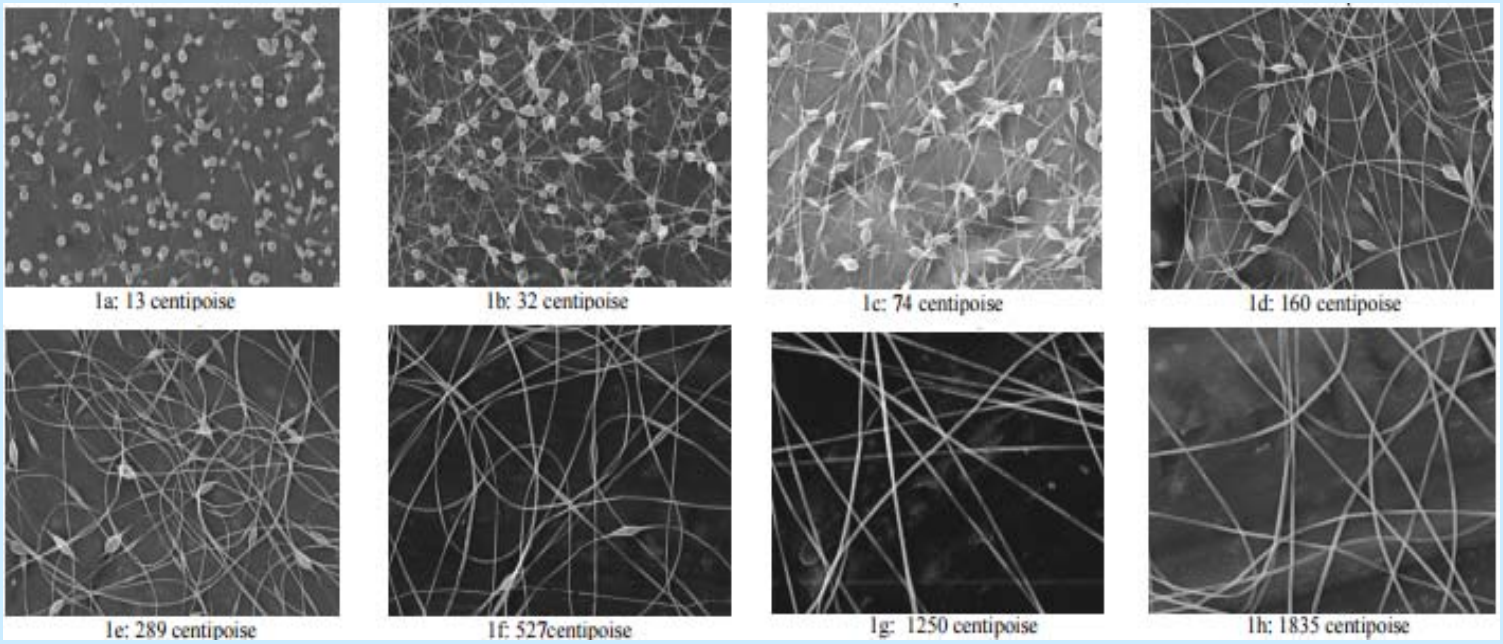
1a: 13 centipoise
1b: 32 centipoise
1c: 74 centipoise
1d: 160 centipoise
1e: 289 centipoise
1f: 527centipoise
1g: 1250 centipoise
1h: 1835 centipoise

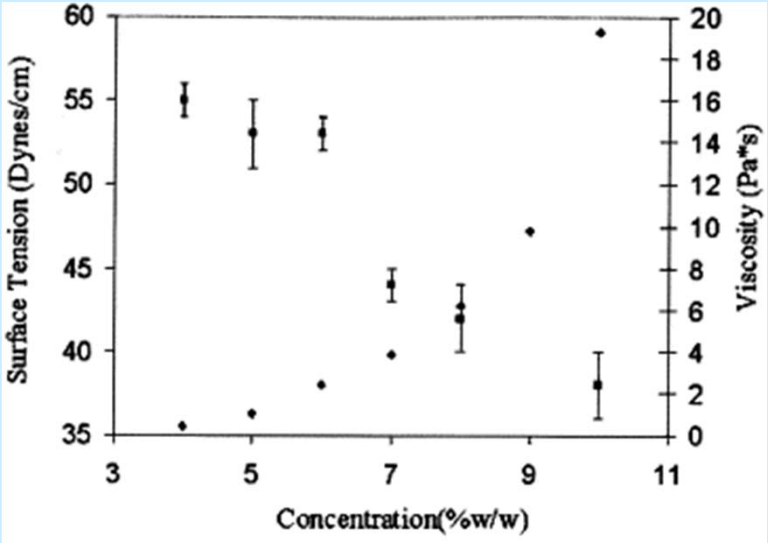
Surface Tension (Dynes/cm)
Viscosity (Pa*s)
Concentration(%w/w)
60
55
50
45
40
35
20
18
16
14
12
10
8
6
4
2
0
3
5
7
9
11

Volume charge density

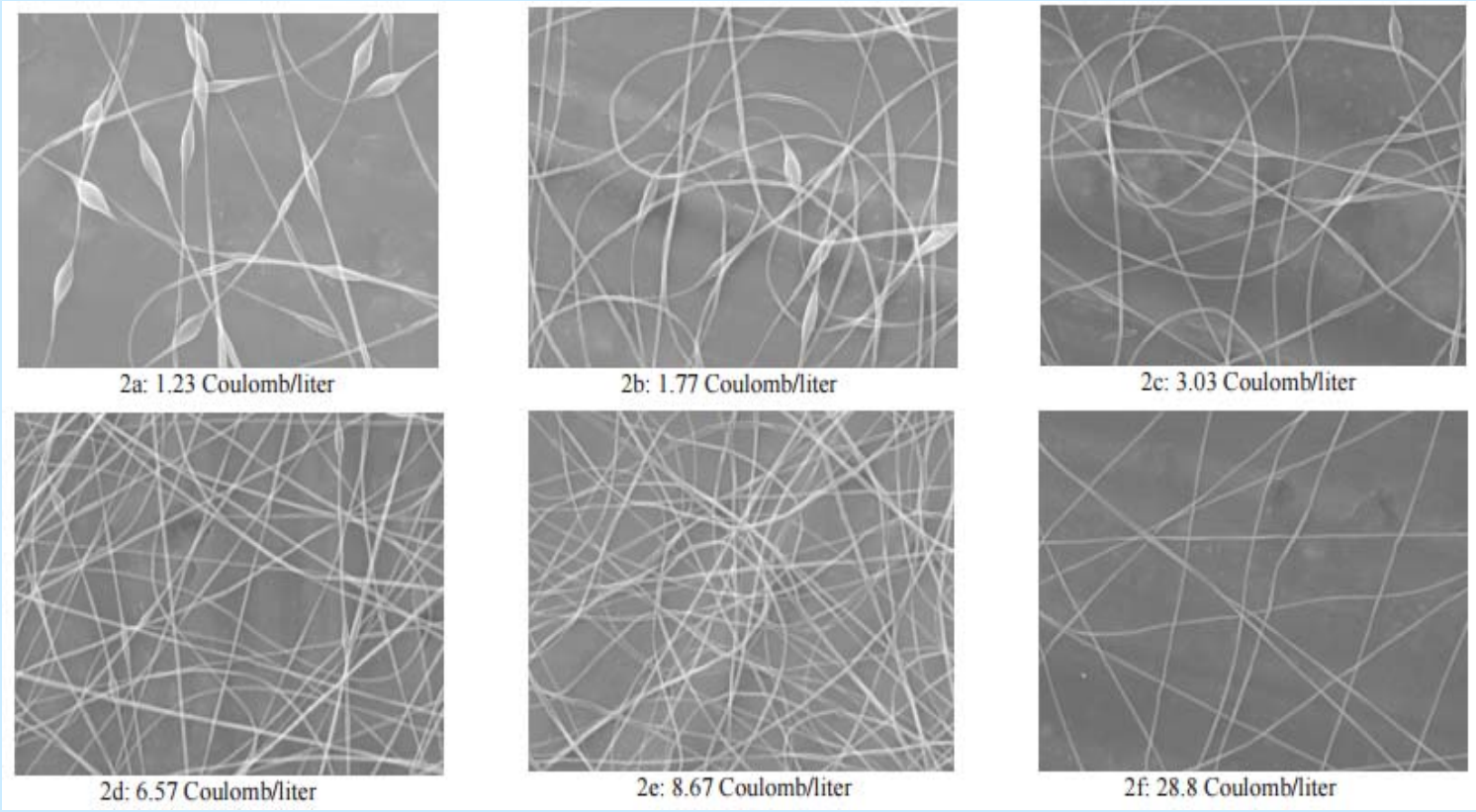

2a: 1.23 Coulomb/liter

2b: 1.77 Coulomb/liter

2c: 3.03 Coulomb/liter

2d: 6.57 Coulomb/liter

2e: 8.67 Coulomb/liter

2f: 28.8 Coulomb/liter

Needle-collector distance

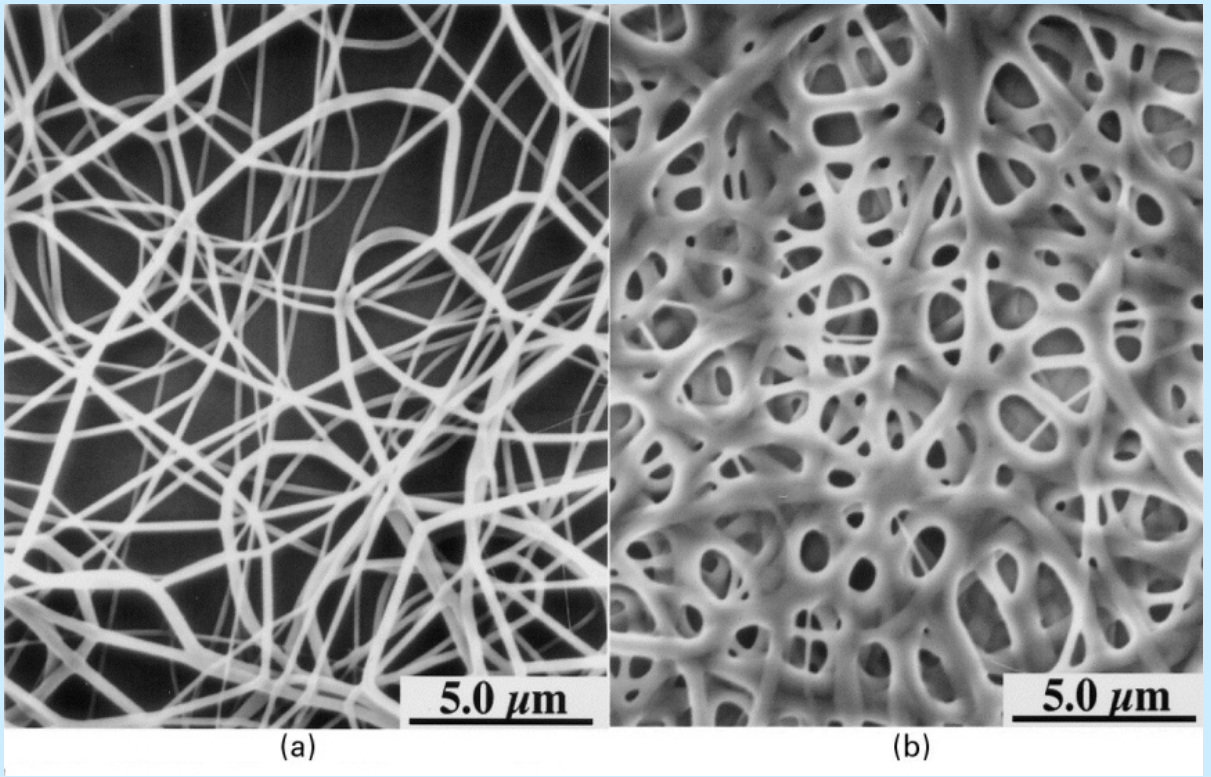

PA fibers, electrode distance 2 cm (a) and 0.5 cm (b)

Conductivity

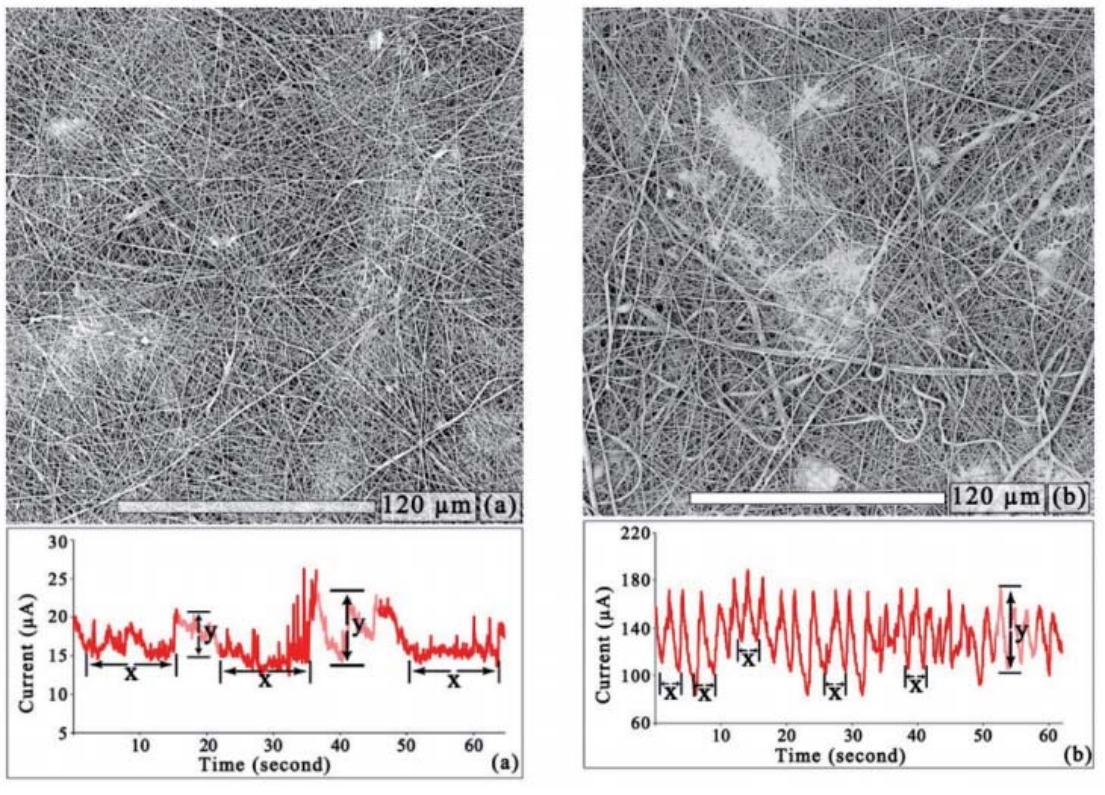

Morphology of fibers as a function of electric current
(a) 20 hm.% PU (b) 20 hm.% PU with addition of 1.27% TEAB

Relative humidity

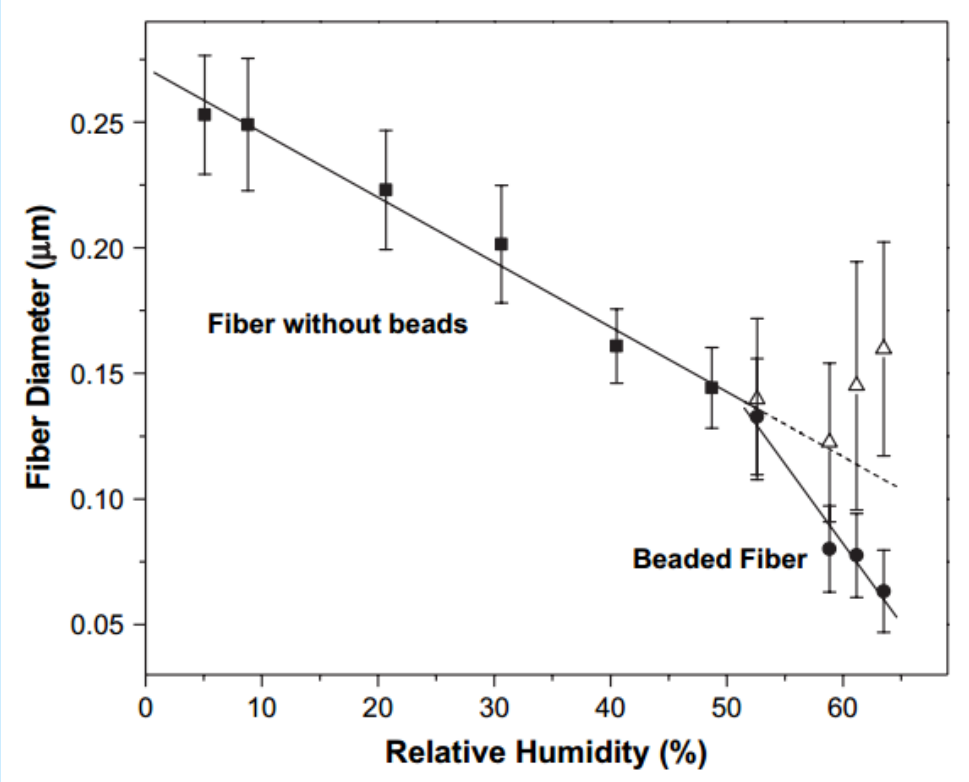

PEO fiber diameter as a function of relative humidity

Coaxial electrospinning

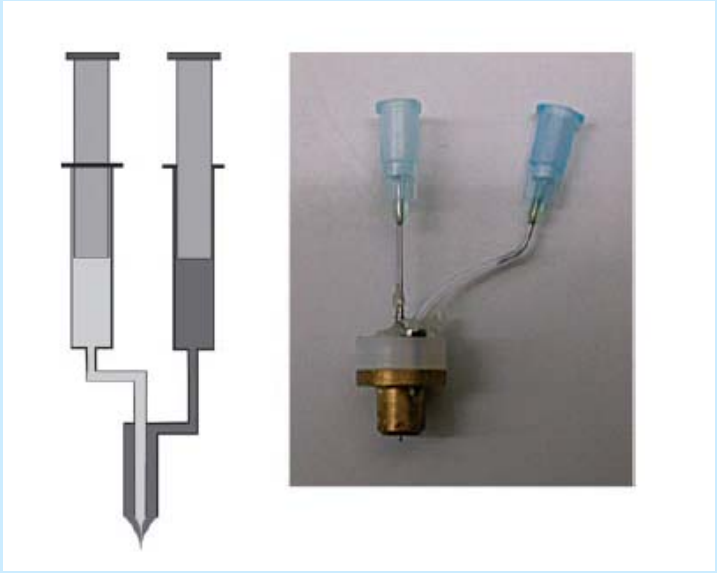

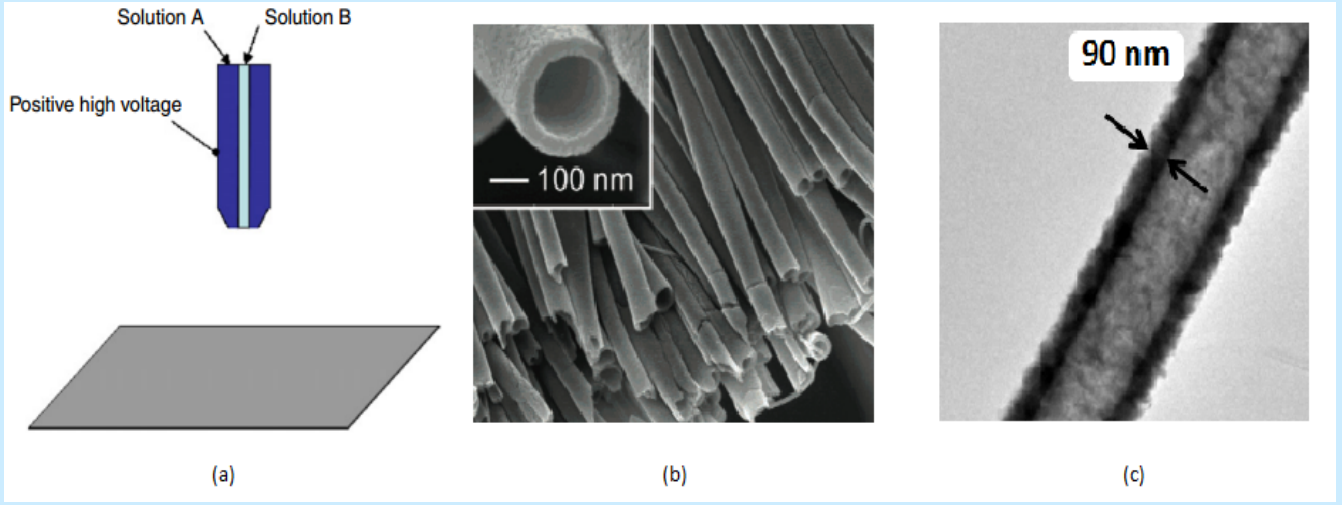

Side-by-side electrospinning

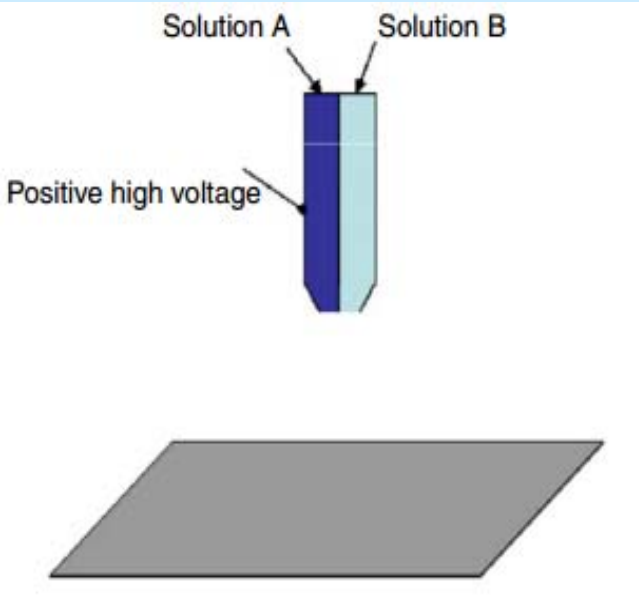

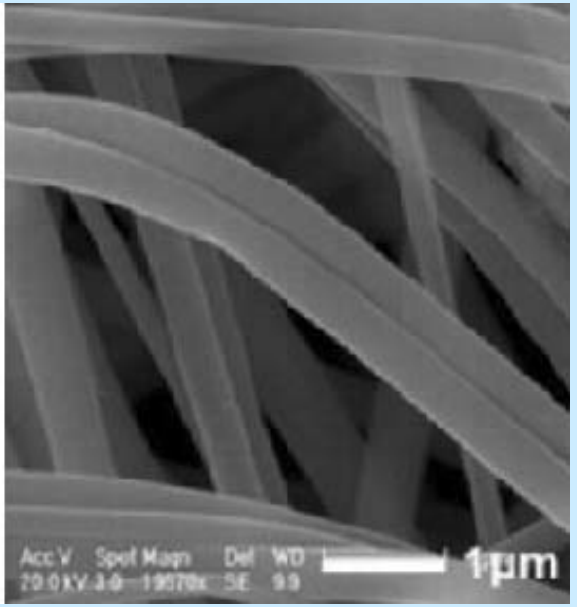

Multijet electrospinning

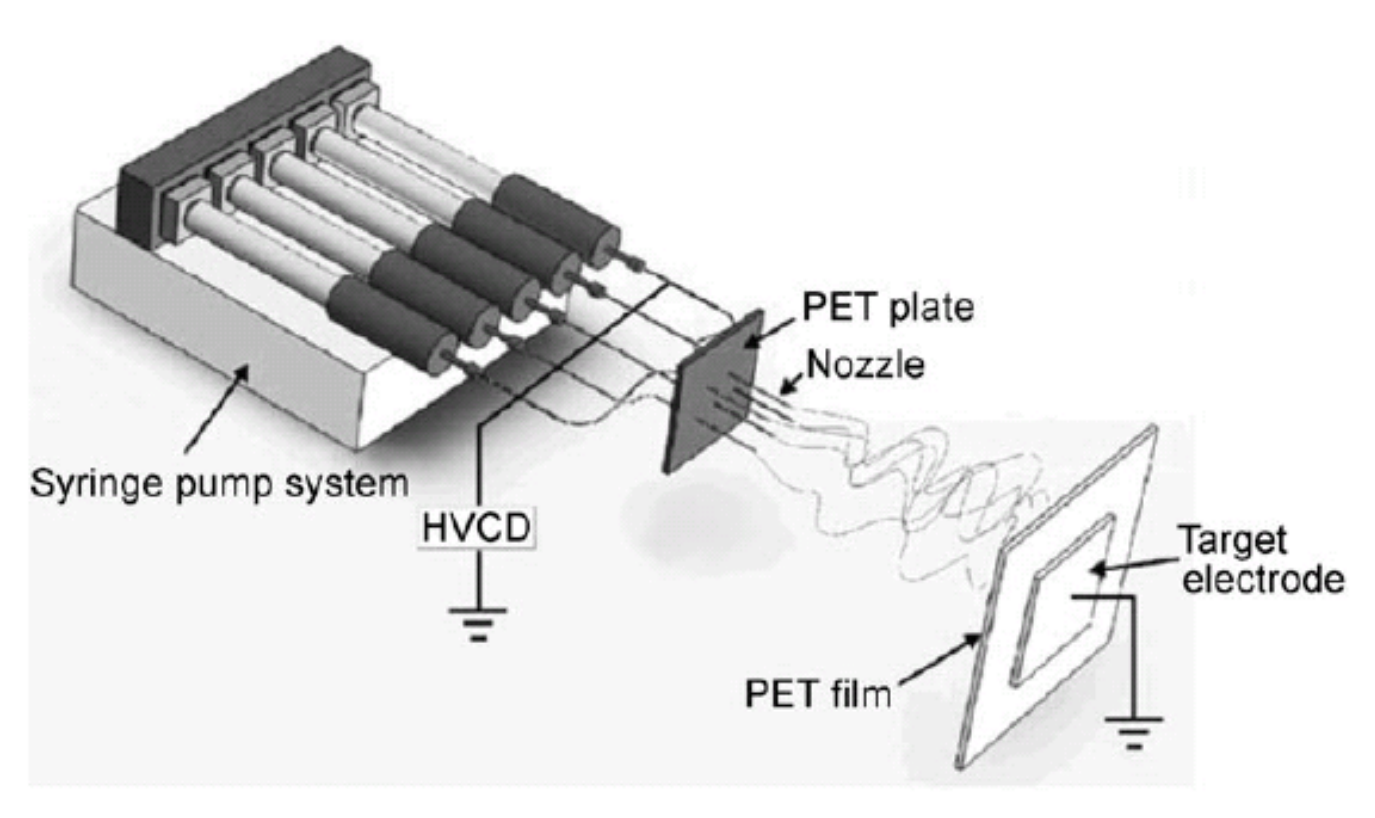

Needle-less spinning

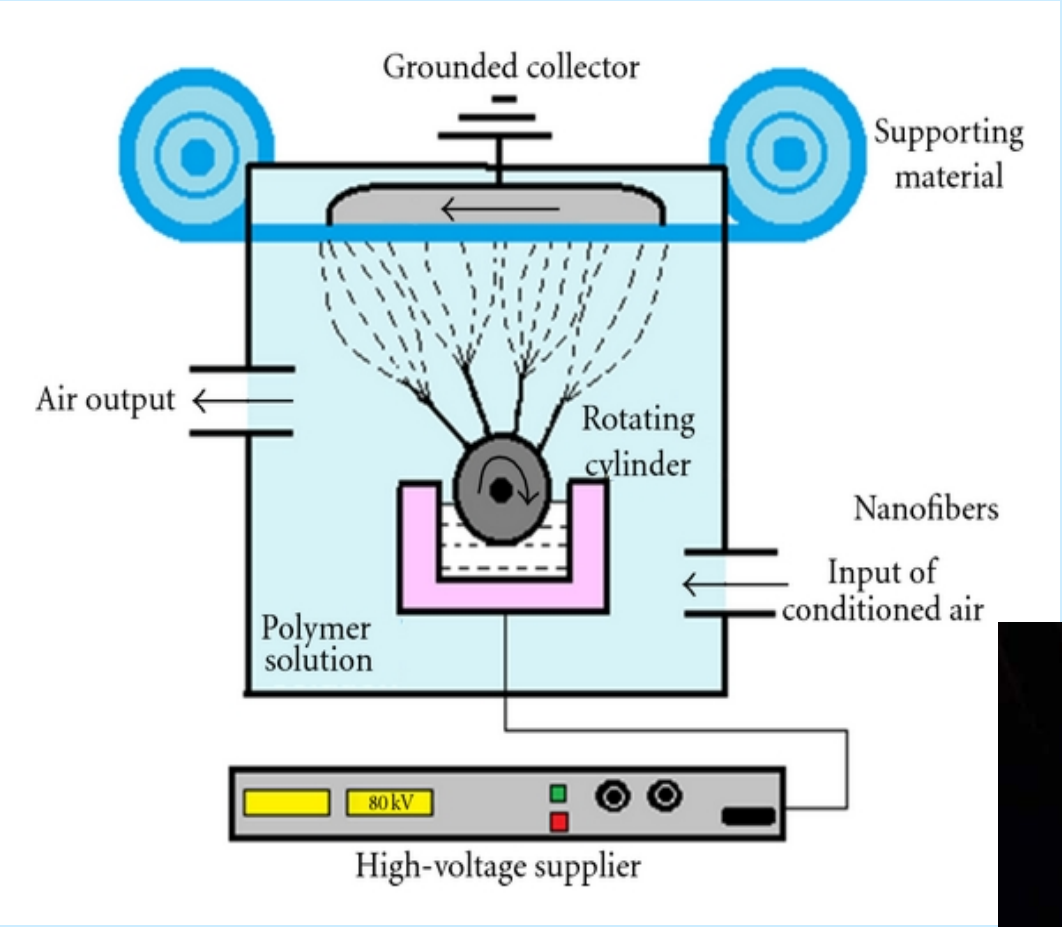

Inorganic fibers

$Th(acac)_4$; PVP; EtOH; acetone

Electrospinning

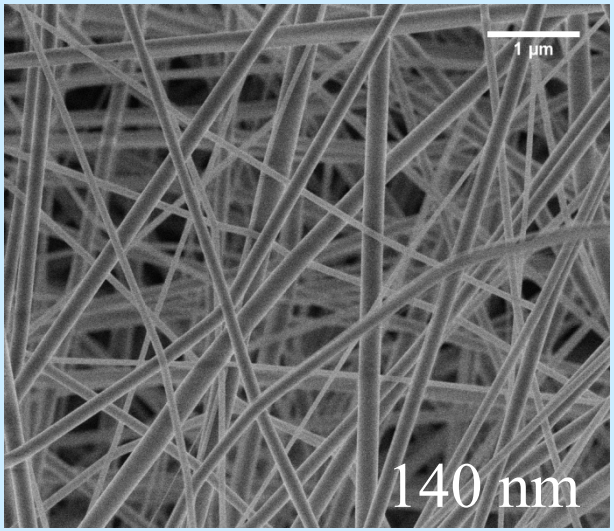

Calcination at
400 °C

ThO_2